# DESIGN AND PERFORMANCE EVALUATION OF RAKE FINGER MANAGEMENT SCHEMES IN THE SOFT HANDOVER REGION

A Dissertation

by

SEYEONG CHOI

Submitted to the Office of Graduate Studies of
Texas A&M University
in partial fulfillment of the requirements for the degree of

DOCTOR OF PHILOSOPHY

August 2007

Major Subject: Electrical Engineering

# DESIGN AND PERFORMANCE EVALUATION OF RAKE FINGER MANAGEMENT SCHEMES IN THE SOFT HANDOVER REGION

A Dissertation

by

SEYEONG CHOI

Submitted to the Office of Graduate Studies of
Texas A&M University
in partial fulfillment of the requirements for the degree of

DOCTOR OF PHILOSOPHY

Approved by:

| | |
|---|---|
| Co-Chairs of Committee, | Mohamed-Slim Alouini |
| | Costas N. Georghiades |
| Committee Members, | Khalid A. Qaraqe |
| | Narasimha Reddy |
| | Eyad A. Masad |
| Head of Department, | Costas N. Georghiades |

August 2007

Major Subject: Electrical Engineering

# ABSTRACT

Design and Performance Evaluation of RAKE Finger

Management Schemes in the Soft Handover Region. (August 2007)

Seyeong Choi, B.S., Hanyang University;

M.S., Hanyang University

Co–Chairs of Advisory Committee: Dr. Mohamed-Slim Alouini
Dr. Costas N. Georghiades

We propose and analyze new finger assignment/management techniques that are applicable for RAKE receivers when they operate in the soft handover region. Two main criteria are considered: minimum use of additional network resources and minimum call drops. For the schemes minimizing the use of network resources, basic principles are to use the network resources only if necessary while minimum call drop schemes rely on balancing or distributing the signal strength/paths among as many base stations as possible. The analyses of these schemes require us to consider joint microscopic/macroscopic diversity techniques which have seldom been considered before and as such, we tackle the statistics of several correlated generalized selection combining output signal-to-noise ratios in order to obtain closed-form expressions for the statistics of interest. To provide a general comprehensive framework for the assessment of the proposed schemes, we investigate not only the complexity in terms of the average number of required path estimations/comparisons, the average number of combined paths, and the soft handover overhead but also the error performance of the proposed schemes over independent and identically distributed fading channels. We also examine via computer simulations the effect of path unbalance/correlation as well as outdated/imperfect channel estimations. We show through numerical exam-

ples that the proposed schemes which are designed for the minimum use of network resources can save a certain amount of complexity load and soft handover overhead with a very slight performance loss compared to the conventional generalized selection combining-based diversity systems. For the minimum call drop schemes, by accurately quantifying the average error rate, we show that in comparison to the conventional schemes, the proposed distributed schemes offer the better error performance when there is a considerable chance of loosing the signals from one of the active base stations.

# DEDICATION

*To my wife, Kyung En Gong*

*my son, Joshua Choi*

*and*

*my parents*

I could not have completed my study without their love, encouragement, and patience.

# ACKNOWLEDGMENTS

I would like to acknowledge the contributions of the following individuals and groups to the development of my dissertation. First, I am very grateful to Professor Mohamed-Slim Alouini, my dissertation advisor, for his wonderful insight and guidance in my research. I am greatly indebted to him for his full support, constant encouragement, and advice in both technical and non-technical matters.

I would also like to thank Professor Costas N. Georghiades for being a co-chair and Professor Khalid A. Qaraqe, Professor Narasimha Reddy, and Professor Eyad A. Masad for being committee members and reviewing this dissertation.

I am particularly thankful to my colleagues, Professor Young-Chai Ko and Professor Hong-Chuan Yang, for their broad expertise and superb intuition which have been a source of inspiration to me during the course of this work. I am also grateful to Professor Edward J. Powers, my former supervisor at the University of Texas at Austin, for his warmhearted kindness during my stay at UT Austin.

During my last one and one-half years, I had the great fortune to join Texas A&M University at Qatar where I could finish my graduate programs with the full support of the Qatar Foundation and Qatar Telecom, which are gratefully acknowledged.

Thanks also to my friends and department faculty and staff in both UT Austin and TAMU(Q) (too many to be listed here) for making my time in Austin, College Station, and Doha such an unforgettable experience. I would also like to extend my gratitude to all group members in YOUNGWOO and SASA for their love.

Last, but certainly not least, I would also like to express my thanks to my parents for their love, belief, sacrifice, and support which have always motivated me. I would also like to acknowledge the most important contributions made by my wife Kyung En Gong and my son Joshua. In reality, this dissertation is partly theirs too.

# NOMENCLATURE

| | |
|---|---|
| BER | Bit Error Rate |
| BPSK | Binary Phase Shift Keying |
| BS | Base Station |
| CDF | Cumulative Distribution Function |
| CDMA | Code Division Multiple Access |
| EGC | Equal Gain Combining |
| GSC | Generalized Selection Combining |
| HO | HandOver |
| i.i.d. | Independent and Identically Distributed |
| LOS | Line-Of-Sight |
| MEC GSC | Minimum Estimation and Combining Generalized Selection Combining |
| MGF | Moment Generating Function |
| MRC | Maximal Ratio Combining |
| MS GSC | Minimum Selection Generalized Selection Combining |
| OT GSC | Output Threshold Generalized Selection Combining |
| PDF | Probability Density Function |
| PDP | Power Delay Profile |
| SC | Selection Combining |
| SHO | Soft HandOver |
| SNR | Signal-to-Noise Ratio |
| SWC | SWitched Combining |
| WCDMA | Wideband Code Division Multiple Access |

# TABLE OF CONTENTS

Page

CHAPTER Page

CHAPTER Page

CHAPTER Page

# LIST OF FIGURES

FIGURE Page

FIGURE Page

FIGURE Page

# CHAPTER I

# INTRODUCTION

## A. Motivation and Objective

In wireless communications, multi-path is the propagation phenomenon that results in radio signals' reaching the receiver by two or more paths. Causes of multi-path can be atmospheric ducting, ionospheric reflection and refraction, and reflection from terrestrial objects such as mountains and buildings. Although the effects of multi-path include both constructive and destructive interferences, and phase shifting of the signal, they significantly deteriorate the performance of wireless communications overall. Hence a multi-path environment is undesirable for receiving signals but also unavoidable. To mitigate the effects of multi-path fading and to therefore improve the performance, various diversity techniques have been investigated. The main principle behind diversity techniques is to make use of multiple independently faded replicas of signals at the receiver to achieve more reliable detection.

In wideband systems that use for example code division multiple access (CDMA) as the air access technology, different path delays of a signal can be discriminated (resolved) due to its nature of high time-resolution. Therefore, energy from all the paths can be summed by adjusting their phases and delays in order to utilize multi-path diversity. As a commonly used diversity technique in conjunction with wideband systems, a RAKE receiver is designed to optimally detect a signal transmitted over a dispersive multi-path channel. It is an extension of the concept of the matched filter. In the RAKE receiver, one RAKE finger is assigned to each multi-path, thus

---

The journal model is *IEEE Transactions on Automatic Control.*

maximizing the amount of received signal energy. Each of these different paths are combined to form a composite signal that is expected to have substantially better characteristics for the purpose of demodulation than just a single path.

Due to the limited number of fingers in comparison to the large number of multi-paths, the RAKE receiver has to have a certain form of path selection algorithm. Moreover, in the soft handover (SHO) region, this issue becomes more critical since the receiver relies on the additional network resources available in the SHO. Hence, in order to meet the requirement of the performance as well as the network resource limitations, more sophisticated diversity combining techniques are imperative. Although many of researchers have been dedicated to the study of the finger assignment issue, there are only very few detailed investigations on diversity combining techniques which can distinguish the resolvable paths from different base stations (BSs).

In this dissertation, by considering macroscopic diversity techniques, we propose and analyze new finger assignment/management schemes for RAKE receivers in the SHO region. The main idea behind the proposed finger assignment schemes is that in the SHO region the receiver uses the additional network resources only if necessary so as to reduce the unnecessary path estimations/comparisons and the SHO overhead with a slight performance loss compared to the conventional schemes. With the finger management schemes, we consider the schemes minimizing the probability of call drops. These schemes are devised to distribute paths among BSs so as to secure a certain proportion of total combined signal strength in case of disconnecting one of the active BSs.

We thoroughly quantify the performance of all the proposed schemes by providing analytical (closed-from) expressions for the statistic of the output signal-to-noise ratio (SNR) and for the performance measures of our interests. Based on these analytical results, we examine the tradeoff between performance and complexity.

## B. Outline

The outline of the dissertation is as follows. We begin in Chapter II with a brief review of the fading channels, diversity techniques, and RAKE combining schemes in the SHO region in view of diversity combining techniques. We then present new finger assignment/management schemes throughout the dissertation. From Chapter III to Chapter VII, our main concern is focused on the schemes for the minimum use of network resources, while we deal with in Chapter VIII the schemes for the minimum call drops. In all chapters except Chapter VII, one of our main goals is to obtain analytical expressions for the performance measures so as to allow system designers to immediately investigate tradeoff between performance and complexity among various proposed schemes.

In Chapter III, a new finger reassignment technique with two-BS which is applicable for RAKE receivers in the SHO region is proposed and analyzed. This scheme employs a new version of generalized selection combining (GSC). More specifically, in the SHO region, the receiver uses by default only the strongest paths from the serving BS and only when the combined SNR falls below a certain pre-determined threshold, the receiver uses more resolvable paths from the target BS to improve the performance. In this chapter, we attack the statistics of two correlated GSC stages and provide approximate but accurate closed-form expressions for the statistics of the output SNR. In Chapter IV, we extend the results in Chapter III to the multi-BS situation by attacking the statistics of several correlated GSC stages and providing closed-form expressions for the statistics of the output SNR. In this chapter, we consider two different path scanning schemes: full scanning and sequential scanning schemes.

Next, we propose and analyze in Chapter V an alternative new finger replacement

technique with two-BS. With this scheme, instead of changing the configuration for all fingers which is essential for the schemes proposed in Chapters III and IV, the receiver just compares the sum of the weakest paths out of the currently connected paths from the serving BS with the sum of the strongest paths from the target BS and selects the better group and as such, a further reduction in complexity as well as the use of additional network resources can be obtained. Similar to Chapter IV, we extend this replacement scheme to multi-BS situation in Chapter VI.

In Chapter VII, we present the effects of practical channel environments on the performance of new finger assignment schemes analyzed over independent and identically distributed (i.i.d.) Rayleigh fading channels in Chapters III-VI. In this chapter, we consider an exponentially decaying power delay profile among paths along with an exponential and constant correlation models. The effect of outdated/imperfect channel estimations is also evaluated. Simulation results show that our proposed schemes are still offering an interesting performance versus network overhead tradeoff in the practical channel environments considered in this chapter.

We propose and analyze in Chapter VIII new finger management techniques employing "distributed" types of GSC and minimum selection GSC schemes in order to minimize the impact of sudden connection loss of one of the active base stations. By accurately quantifying the average error rate, we show through numerical examples that our newly proposed distributed schemes offer a clear advantage in comparison with their conventional counterparts.

# CHAPTER II

# BACKGROUND

## A. Fading Channels

Fading (or fading channels) refers to the distortion of a carrier-modulated telecommunication signal which experiences over certain propagation media between the transmitter and the receiver. Fading results from the interference among several versions of the same transmitted signals arriving from many different directions with random attenuation, delay, and phase shift. It may also be caused by attenuation of a single signal. The most common way of classification of fading is as follows [1–6]:

- Large-Scale fading (Shadowing) : An average signal power attenuation caused by larger movements of a mobile or obstructions within the propagation environment. This is often modeled as log-normal distribution with a standard deviation according to the log distance path loss model.
- Small-Scale fading (Multi-path fading) : A rapid fluctuation of the amplitudes, phases, or multi-path delays of a radio signal over a short period of time or travel distance occurring with small movements of a mobile or obstacle. This kind of fading is mainly due to multi-path propagation. The Rayleigh distribution is frequently used to model multi-path fading with no direct line-of-sight (LOS) path.
  - Frequency-Flat and Frequency-Selective fading based on multi-path time delay spread
    - Frequency-Flat fading : The bandwidth of the signal is less than the

coherence bandwidth of the channel or the delay spread is less than the symbol period.

  - Frequency-Selective fading : The bandwidth of the signal is greater than the coherence bandwidth of the channel or the delay spread is greater than the symbol period.

- Slow and Fast fading based on Doppler spread

  - Fast fading : The coherence time is less than the symbol period, and the channel variations are faster than baseband signal variations.
  - Slow fading : The coherence time is greater than the symbol period and the channel variations are slower than the baseband signal variations.

Note that large-scale fading is more relevant to issues such as cell-site planning while small-scale fading is more relevant to the design of reliable and efficient communication systems. In this dissertation, we focus on small-scale fading caused mainly by multiple paths.

## B. Diversity Techniques

The best way to combat fading is to ensure that multiple versions of the same signal are transmitted, received, and coherently combined. This is usually termed diversity. The intuition behind this concept is to exploit the low probability of concurrence of deep fades in all the diversity channels to lower the probability of error and of outage. In telecommunications, a diversity scheme refers to a method for improving the reliability of a message signal by utilizing two or more communication channels with different characteristics and as such, it plays an important role in combatting fading and co-channel interference and avoiding error bursts.

Diversity combining is the technique applied to combine the multiple received signals of a diversity reception device into a single improved signal. Various classical pure diversity combining techniques can be distinguished as follows [1–5, 7]:

- Selection Combining (SC) : Of all the received signals, the strongest signal is selected.
- Equal Gain Combining (EGC) : All the received signals are summed coherently.
- Maximal Ratio Combining (MRC) : The received signals are weighted with respect to their SNRs and then summed.
- Switched Combining (SWC) [8–15] : The receiver switches to another signal when current signal drops below a predefined threshold.

Due to additional complexity constraints and/or the potential of a higher diversity gain with more sophisticated diversity scheme, recently newly proposed hybrid diversity techniques have been a great deal of attention in view of their promising offer to meet the specifications of emerging wideband communications system. Among them is GSC [16–20] which is a generalization of SC and which chooses a fixed number of paths with the largest instantaneous SNR from all available diversity paths and then combines them as per the rules of MRC. As a power-saving implementation of GSC, minimum selection GSC (MS GSC) [21–24], minimum estimation and combining GSC (MEC GSC) [25], and output-threshold GSC (OT GSC) [26,27] were recently proposed. With MS GSC, after examining and ranking all available paths, the receiver tries to raise the combined SNR above a certain threshold by combining in an MRC fashion the least number of the best diversity paths and as such, MS GSC can save considerable amount of processing power by keeping less MRC branch active on average in comparison to the conventional GSC scheme. Further estimation

savings can be done by using MEC GSC. On an other hand, OT GSC successively estimates available diversity paths and applies MRC or GSC to them in order to make the combined SNR exceed a certain SNR threshold.

### C. RAKE Combining Scheme in the Soft Handover Region

While usually viewed as a deteriorating factor, multi-path fading can also be exploited to improve the performance by using RAKE type of receivers [28]. RAKE reception is a technique which uses several baseband correlators called fingers to individually process multi-path signal components from different BSs. The outputs from the different correlators are coherently combined to improve the SNR and to therefore lower the probability of deep fades. Since they rely on resolvable multi-paths to operate and the diversity branches correspond to the different resolvable multi-paths, RAKE receivers are usually used in conjunction with wideband systems such as wideband code division multiple access (WCDMA) in order to mitigate the effect of multi-path fading.

In the handover (HO) region, the number of available resolvable paths can be quite large since they come from the serving BS as well as the target BS. However, due to the hardware and complexity constraints, the number of fingers in the mobile unit is very limited. Usually, the mobile unit receiver is limited to 3 fingers while the BS receiver can use 4 or 5 fingers depending on the equipment manufacturer [29]. Hence, we are faced with the problem of how to judiciously select a subset of paths for the RAKE reception in the SHO region. Although many newly proposed low complexity diversity combining approaches considered in the above section can be used for our problem of interest (i.e., combining in the SHO region), all the combining schemes base their selection criteria on all the available paths regardless of the BSs and did not

take into consideration the network overhead. In other words, the way they operate does not make them distinguish the resolvable paths coming from the serving and the target BS. As such, if they are used without any modification or adaptation to the SHO, they end up using continuously the hardware/transmission resources of the serving and the target BS and result therefore in a considerable increase in overhead on the network (known as SHO overhead [30, Section 9.3.1.4]). As such, it is of interest to develop diversity combining schemes which can achieve the required performance while (i) maintaining a low complexity and low processing power consumption and (ii) using a minimal amount of additional network resources.

Based on the fact, to the best knowledge, that detailed investigation on diversity techniques which can distinguish the resolvable paths from different base stations has seldom been considered before, we propose and analyze in this dissertation new finger assignment/management schemes that either maintain a low complexity and reduce the SHO overhead and or minimize the possibility of call drops.

# CHAPTER III

# FINGER REASSIGNMENT SCHEME WITH TWO BASE STATIONS

## A. Introduction

In this chapter, we propose and study a new finger reassignment-based scheme that is specifically applicable for RAKE reception in the SHO region. With this scheme, we assume that the $L_c$ out of total $L$ resolvable paths from the serving BS are by default assigned to the RAKE fingers of the mobile unit in the SHO region following $L_c/L$-GSC type of combining. Only when the output SNR falls below a pre-determined SNR threshold (known also as a target SNR), the receiver asks for the additional resources from the target BS. More specifically, the receiver scans the additional $L_a$ resolvable paths from the target BS and selects again the strongest $L_c$ paths but now among the $L + L_a$ available paths (i.e., the receiver uses $L_c/(L + L_a)$-GSC). Unlike minimum MS GSC and OT GSC, our proposed scheme always uses a fixed number of fingers, i.e., $L_c$, but as we will show in the performance results part, it can reduce the unnecessary path estimations and the SHO overhead compared to the conventional GSC scheme.

The main contribution of this chapter is to derive the statistics of the receiver output SNR for our newly proposed scheme, including its probability density function (PDF), cumulative distribution function (CDF), and moment generating function (MGF). We provide not only the analytical framework that leads to exact but complicated expressions but also an alternative approximate approach which yield relatively simple expressions that come close to the exact solutions. These results are then used (i) to analyze the performance in terms of the average probability of error and (ii) to investigate the tradeoff between complexity and performance. Some selected nu-

merical results show that in poor channel conditions our scheme can essentially give the same performance as the GSC scheme while it offers in good channel conditions a smaller path estimation load and considerable reduction in the SHO overhead.

The chapter is organized as follows. In Section III.B, we present the system and channel model under consideration as well as the mode of operation of the proposed scheme. Based on this mode of operation, we derive the expressions for the statistics of the combined SNR in Section III.C. These results are next applied to the performance analysis of the proposed system in Section III.D. Section III.E illustrates the tradeoff of complexity versus performance by comparing the number of path estimations and the SHO overhead of our proposed systems to that of conventional GSC and MRC. Finally, Section III.F provides some concluding remarks.

## B. System Model

### 1. System and Channel Model

We consider a multi-cell CDMA system with universal frequency reuse. Each cell uses different sets of spreading codes to control the intercell interference. We focus on the receiver operation when the mobile unit is moving from the coverage area of its serving BS to that of a target BS. We assume that the mobile unit is equipped with an $L_c$ finger RAKE receiver and is capable of despreading signals from different BSs using different fingers, and thus facilitating SHO. The RAKE receiver also implements a GSC-based path selection mechanism to select the $L_c$ best paths for RAKE combining among all the resolvable paths.

Note that in the SHO region the mobile unit is of roughly the same long distance from the serving and the target BSs and as such, we assume that the average signal strength on a path from both BSs is the same. To simplify our analysis and

make it tractable, we further assume that the receiver operates over a "perfect" uniform average power delay profile provided by a multi-path searcher in a way that the multi-path components are correctly assigned to the RAKE fingers. Moreover, we do not consider the effect of inter-symbol/channel interferences by assuming, for example, perfect spreading codes. As such, we assume that the received signals on all the resolvable paths from the serving and the target BSs experience i.i.d. Rayleigh fading[1]. If we let $\gamma_i$ denote the instantaneous received SNR of the $i$th resolved path, then $\gamma_i$ follows the same exponential distribution, with common PDF and CDF given as [3, Eq. (6.5)]

$$f_\gamma(x) = \frac{1}{\overline{\gamma}} \exp\left(-\frac{x}{\overline{\gamma}}\right), \quad x \geq 0 \tag{3.1}$$

and

$$F_\gamma(x) = 1 - \exp\left(-\frac{x}{\overline{\gamma}}\right), \quad x \geq 0, \tag{3.2}$$

respectively, where $\overline{\gamma}$ is the common average faded SNR.

## 2. Mode of Operation

We assume without loss of generality that in the SHO region, the mobile unit resolves $L$ multi-paths from the serving BS and $L_a$ additional paths from the target BS. As the mobile unit enters the SHO region, the RAKE receiver relies at first on the $L$ resolvable paths gathered from the serving BS and as such, starts with $L_c/L$-GSC. If we let $\Gamma_{i:j}$ be the sum of the $i$ largest SNRs among $j$ ones, i.e., $\Gamma_{i:j} = \sum_{k=1}^{i} \gamma_{k:j}$ where $\gamma_{k:j}$ is the $k$th order statistics (see [18] for terminology), then the total received SNR after GSC is given by $\Gamma_{L_c:L}$. At the beginning of every time slot, the receiver compares the received SNR, $\Gamma_{L_c:L}$, with a certain target SNR, denoted by $\gamma_T$. If $\Gamma_{L_c:L}$ is greater

[1]In Chapter VII, more practical channel environments, such as non-identical/correlated fading channels and outdated channel estimation, are considered.

than or equal to $\gamma_T$, a one-way SHO[2] is used and no finger reassignment is needed. On the other hand, whenever $\Gamma_{L_c:L}$ falls below $\gamma_T$, a two-way SHO[3] is attempted. In this case, the RAKE reassigns its $L_c$ fingers to the $L_c$ strongest paths among the $L + L_a$ available resolvable paths (i.e., the RAKE receiver uses $L_c/(L + L_a)$-GSC). Now the total received SNR is given by $\Gamma_{L_c:L+L_a}$.

Based on the above mode of operation, we can see that the final combined SNR, denoted by $\gamma_t$, is mathematically given by

$$\gamma_t = \begin{cases} \Gamma_{L_c:L+L_a}, & 0 \leq \Gamma_{L_c:L} < \gamma_T; \\ \Gamma_{L_c:L}, & \Gamma_{L_c:L} \geq \gamma_T. \end{cases} \tag{3.3}$$

## C. Statistics of the Combined SNR

Although the mode of operation in (3.3) describes a scheme that essentially switches between $L_c/L$-GSC and $L_c/(L + L_a)$-GSC depending on the channel conditions, we can not obtain the statistics of $\gamma_t$ directly from the statistics of the output SNR with conventional GSC. Hence, in this section, we rely on some recent results on order statistics [22, 27] to derive the statistics of the combined SNR, $\gamma_t$.

### 1. CDF

From (3.3), the CDF of $\gamma_t$, $F_{\gamma_t}(x)$, can be written as

$$\begin{aligned} F_{\gamma_t}(x) &= \Pr\left[\gamma_t < x\right] \\ &= \Pr\left[\gamma_T \leq \Gamma_{L_c:L} < x\right] + \Pr\left[\Gamma_{L_c:L+L_a} < x, \Gamma_{L_c:L} < \gamma_T\right]. \end{aligned} \tag{3.4}$$

[2]One-way SHO refers to the scenario in which the mobile unit is connected only to the serving BS while being in the SHO region.

[3]Two-way SHO refers to the scenario in which the mobile unit is connected to the serving and the target BSs while being in the SHO region.

Since it is clear that $\Gamma_{L_c:L} \leq \Gamma_{L_c:L+L_a}$, we can rewrite $\Pr\left[\Gamma_{L_c:L+L_a} < x, \Gamma_{L_c:L} < \gamma_T\right]$ in (3.4) as

$$\begin{aligned} &\Pr\left[\Gamma_{L_c:L+L_a} < x, \Gamma_{L_c:L} < \gamma_T\right] \qquad (3.5)\\ &= \begin{cases} \Pr\left[\Gamma_{L_c:L+L_a} < x\right], & 0 \leq x < \gamma_T; \\ \Pr[\Gamma_{L_c:L+L_a} < \gamma_T] & \\ + \Pr\left[\gamma_T \leq \Gamma_{L_c:L+L_a} < x, \Gamma_{L_c:L} < \gamma_T\right], & x \geq \gamma_T. \end{cases} \end{aligned}$$

Substituting (3.5) into (3.4), we can express the CDF of $\gamma_t$, $F_{\gamma_t}(x)$, as

$$F_{\gamma_t}(x) = \begin{cases} \Pr\left[\Gamma_{L_c:L+L_a} < x\right], & 0 \leq x < \gamma_T; \\ \Pr\left[\gamma_T \leq \Gamma_{L_c:L} < x\right] + \Pr[\Gamma_{L_c:L+L_a} < \gamma_T] & \\ + \Pr\left[\gamma_T \leq \Gamma_{L_c:L+L_a} < x, \Gamma_{L_c:L} < \gamma_T\right], & x \geq \gamma_T. \end{cases} \qquad (3.6)$$

To obtain a closed-form expression for $F_{\gamma_t}(x)$, we just need to find a closed-form expression of the joint probability, $\Pr\left[\gamma_T \leq \Gamma_{L_c:L+L_a} < x, \Gamma_{L_c:L} < \gamma_T\right]$, in (3.6). This joint probability can be calculated as

$$\begin{aligned} &\Pr\left[\gamma_T \leq \Gamma_{L_c:L+L_a} < x, \Gamma_{L_c:L} < \gamma_T\right] \qquad (3.7)\\ &= \Pr[\Gamma_{L_c:L} < \gamma_T] \Pr\left[\gamma_T \leq \Gamma_{L_c:L+L_a} < x | \Gamma_{L_c:L} < \gamma_T\right] \\ &= \Pr[\Gamma_{L_c:L} < \gamma_T] \int_{\gamma_T}^{x} f_{\Gamma_{L_c:L+L_a}|\Gamma_{L_c:L}<\gamma_T}(y_0) dy_0. \end{aligned}$$

By recursively performing the following integration

$$f_{\Gamma_{L_c:L+2}|\Gamma_{L_c:L}<\gamma_T}(y_0) = \int_0^{\infty} f_{\Gamma_{L_c:L+2},\Gamma_{L_c:L+1}}(y_0, y_1) f_{\Gamma_{L_c:L+1}|\Gamma_{L_c:L}<\gamma_T}(y_1) dy_1, \qquad (3.8)$$

we can express the conditional PDF in (3.7), for the general value of $L_a\,(\geq 2)$, as

$$\begin{aligned} &f_{\Gamma_{L_c:L+L_a}|\Gamma_{L_c:L}<\gamma_T}(y_0) \\ &= \underbrace{\int_0^\infty \cdots \int_0^\infty}_{L_a-1\,\text{folds}} \prod_{j=L+1}^{L+L_a-1} f_{\Gamma_{L_c:j+1},\Gamma_{L_c:j}}(y_{L+L_a-j-1}, y_{L+L_a-j}) \\ &\qquad \times f_{\Gamma_{L_c:L+1}|\Gamma_{L_c:L}<\gamma_T}(y_{L_a-1}) dy_1 \cdots dy_{L_a-1}. \end{aligned} \tag{3.9}$$

Even though the joint PDFs and the conditional PDF in (3.9) are available in closed-form using some results that will be shown in what follows, the resulting expressions are complicated and quite tedious to obtain. Here, we rather use in what follows another approximate approach which leads to results that are very close to the exact solutions as we will demonstrate it by computer simulations in Section III.D.

Going back to Eq. (3.7) and based on the derivations in Appendix A, we can show that $\Pr\left[\gamma_T \leq \Gamma_{L_c:L+L_a} < x, \Gamma_{L_c:L} < \gamma_T\right]$ can be expressed approximately as

$$\begin{aligned} &\Pr\left[\gamma_T \leq \Gamma_{L_c:L+L_a} < x, \Gamma_{L_c:L} < \gamma_T\right] \\ &= \Pr\left[\gamma_T \leq \Gamma_{L_c:L+L_a} < x\right] - \frac{1-\Pr[\Gamma_{L_c:L} < \gamma_T]}{1-\Pr[\Gamma_{L_c:L+L_a-1} < \gamma_T]} \\ &\quad \times \left(\Pr\left[\gamma_T \leq \Gamma_{L_c:L+L_a} < x\right] - \Pr\left[\gamma_T \leq \Gamma_{L_c:L+L_a} < x, \Gamma_{L_c:L+L_a-1} < \gamma_T\right]\right). \end{aligned} \tag{3.10}$$

Substitution (3.10) into (3.6) gives the CDF of $\gamma_t$, $F_{\gamma_t}(x)$, as

$$\begin{aligned} &F_{\gamma_t}(x) \\ &= \begin{cases} \Pr\left[\Gamma_{L_c:L+L_a} < x\right], & 0 \leq x < \gamma_T; \\ \Pr\left[\gamma_T \leq \Gamma_{L_c:L} < x\right] + \Pr[\Gamma_{L_c:L+L_a} < \gamma_T] & \\ + \Pr[\gamma_T \leq \Gamma_{L_c:L+L_a} < x] - \frac{1-\Pr[\Gamma_{L_c:L} < \gamma_T]}{1-\Pr[\Gamma_{L_c:L+L_a-1} < \gamma_T]} & \\ \times \left(\Pr[\gamma_T \leq \Gamma_{L_c:L+L_a} < x] - \mathcal{J}(x)\right), & x \geq \gamma_T, \end{cases} \end{aligned} \tag{3.11}$$

where

$$\mathcal{J}(x) = \Pr\left[\gamma_T \leq \Gamma_{L_c:L+L_a} < x, \Gamma_{L_c:L+L_a-1} < \gamma_T\right]. \tag{3.12}$$

Although (3.11) looks more complicate than (3.6), it actually leads to the desired final result, as we show in what follows. Since for i.i.d. Rayleigh fading channels, all probabilities, Pr[·], in (3.11) can be easily obtained by using the well-known CDF of the GSC output SNR [5, Eq. (9.440)], we just need to derive a closed-form expression for $\mathcal{J}(x)$ in (3.12). This joint probability can be expressed as

$$\begin{aligned} &\Pr\left[\gamma_T \leq \Gamma_{L_c:L+L_a} < x, \Gamma_{L_c:L+L_a-1} < \gamma_T\right] \\ &= \Pr\left[\gamma_T \leq \Gamma_{L_c-1:L+L_a-1} + \gamma_{L+L_a} < x, \Gamma_{L_c-1:L+L_a-1} + \gamma_{L_c:L+L_a-1} < \gamma_T\right]. \end{aligned} \tag{3.13}$$

Since all branch SNRs are i.i.d. random variables, $\gamma_{L+L_a}$ is independent of both $\Gamma_{L_c-1:L+L_a-1}$ and $\gamma_{L_c:L+L_a-1}$. As such, we can compute the joint probability in (3.13) by using the joint PDF of $\Gamma_{L_c-1:L+L_a-1}$ and $\gamma_{L_c:L+L_a-1}$, $f_{\gamma_{L_c:L+L_a-1},\Gamma_{L_c-1:L+L_a-1}}(y,z)$, and the single-branch CDF of $\gamma_{L+L_a}$, $F_{\gamma_{L+L_a}}(\cdot)$, given in (3.2), as

$$\begin{aligned} &\Pr\left[\gamma_T \leq \Gamma_{L_c:L+L_a} < x, \Gamma_{L_c:L+L_a-1} < \gamma_T\right] \\ &= \int_0^{\frac{\gamma_T}{L_c}} \int_{(L_c-1)y}^{\gamma_T - y} f_{\gamma_{L_c:L+L_a-1},\Gamma_{L_c-1:L+L_a-1}}(y,z) \\ &\quad \times (F_{\gamma_{L+L_a}}(x-z) - F_{\gamma_{L+L_a}}(\gamma_T - z)) dz dy. \end{aligned} \tag{3.14}$$

For i.i.d. Rayleigh fading channels, it has been shown in [22, Eq. (9)] that the joint PDF in (3.14) is given by

$$\begin{aligned} &f_{\gamma_{L_c:L+L_a-1},\Gamma_{L_c-1:L+L_a-1}}(y,z) \\ &= \sum_{t=0}^{L+L_a-L_c-1} \frac{(-1)^t (L+L_a-1)!(z-(L_c-1)y)^{L_c-2}}{(L+L_a-L_c-1-t)!(L_c-1)!(L_c-2)!t!\overline{\gamma}^{L_c}} e^{-\frac{z+(t+1)y}{\overline{\gamma}}}, \\ &\qquad y \geq 0, z \geq (L_c-1)y. \end{aligned} \tag{3.15}$$

After substitution (3.15) into (3.14) and integrations, we can obtain the closed-form

expression for $\mathcal{J}(x)$ as

$$\mathcal{J}(x) = \left(e^{-\frac{\gamma_T}{\overline{\gamma}}} - e^{-\frac{x}{\overline{\gamma}}}\right)\left(\frac{\gamma_T}{\overline{\gamma}}\right)^{L_c} \sum_{t=0}^{L+L_a-L_c-1} \sum_{u=0}^{L_c-1} \frac{(-1)^{t+u}\binom{L+L_a-1}{L_c, L+L_a-L_c-t-1, t}}{(L_c-u-1)!\left((t+1)\gamma_T/(\overline{\gamma}L_c)\right)^{u+1}} \times \left[1 - e^{-\frac{(t+1)\gamma_T}{\overline{\gamma}L_c}} \sum_{v=0}^{u} \left(\frac{(t+1)\gamma_T}{\overline{\gamma}L_c}\right)^{v} / v!\right], \tag{3.16}$$

where $\binom{A}{a_1, a_2, \cdots, a_n}$ is the multinomial coefficient, defined as $\binom{A}{a_1, a_2, \cdots, a_n} = \frac{A!}{a_1! a_2! \cdots a_n!}$, $A = \sum_{w=1}^{n} a_w$. Hence, we can obtain the closed-form expression for the CDF of $\gamma_t$ by substituting (3.16) in (3.11).

## 2. PDF

Differentiation of (3.11) gives the PDF of $\gamma_t$, $f_{\gamma_t}(x)$, as

$$f_{\gamma_t}(x) = \begin{cases} f_{\Gamma_{L_c:L+L_a}}(x), & 0 \le x < \gamma_T; \\ f_{\Gamma_{L_c:L}}(x) + f_{\Gamma_{L_c:L+L_a}}(x) & \\ \quad - \frac{1-F_{\Gamma_{L_c:L}}(\gamma_T)}{1-F_{\Gamma_{L_c:L+L_a-1}}(\gamma_T)} \left(f_{\Gamma_{L_c:L+L_a}}(x) - \mathcal{I}(x)\right), & x \ge \gamma_T, \end{cases} \tag{3.17}$$

where

$$\mathcal{I}(x) = \frac{d}{dx}\mathcal{J}(x) = \frac{1}{\overline{\gamma}} e^{-\frac{x}{\overline{\gamma}}} \left(\frac{\gamma_T}{\overline{\gamma}}\right)^{L_c} \sum_{t=0}^{L+L_a-L_c-1} \sum_{u=0}^{L_c-1} \frac{(-1)^{t+u}\binom{L+L_a-1}{L_c, L+L_a-L_c-t-1, t}}{(L_c-u-1)!\left((t+1)\gamma_T/(\overline{\gamma}L_c)\right)^{u+1}} \times \left[1 - e^{-\frac{(t+1)\gamma_T}{\overline{\gamma}L_c}} \sum_{v=0}^{u} \left(\frac{(t+1)\gamma_T}{\overline{\gamma}L_c}\right)^{v} / v!\right]. \tag{3.18}$$

For i.i.d. Rayleigh fading channels, $f_{\Gamma_{i:j}}(x)$ and $F_{\Gamma_{i:j}}(x)$ are the well-known PDF and CDF of $i/j$-GSC output SNR, respectively, which can be found in [5, Eqs.

(9.433)(9.440)] as

$$f_{\Gamma_{i:j}}(x) = \binom{j}{i}\left[\frac{x^{i-1}e^{-x/\overline{\gamma}}}{\overline{\gamma}^{i}(i-1)!} + \frac{1}{\overline{\gamma}}\sum_{l=1}^{j-i}(-1)^{i+l-1}\binom{j-i}{l}\left(\frac{i}{l}\right)^{i-1}e^{-x/\overline{\gamma}}\right. \tag{3.19}$$
$$\left.\times\left(e^{-lx/(i\overline{\gamma})} - \sum_{m=0}^{i-2}\frac{1}{m!}\left(\frac{-lx}{i\overline{\gamma}}\right)^{m}\right)\right]$$

and

$$F_{\Gamma_{i:j}}(x) = \binom{j}{i}\left\{1 - e^{-x/\overline{\gamma}}\sum_{l=0}^{i-1}\frac{(x/\overline{\gamma})^{l}}{l!} + \sum_{l=1}^{j-i}(-1)^{i+l-1}\binom{j-i}{l}\left(\frac{i}{l}\right)^{i-1}\right. \tag{3.20}$$
$$\left.\times\left[\frac{1-e^{-(1+l/i)(x/\overline{\gamma})}}{1+l/i} - \sum_{m=0}^{i-2}\left(\frac{-l}{i}\right)^{m}\left(1 - e^{-x/\overline{\gamma}}\sum_{k=0}^{m}\frac{(x/\overline{\gamma})^{k}}{k!}\right)\right]\right\}.$$

### 3. MGF

Substituting (3.18), (3.19), and (3.20) into (3.17) leads to the desired closed-form expression for the PDF of the proposed scheme. With this PDF in hand, the MGF of $\gamma_t$, $\mathcal{M}_{\gamma_t}(s) = \int_0^\infty e^{sx} f_{\gamma_t}(x)dx$, can be obtained in closed-form after lengthy and tedious calculations as

$$\mathcal{M}_{\gamma_t}(s) = A(L_c : L + L_a, 0, s) + A(L_c : L, \gamma_T, s) \tag{3.21}$$
$$-\frac{1 - B(L_c : L, \gamma_T)}{1 - B(L_c : L + L_a - 1, \gamma_T)}\left(A(L_c : L + L_c, \gamma_T, s) - C(\gamma_T, s)\right),$$

where

$$A(i : j, k, s) = \int_k^\infty e^{sx} f_{\Gamma_{i:j}}(x)dx \tag{3.22}$$
$$= \binom{j}{i}\left[\frac{\Gamma\left[i, (1-s\overline{\gamma})k/\overline{\gamma}\right]}{(i-1)!(1-s\overline{\gamma})^{i}} + \sum_{l=1}^{j-i}(-1)^{i+l-1}\binom{j-i}{l}\left(\frac{i}{l}\right)^{i}\right.$$
$$\left.\times\left(\frac{e^{k\left(s-\frac{1}{\overline{\gamma}}-\frac{l}{i\overline{\gamma}}\right)}}{1+i(1-s\overline{\gamma})/l} + \sum_{m=0}^{i-2}\left(\frac{l}{i(s\overline{\gamma}-1)}\right)^{m+1}\frac{\Gamma\left[m+1, (1-s\overline{\gamma})k/\overline{\gamma}\right]}{m!}\right)\right],$$

$$B(i:j,k) = F_{\Gamma_{i:j}}(k) = \int_0^k f_{\Gamma_{i:j}}(x)dx \tag{3.23}$$
$$= \binom{j}{i}\left[\frac{\gamma\left[i, k/\overline{\gamma}\right]}{(i-1)!} + \sum_{l=1}^{j-i}(-1)^{i+l-1}\binom{j-i}{l}\left(\frac{i}{l}\right)^i \times\left(\frac{1-e^{-\left(1+\frac{l}{i}\right)\frac{k}{\overline{\gamma}}}}{(1+i/l)} - \sum_{m=0}^{i-2}(-1)^m\left(\frac{l}{i}\right)^{m+1}\frac{\gamma\left[m+1, k/\overline{\gamma}\right]}{m!}\right)\right],$$

and

$$C(k,s) = \int_k^\infty e^{sx}\mathcal{I}(x)dx \tag{3.24}$$
$$= \frac{e^{k\left(s-\frac{1}{\overline{\gamma}}\right)}}{1-s\overline{\gamma}}\left(\frac{\gamma_T}{\overline{\gamma}}\right)^{L_c}\sum_{t=0}^{L+L_a-L_c-1}\sum_{u=0}^{L_c-1}\frac{(-1)^{t+u}\binom{L+L_a-1}{L_c, L+L_a-L_c-t-1, t}}{(L_c-u-1)!\left((t+1)\gamma_T/(\overline{\gamma}L_c)\right)^{u+1}} \times\left[1-e^{-\frac{(t+1)\gamma_T}{\overline{\gamma}L_c}}\sum_{v=0}^{u}\left(\frac{(t+1)\gamma_T}{\overline{\gamma}L_c}\right)^v/v!\right],$$

where $\Gamma[\cdot,\cdot]$ and $\gamma[\cdot,\cdot]$ are the upper and lower incomplete gamma functions, respectively, defined as [31, Eq. (8.350)]

$$\Gamma[\alpha,\beta] = \int_\beta^\infty e^{-t}t^{\alpha-1}dt, \qquad \gamma[\alpha,\beta] = \int_0^\beta e^{-t}t^{\alpha-1}dt. \tag{3.25}$$

## D. Average BER

In this section, we apply the closed-form results from the previous section for the performance analysis of our proposed combining scheme over Rayleigh fading channels. More specifically, we first examine its average bit error rate (BER) by using the well-known MGF-based approach [5, Sec. 9.2.3]. For example, the average BER of binary phase shift keying (BPSK) signals is given by

$$P_B(E) = \frac{1}{\pi}\int_0^{\pi/2}\mathcal{M}_{\gamma_t}\left(\frac{-1}{\sin^2\phi}\right)d\phi. \tag{3.26}$$

First, we consider the relationship between the number of resolvable paths from the serving BS and the average BER performance. In Fig. 1, the average BER of

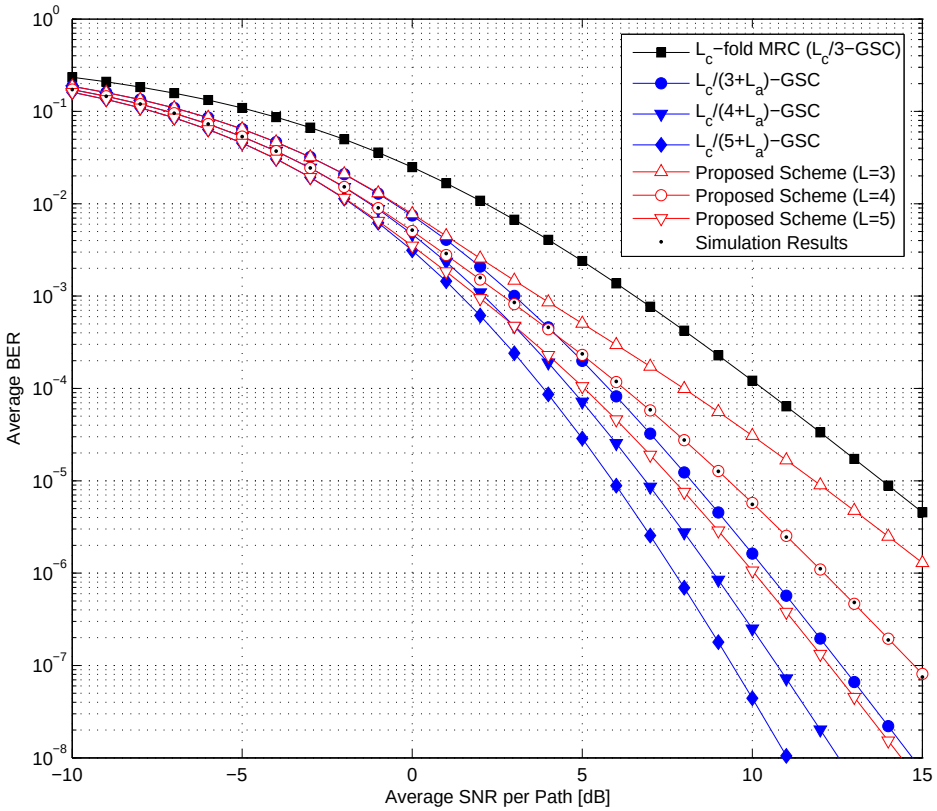


Fig. 1. Average BER of BPSK versus the average SNR per path, $\overline{\gamma}$, with MRC, GSC, and the proposed scheme for various values of $L$ over i.i.d. Rayleigh fading channels when $L_c = 3, L_a = 2$, and $\gamma_T = 5$ dB.

BPSK versus the average SNR per path, $\overline{\gamma}$, of the proposed scheme for various values of $L$ over i.i.d. Rayleigh fading channels is plotted. For comparison purpose, we also plot the average BER of BPSK with $L_c$-MRC and $L_c/(L + L_a)$-GSC. In this graph, we set $L_c = 3, L_a = 2$, and $\gamma_T = 5$ dB. The simulation result for the case of $L = 4$ shows that our alternative simple approach is indeed a good approximation[4]. It is

[4]We note that all other numerical evaluations obtained from the analytical results derived here have been also compared by Monte Carlo simulations of the system under consideration in order to justify our approach.

clear from this figure that our proposed scheme always outperforms MRC. Also it is very interesting to note that when the channel condition is poor, i.e, $\overline{\gamma}$ is relatively small compared to $\gamma_T$, our scheme has the same error performance as GSC. This behavior can be explained as follows. When $\overline{\gamma}$ is small compared to $\gamma_T$, our proposed scheme acts most of the times as $L_c/(L+L_a)$-GSC since $L_c/L$-GSC output SNR has a high chance of not exceeding the required target SNR. On the other hand, in good channel conditions, our scheme shows a higher error probability. This is because when $\overline{\gamma}$ becomes larger, the combined SNR of $L_c/L$-GSC has a higher chance to exceed the target SNR, $\gamma_T$, and as such, does not need to rely on the additional resolvable paths from the target BS. Hence, we can conclude that our proposed combiner relies on the additional resources provided by the target BS only in poor channel conditions. For a better understanding of our scheme, we study when $L$ is fixed and $L_a$ is variable in what follows.

Fig. 2 shows the average BER of BPSK with MRC, GSC, and the proposed combining scheme versus the average SNR per path, $\overline{\gamma}$, for various values of $L_a$ over i.i.d. Rayleigh fading channels when $L = 4$, $L_c = 3$, and $\gamma_T = 5$ dB. Similar trends to those observed in Fig. 1 can also be seen in this figure, but since $L$ is fixed, as one expects intuitively, all the curves of our proposed scheme are converging to the case of $L_c$/4-GSC in the higher average SNR region.

We now study the average BER dependence on the threshold SNR, $\gamma_T$. Fig. 3 represents the average BER of BPSK versus the average SNR per path, $\overline{\gamma}$, with MRC, GSC, and the proposed scheme for various values of $\gamma_T$ over i.i.d. Rayleigh fading channels when $L = 4, L_c = 3$, and $L_a = 2$. From this figure, it is clear that the higher the threshold, the better the performance, as one expects. However, high thresholds increase the path estimation load. We examine in what follows this issue in details.

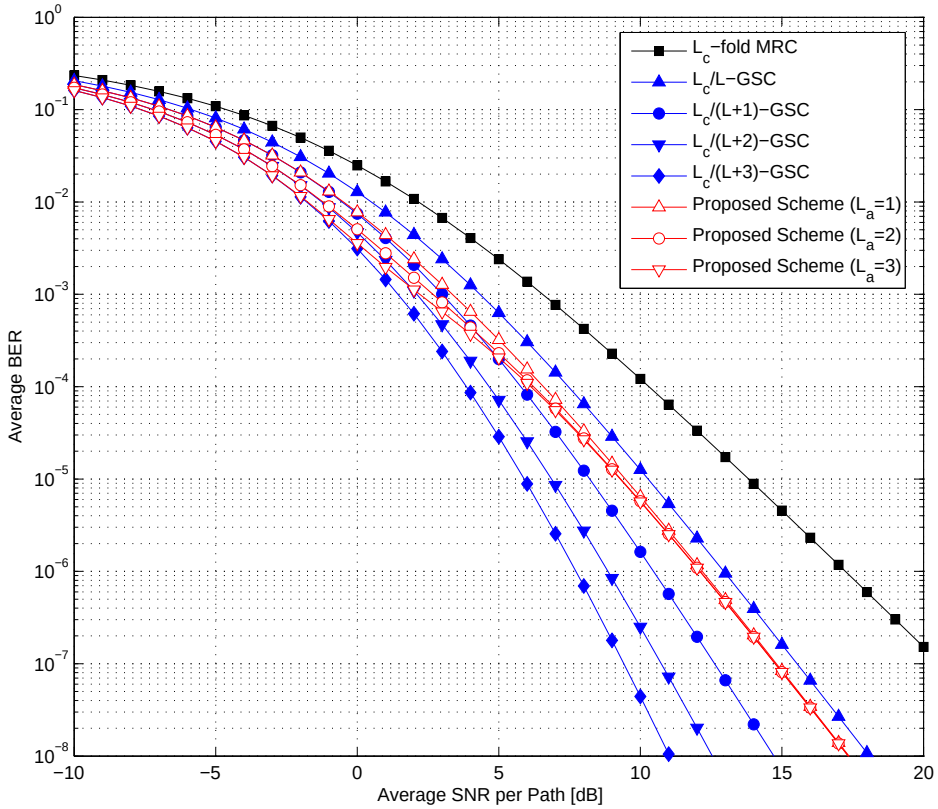


Fig. 2. Average BER of BPSK versus the average SNR per path, $\overline{\gamma}$, with MRC, GSC, and the proposed scheme for various values of $L_a$ over i.i.d. Rayleigh fading channels when $L = 4, L_c = 3$, and $\gamma_T = 5$ dB.

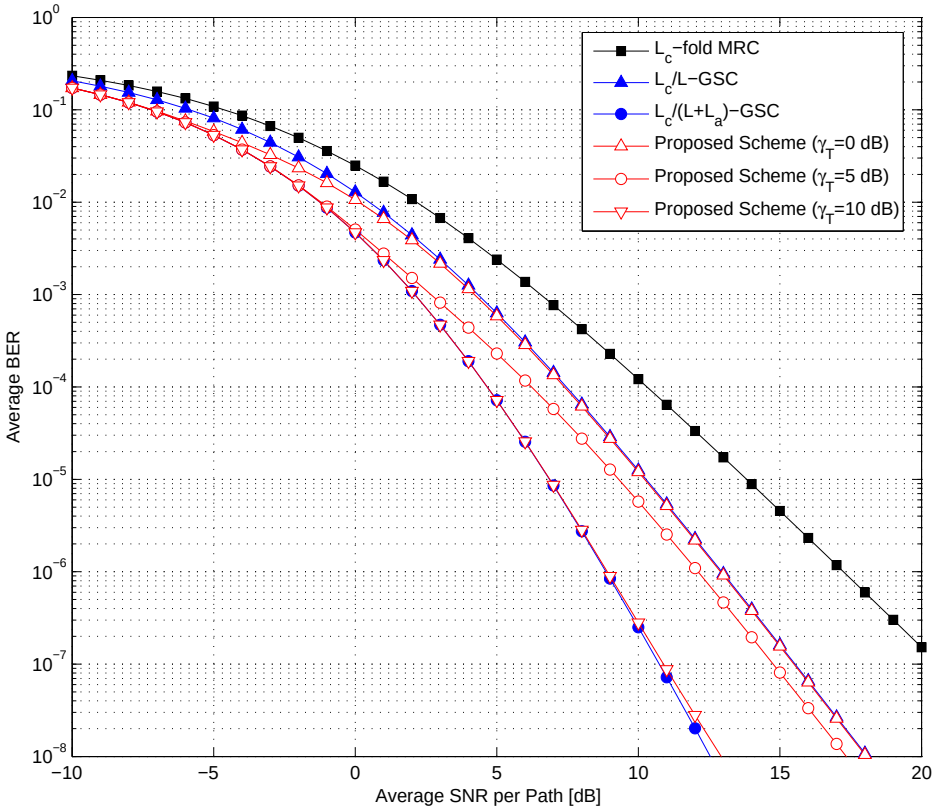


Fig. 3. Average BER of BPSK versus the average SNR per path, $\overline{\gamma}$, with MRC, GSC, and the proposed scheme for various values of $\gamma_T$ over i.i.d. Rayleigh fading channels when $L = 4, L_c = 3$, and $L_a = 2$.

## E. Complexity Comparison

In this section, we look into the average number of path estimations and the SHO overhead it requires.

### 1. Average Number of Path Estimations

With the proposed scheme, the RAKE receiver estimates $L$ paths in the case of $\Gamma_{L_c:L} \geq \gamma_T$ or $L + L_a$ in the case of $\Gamma_{L_c:L} < \gamma_T$. Hence, we can easily quantify the average number of path estimations, denoted by $N_E$, as

$$N_E = L \cdot \Pr\left[\Gamma_{L_c:L} \geq \gamma_T\right] + (L + L_a) \cdot \Pr\left[\Gamma_{L_c:L} < \gamma_T\right], \tag{3.27}$$

which reduces to

$$N_E = L + L_a \cdot F_{\Gamma_{L_c:L}}(\gamma_T), \tag{3.28}$$

where $F_{\Gamma_{L_c:L}}(\gamma_T)$ can be calculated from (3.23) for i.i.d. Rayleigh fading channels. Note that $L_c$-MRC and $L_c/(L + L_a)$-GSC always require $L_c$ and $L + L_a$ estimations, respectively. Fig. 4 shows the average number of path estimations versus the output threshold, $\gamma_T$, with MRC, GSC, and the proposed scheme for various values of $L_a$ over i.i.d. Rayleigh fading channels when $L = 4$, $L_c = 3$, and $\overline{\gamma} = 0$ dB. For a better illustration of the tradeoff between complexity and performance, Fig. 5 shows the average BER of BPSK versus the output threshold, $\gamma_T$, with MRC, GSC, and the proposed scheme. As we can see, the error rate of the proposed scheme decreases to that of $L_c/(L + L_a)$-GSC when the output threshold increases. Considering Figs. 4 and 5 together, we observe that the proposed scheme can save a certain amount of estimation load with a slight performance loss compared to GSC if the required threshold is 2 to 6 dB above $\overline{\gamma}$ for our chosen set of parameters.

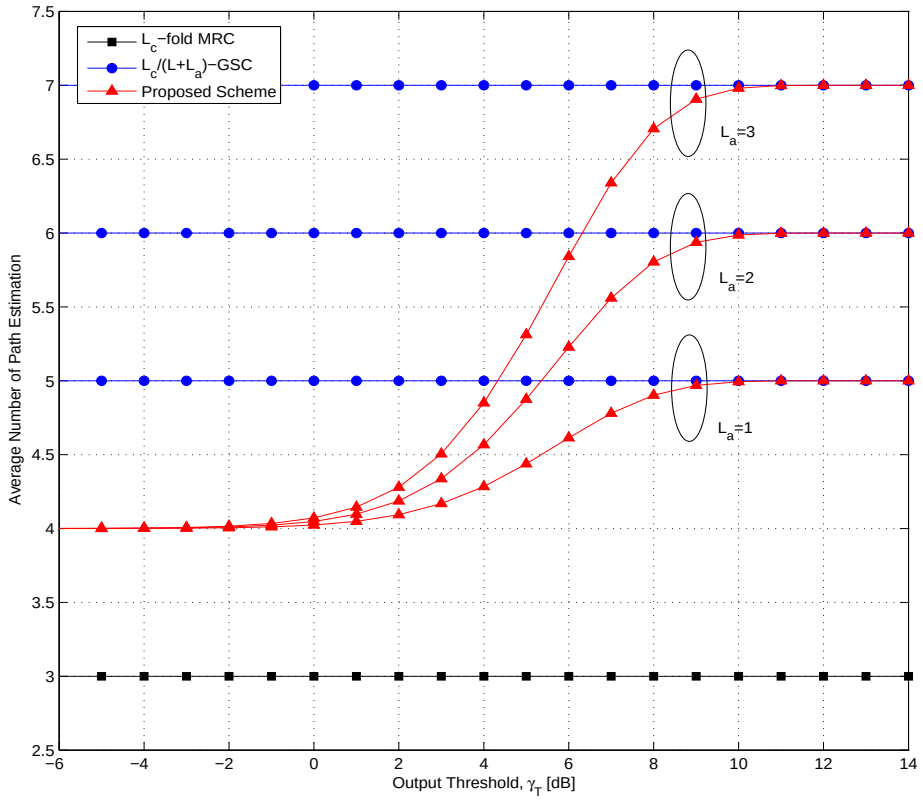


Fig. 4. Average number of path estimations versus the output threshold, $\gamma_T$, with MRC, GSC, and the proposed scheme for various values of $L_a$ over i.i.d. Rayleigh fading channels when $L = 4, L_c = 3$, and $\overline{\gamma} = 0$ dB.

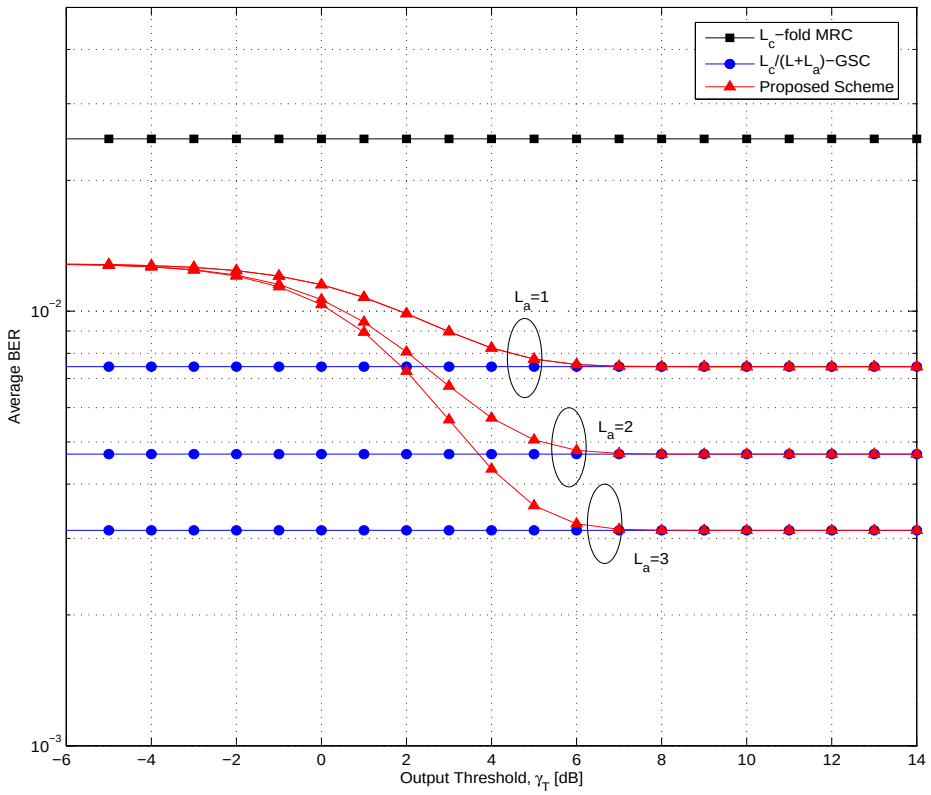


Fig. 5. Average BER of BPSK versus the output threshold, $\gamma_T$, with MRC, GSC, and the proposed scheme for various values of $L_a$ over i.i.d. Rayleigh fading channels with $L = 4, L_c = 3$, and $\overline{\gamma} = 0$ dB.

### 2. SHO Overhead

In this subsection, we investigate the probability of the SHO attempt and the SHO overhead. In our proposed scheme, the SHO is attempted whenever $\Gamma_{L_c:L}$ is below $\gamma_T$. Hence, the probability of the SHO attempt is same as the outage probability of $L_c/L$-GSC evaluated at $\gamma_T$, i.e., $F_{\Gamma_{L_c:L}}(\gamma_T)$. The SHO overhead, denoted by $\beta$, is commonly used to quantify the SHO activity in a network and is defined as [30, Eq. (9.2)]

$$\beta = \sum_{n=1}^{N} nP_n - 1, \tag{3.29}$$

where $N$ is the number of active BSs and $P_n$ is the average probability that the mobile unit uses $n$-way SHO.

#### a. $L_a < L_c$

Based on the mode of operation in Section III.B.2 in Page 12, $P_1$ and $P_2$ can be defined as

$$P_1 = \Pr\left[\Gamma_{L_c:L} \geq \gamma_T\right] + \Pr\left[\Gamma_{L_c:L} < \gamma_T, \gamma_{L_c:L} \geq \gamma_{1:L_a}\right], \tag{3.30}$$

and

$$P_2 = 1 - P_1, \tag{3.31}$$

where $\gamma_{L_c:L}$ is the $L_c$th strongest path among $L$ ones from the serving BS and $\gamma_{1:L_a}$ is the strongest path among $L_a$ ones from the target BS. Substituting (3.30) and (3.31) into (3.29), we can express the SHO overhead, $\beta$, as

$$\begin{aligned} \beta &= P_1 + 2P_2 - 1 \\ &= F_{\Gamma_{L_c:L}}(\gamma_T) \Pr\left[\gamma_{L_c:L} < \gamma_{1:L_a} | \Gamma_{L_c:L} < \gamma_T\right]. \end{aligned} \tag{3.32}$$

Since $\gamma_{1:L_a}$ is independent to $\gamma_{Lc:L}$ and $\Gamma_{Lc:L}$, we can calculate the conditional probability, $\Pr\left[\gamma_{L_c:L} < \gamma_{1:L_a} | \Gamma_{L_c:L} < \gamma_T\right]$, as

$$\Pr\left[\gamma_{L_c:L} < \gamma_{1:L_a} | \Gamma_{L_c:L} < \gamma_T\right] = \int_0^\infty F_{\gamma_{L_c:L}|\Gamma_{L_c:L}<\gamma_T}(x) f_{\gamma_{1:L_a}}(x) dx. \tag{3.33}$$

The conditional CDF in (3.33) can be written as

$$\begin{aligned} F_{\gamma_{L_c:L}|\Gamma_{L_c:L}<\gamma_T}(x) &= \frac{\Pr\left[\gamma_{L_c:L} < x, \Gamma_{L_c:L} < \gamma_T\right]}{\Pr\left[\Gamma_{L_c:L} < \gamma_T\right]} \\ &= \frac{\Pr\left[\gamma_{L_c:L} < x, \Gamma_{L_c-1:L} + \gamma_{L_c:L} < \gamma_T\right]}{\Pr\left[\Gamma_{L_c:L} < \gamma_T\right]} \\ &= \frac{1}{F_{\Gamma_{L_c:L}}(\gamma_T)} \begin{cases} \int_0^x \int_{(L_c-1)y}^{\gamma_T - y} f_{\gamma_{L_c:L}, \Gamma_{L_c-1:L}}(y,z) dz dy, & 0 \le x < \frac{\gamma_T}{L_c}; \\ \int_0^{\gamma_T/L_c} \int_{(L_c-1)y}^{\gamma_T - y} f_{\gamma_{L_c:L}, \Gamma_{L_c-1:L}}(y,z) dz dy, & x \ge \frac{\gamma_T}{L_c}, \end{cases} \end{aligned} \tag{3.34}$$

where $f_{\gamma_{L_c:L}, \Gamma_{L_c-1:L}}(y,z)$ can be obtained from (3.15). After successive substitutions from (3.34) to (3.32), we can express the SHO overhead, $\beta$, as

$$\begin{aligned} \beta = &\int_0^{\frac{\gamma_T}{L_c}} \left( f_{\gamma_{1:L_a}}(x) \int_0^x \int_{(L_c-1)y}^{\gamma_T - y} f_{\gamma_{L_c:L}, \Gamma_{L_c-1:L}}(y,z) dz dy \right) dx \\ &+ \left[ 1 - F_{\gamma_{1:L_a}} \left( \frac{\gamma_T}{L_c} \right) \right] \int_0^{\frac{\gamma_T}{L_c}} \int_{(L_c-1)y}^{\gamma_T - y} f_{\gamma_{L_c:L}, \Gamma_{L_c-1:L}}(y,z) dz dy. \end{aligned} \tag{3.35}$$

Finally, by integrating (3.35), we can obtain the exact closed-from expression for the SHO overhead, $\beta$, which is given in Appendix B.

b. $L_a \ge L_c$

In this case, we need to consider the probability that a call is completely handed over to the target BS. Hence, the joint probability, $\Pr[\Gamma_{L_c:L} < \gamma_T, \gamma_{1:L} \le \gamma_{L_c:L_a}]$, should be added to $P_1$ in (3.30) where $\gamma_{1:L}$ is the strongest path among $L$ ones from the serving BS and $\gamma_{L_c:L_a}$ is the $L_c$th strongest path among $L_a$ ones from the target BS. This

joint probability is given by the following analytical expression

$$\begin{aligned}
&\Pr[\Gamma_{L_c:L} < \gamma_T, \gamma_{1:L} \le \gamma_{L_c:L_a}] \qquad (3.36)\\
&= \int_0^{\infty} \int_0^{\min[\gamma_T, \gamma_{L_c:L_a}]} \int_0^{\min[\gamma_T - \gamma_{1:L}, \gamma_{1:L}]} \int_0^{\min[\gamma_T - \gamma_{1:L} - \gamma_{2:L}, \gamma_{2:L}]} \\
&\quad \cdots \int_0^{\min[\gamma_T - \sum_{j=1}^{L_c-1} \gamma_{j:L}, \gamma_{L_c-1:L}]} f_{\gamma_{L_c:L_a}}(\gamma_{L_c:L_a}) \\
&\quad \times f_{\gamma_{1:L}, \gamma_{2:L}, \gamma_{3:L}, \cdots, \gamma_{L_c:L}}(\gamma_{1:L}, \gamma_{2:L}, \gamma_{3:L}, \cdots, \gamma_{L_c:L}) d\gamma_{1:L} d\gamma_{2:L} d\gamma_{3:L} \cdots d\gamma_{L_c:L} d\gamma_{L_c:L_a},
\end{aligned}$$

where $f_{\gamma_{1:L}, \gamma_{2:L}, \gamma_{3:L}, \cdots, \gamma_{L_c:L}}(\cdots)$ is the joint PDF of the first $L_c$ order statistics out of $L$ ones [5, Eq. (9.420)]. Unfortunately, it seems difficult to obtain a simple close-form expression for this nested $L_c + 1$ multi-fold integral.

Fig. 6 shows the SHO overhead versus the output threshold, $\gamma_T$, with GSC and the proposed scheme for various values of $L_a$ over i.i.d. Rayleigh fading channels when $L = 4, L_c = 3$, and $\overline{\gamma} = 0$ dB. The SHO overhead of $L_c/(L + L_a)$-GSC is plotted by calculating $P_1$ and $P_2$ as

$$P_1 = \begin{cases} \Pr\left[\gamma_{L_c:L} \ge \gamma_{1:L_a}\right], & L_a < L_c; \\ \Pr\left[\gamma_{L_c:L} \ge \gamma_{1:L_a}\right] + \Pr[\gamma_{1:L} \le \gamma_{L_c:L_a}], & L_a \ge L_c, \end{cases} \qquad (3.37)$$

and

$$P_2 = 1 - P_1. \qquad (3.38)$$

It is clear from this figure that we have a higher chance to use 2-way SHO, as the number of additional paths from the target BS increases. Note that our proposed scheme acts as $L_c/(L + L_a)$-GSC when the output threshold is very high. Hence, we can observe that the SHO overhead of the proposed scheme converges to that of GSC as $\gamma_T$ increases. From this figure together with Fig. 5, we can see the SHO overhead reduction of our proposed scheme. For example, if the required threshold is 6 dB above $\overline{\gamma}$, our scheme shows for $L_a = 2$ around 0.55 SHO overhead while maintaining

the same error rate as GSC which requires 0.8 SHO overhead.

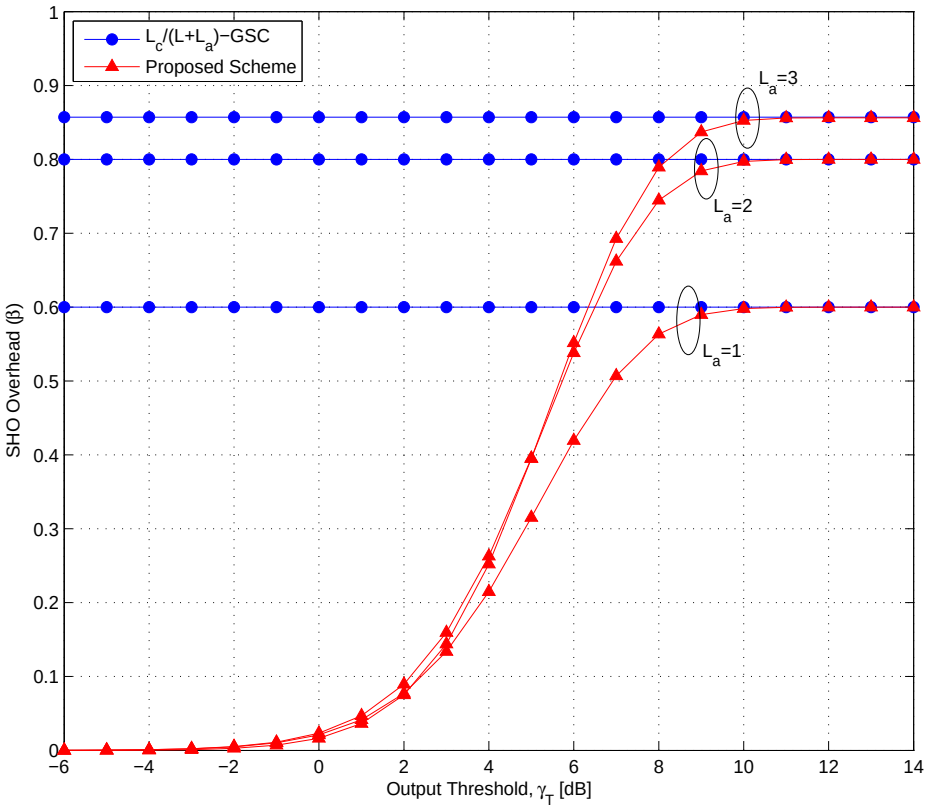


Fig. 6. SHO overhead versus the output threshold, $\gamma_T$, with GSC and the proposed scheme for various values of $L_a$ over i.i.d. Rayleigh fading channels with $L = 4, L_c = 3$, and $\overline{\gamma} = 0$ dB.

## F. Conclusion

In this chapter, we proposed a new finger assignment scheme for RAKE receivers in the SHO region. In this scheme, the receiver checks the GSC output SNR from the serving BS against a certain pre-determined output threshold. If the output SNR is below this threshold, the receiver performs a finger reassignment after using GSC on

the paths coming from the serving BS and the target BS. We derived the statistics of the output SNR of the proposed scheme in accurate approximate closed-form, based on which we carried out the performance analysis of the resulting systems. We showed through numerical examples that the new scheme offers commensurate performance in comparison with more complicated GSC-based diversity systems while requiring a smaller estimation load and SHO overhead.

# CHAPTER IV

# FINGER REASSIGNMENT SCHEME WITH MULTIPLE BASE STATIONS

## A. Introduction

In this chapter, we generalize the scheme proposed in Chapter III to the multi-BS situation. We propose two assignment schemes denoted as *the full scanning scheme* and *the sequential scanning scheme*. For the full scanning scheme, whenever the GSC output SNR of the paths from the serving BS is below a certain pre-determined SNR threshold (known as a target SNR), the RAKE receiver scans all the available paths from all the target BSs while for the sequential scanning scheme, the RAKE receiver sequentially scans the target BSs until the combined SNR is satisfactory or all target BSs are scanned.

We provide an analytical framework deriving the statistics of the receiver output SNR of our proposed schemes, including the CDF, PDF, and MGF of the output SNR. In our derivations, we specifically tackle the statistics of the output SNR which is the sum of correlated GSC output SNRs. These results are then used first to analyze the performance in terms of the average probability of error and then to investigate the tradeoff between complexity and performance by quantifying the average number of path estimations, the average number of SNR comparisons, and the SHO overhead versus the target SNR.

The remainder of this chapter is organized as follows. In Section IV.B, we present the channel and system model under consideration as well as the mode of operation of the proposed schemes. Based on this mode of operation, we derive the expressions for the statistics of the combined SNR in Section IV.C. These results are next applied to the average BER performance analysis of the proposed systems in Section IV.D.

Section IV.E illustrates the tradeoff of complexity versus performance by comparing the average number of path estimations, the average number of SNR comparisons, and the SHO overhead of our proposed systems to that of conventional GSC and MRC. Finally, Section IV.F provides some concluding remarks.

## B. System Model

### 1. System and Channel Model

Let $\gamma_j$ denote the instantaneous received SNR of the $j$th resolvable path, where $j = 1, 2, \cdots, \sum_{i=1}^{N} L_i$, $L_i$ is the number of resolvable paths from $i$th BS, and $N$ is the number of available BSs in the SHO region. By following the same channel model described in Section III.B.1 in Page 11, we assume the average signal strength on a path from BSs is the same and the received signals on all the resolvable paths from the serving and the target BSs experience i.i.d. Rayleigh fading[1]. Then, the faded SNR, $\gamma_j$, follows the same exponential distribution with common PDF and CDF given in (3.1) and (3.2), respectively.

We also consider systems that employ a RAKE receiver with GSC. We assume that the RAKE receiver has $L_c$ fingers and, in the SHO region, depending on the channel conditions only $L_c$ paths among $L_{(k)}$ paths are used for RAKE reception where $L_{(k)} = \sum_{i=1}^{k} L_i$ and $1 \leq k \leq N$. Then, the total received SNR after GSC is given by $\Gamma_{L_c:L_{(k)}}$ where $\Gamma_{i:j}$ is the sum of the $i$ largest SNRs among $j$ ones, i.e., $\Gamma_{i:j} = \sum_{k=1}^{i} \gamma_{k:j}$ where $\gamma_{k:j}$ is the $k$th order statistics (see [18] for terminology).

[1]In Chapter VII, more practical channel environments, such as non-identical/correlated fading channels and outdated channel estimation, are considered.

## 2. Mode of Operation

For convenience, let $L_1$ be the number of resolvable paths from the serving BS and $L_2$, $L_3$, $\cdots$, $L_N$ be those from the target BSs. Without loss of generality, we assume that at first the receiver relies only on $L_1$ resolvable paths and as such, starts with $L_c/L_1$-GSC. In the SHO region, the receiver compares the received SNR, $\Gamma_{L_c:L_1}$, with a certain target SNR, denoted by $\gamma_T$. If $\Gamma_{L_c:L_1}$ is greater than or equal to $\gamma_T$, a one-way SHO is used and no finger reassignment is needed. On the other hand, whenever $\Gamma_{L_c:L_1}$ falls below $\gamma_T$, a multi-way SHO[2] is attempted. More specifically, we consider two different finger assignment schemes described below[3].

### a. Case I - Full Scanning

In this case, when $\Gamma_{L_c:L_1} < \gamma_T$, the RAKE at once scans all possible $L_{(N)}$ resolvable paths from $N$ BSs and reassigns its $L_c$ fingers to the $L_c$ strongest paths among the $L_{(N)}$ available resolvable paths (i.e., the RAKE receiver uses $L_c/L_{(N)}$-GSC). Hence, the final combined SNR, denoted by $\gamma_{Full}$, is mathematically given by

$$\gamma_{Full} = \begin{cases} \Gamma_{L_c:L_1}, & \gamma_T \leq \Gamma_{L_c:L_1}; \\ \Gamma_{L_c:L_{(N)}}, & \Gamma_{L_c:L_1} < \gamma_T. \end{cases} \tag{4.1}$$

### b. Case II - Sequential Scanning

In this case, when $\Gamma_{L_c:L_1} < \gamma_T$, the RAKE receiver estimates $L_2$ paths from the first target BS which is randomly chosen and uses $L_c/L_{(2)}$-GSC. The receiver then checks whether the combined SNR, $\Gamma_{L_c:L_{(2)}}$, is above $\gamma_T$ or not. By sequentially adding the

[2]Multi-way SHO refers to the scenario in which the mobile unit is connected to the serving BS and the target BSs while being in the SHO region.

[3]In this work, we focus on macroscopic diversity techniques but possible joint micro/macroscopic diversity schemes can further reduce the usage of network resources.

remaining target BSs, this process is repeated until either the combined SNR, $\Gamma_{L_c:L_{(k)}}$, is above $\gamma_T$ or all the $L_{(N)}$ paths are examined. Based on this mode of operation, we can see that the final combined SNR, denoted by $\gamma_{Seq}$, is mathematically given by

$$\gamma_{Seq} = \begin{cases} \Gamma_{L_c:L_1}, & \gamma_T \leq \Gamma_{L_c:L_1}; \\ \Gamma_{L_c:L_{(2)}}, & \Gamma_{L_c:L_1} < \gamma_T \leq \Gamma_{L_c:L_{(2)}}; \\ \vdots & \vdots \\ \Gamma_{L_c:L_{(N-1)}}, & \Gamma_{L_c:L_{(N-2)}} < \gamma_T \leq \Gamma_{L_c:L_{(N-1)}}; \\ \Gamma_{L_c:L_{(N)}}, & \Gamma_{L_c:L_{(N-1)}} < \gamma_T. \end{cases} \tag{4.2}$$

Note that with the sequential scanning scheme, the receiver checks the paths from another BS only if the output SNR from the currently scanned BSs is below the threshold while with the full scanning scheme, the receiver always checks the paths from all the available BSs. Hence, we can expect that the sequential scanning scheme will lead to a reduction in complexity at the cost of performance gains. We will quantify this tradeoff later on in this chapter.

## C. Statistics of the Combined SNR

Although the mode of operations in (4.1) and (4.2) describe a scheme that essentially switches among $L_c/L_{(k)}$-GSC stages depending on the channel conditions and the output threshold, we can not obtain the statistics of $\gamma_{Full}$ and $\gamma_{Seq}$ directly from that of the output SNR with conventional GSC. Hence, in this section, we rely on some derived order statistics results in Chapter III to derive the statistics of the combined SNRs of $\gamma_{Full}$ and $\gamma_{Seq}$.

### 1. Case I - Full Scanning

Comparing (4.1) and (3.3), we can see that the results in Chapter III can be directly used. The key difference is that $L$ and $L+L_a$ in Chapter III have to be replaced here by $L_1$ and $L_{(N)}$, respectively.

### 2. Case II - Sequential Scanning

If we let $L_t$ be the number of total resolvable paths examined for the finger assignment, then applying the total probability theorem, we can write the CDF of combined SNR, $\gamma_{Seq}$, as

$$F_{\gamma_{Seq}}(x) = \Pr\left[\gamma_{Seq} < x\right] = \sum_{k=1}^{N} \Pr\left[\gamma_{Seq} < x, L_t = L_{(k)}\right]. \tag{4.3}$$

Note that based on the mode of operation in Section IV.B.2.b in Page 34, $L_{(k)}$ $(k < N)$ paths are examined if and only if the GSC-combined SNR of the first $L_{(k-1)}$ paths is less than $\gamma_T$ but the combined SNR of the first $L_{(k)}$ paths is greater than or equal to $\gamma_T$. In addition, if the combined SNR of $L_{(N-1)}$ paths is below $\gamma_T$, then $L_c/L_{(N)}$-GSC is used. Hence, the joint probability in (4.3) can be written as

$$\begin{aligned} &\Pr\left[\gamma_{Seq} < x, L_t = L_{(k)}\right] \\ &= \begin{cases} \Pr\left[\gamma_T \le \Gamma_{L_c:L_1} < x\right], & k = 1; \\ \Pr\left[\gamma_T \le \Gamma_{L_c:L_{(k)}} < x, \Gamma_{L_c:L_{(k-1)}} < \gamma_T\right], & 2 \le k \le N-1; \\ \Pr\left[\Gamma_{L_c:L_{(N)}} < x, \Gamma_{L_c:L_{(N-1)}} < \gamma_T\right], & k = N. \end{cases} \end{aligned} \tag{4.4}$$

Substituting (4.4) into (4.3), we can obtain the CDF of $\gamma_{Seq}$ as

$$\begin{aligned} F_{\gamma_{Seq}}(x) = \Pr\left[\gamma_T \le \Gamma_{L_c:L_1} < x\right] &+ \sum_{k=2}^{N-1} \Pr\left[\gamma_T \le \Gamma_{L_c:L_{(k)}} < x, \Gamma_{L_c:L_{(k-1)}} < \gamma_T\right] \\ &+ \Pr\left[\Gamma_{L_c:L_{(N)}} < x, \Gamma_{L_c:L_{(N-1)}} < \gamma_T\right]. \end{aligned} \tag{4.5}$$

Since it is clear that $\Gamma_{L_c:L_{(N-1)}} \leq \Gamma_{L_c:L_{(N)}}$, we can rewrite $\Pr[\Gamma_{L_c:L_{(N)}} < x, \Gamma_{L_c:L_{(N-1)}} < \gamma_T]$ in (4.5) as

$$\begin{aligned} &\Pr\left[\Gamma_{L_c:L_{(N)}} < x, \Gamma_{L_c:L_{(N-1)}} < \gamma_T\right] \qquad (4.6)\\ &= \begin{cases} \Pr\left[\Gamma_{L_c:L_{(N)}} < x\right], & 0 \leq x < \gamma_T; \\ \Pr\left[\Gamma_{L_c:L_{(N)}} < \gamma_T\right] + \Pr\left[\gamma_T \leq \Gamma_{L_c:L_{(N)}} < x, \Gamma_{L_c:L_{(N-1)}} < \gamma_T\right], & x \geq \gamma_T. \end{cases} \end{aligned}$$

Substituting (4.6) into (4.5), we can express the CDF of $\gamma_{Seq}$, $F_{\gamma_{Seq}}(x)$, as

$$F_{\gamma_{Seq}}(x) = \begin{cases} \Pr\left[\Gamma_{L_c:L_{(N)}} < x\right], & 0 \leq x < \gamma_T; \\ \Pr\left[\gamma_T \leq \Gamma_{L_c:L_1} < x\right] + \Pr\left[\Gamma_{L_c:L_{(N)}} < \gamma_T\right] & \\ + \sum_{k=2}^{N} \Pr\left[\gamma_T \leq \Gamma_{L_c:L_{(k)}} < x, \Gamma_{L_c:L_{(k-1)}} < \gamma_T\right], & x \geq \gamma_T. \end{cases} \qquad (4.7)$$

With the help of Appendix A, we can finally obtain from (4.7) the CDF and the PDF of $\gamma_{Seq}$ as

$$\begin{aligned} &F_{\gamma_{Seq}}(x) \qquad (4.8)\\ &= \begin{cases} \Pr\left[\Gamma_{L_c:L_{(N)}} < x\right], & 0 \leq x < \gamma_T; \\ \Pr\left[\gamma_T \leq \Gamma_{L_c:L_1} < x\right] + \Pr\left[\Gamma_{L_c:L_{(N)}} < \gamma_T\right] & \\ + \sum_{k=2}^{N} \left\{ \Pr[\gamma_T \leq \Gamma_{L_c:L_{(k)}} < x] - \frac{1-\Pr[\Gamma_{L_c:L_{(k-1)}} < \gamma_T]}{1-\Pr[\Gamma_{L_c:L_{(k)-1}} < \gamma_T]} \right. & \\ \left. \times \Big(\Pr[\gamma_T \leq \Gamma_{L_c:L_{(k)}} < x] - \mathcal{J}(x)\Big) \right\}, & x \geq \gamma_T \end{cases} \end{aligned}$$

and

$$f_{\gamma_{Seq}}(x) \tag{4.9}$$
$$= \begin{cases} f_{\Gamma_{L_c:L_{(N)}}}(x), & 0 \le x < \gamma_T; \\ f_{\Gamma_{L_c:L_1}}(x) + \sum_{k=2}^{N} \Bigg[ f_{\Gamma_{L_c:L_{(k)}}}(x) & \\ -\frac{1-F_{\Gamma_{L_c:L_{(k-1)}}}(\gamma_T)}{1-F_{\Gamma_{L_c:L_{(k)}-1}}(\gamma_T)} \Big( f_{\Gamma_{L_c:L_{(k)}}}(x) - \mathcal{I}(x) \Big) \Bigg], & x \ge \gamma_T, \end{cases}$$

respectively, where

$$\mathcal{I}(x) = \frac{d}{dx}\mathcal{J}(x) = \frac{d}{dx} \Pr\left[\gamma_T \le \Gamma_{L_c:L_{(k)}} < x, \Gamma_{L_c:L_{(k)}-1} < \gamma_T\right]. \tag{4.10}$$

Note that for i.i.d. Rayleigh fading channels, $f_{\Gamma_{i:j}}(x)$ and $F_{\Gamma_{i:j}}(x)$ are the well-known PDF and CDF of $i/j$-GSC output SNR which are given in (3.19) and (3.20), respectively, and (4.10) can be obtained by using the result in (3.18). Therefore, (4.8) and (4.9) can be expressed in closed-form. With the PDF in (4.9), the closed-form expression for MGF of $\gamma_{Seq}$, $\mathcal{M}_{\gamma_{Seq}}(s) = \int_0^\infty e^{sx} f_{\gamma_{Seq}}(x)dx$, can be routinely obtained as

$$\begin{aligned} \mathcal{M}_{\gamma_{Seq}}(s) = {} & \mathcal{A}(L_c : L_{(N)}, 0, s) - \mathcal{A}(L_c : L_{(N)}, \gamma_T, s) + \mathcal{A}(L_c : L_1, \gamma_T, s) \\ & + \sum_{k=2}^{N} \Big[ \mathcal{A}(L_c : L_{(k)}, \gamma_T, s) - \frac{1 - \mathcal{B}(L_c : L_{(k-1)}, \gamma_T)}{1 - \mathcal{B}(L_c : L_{(k)} - 1, \gamma_T)} \\ & \times \big( \mathcal{A}(L_c : L_{(k)}, \gamma_T, s) - \mathcal{C}(\gamma_T, s) \big) \Big], \end{aligned} \tag{4.11}$$

where $\mathcal{A}(i : j, k, s)$, $\mathcal{B}(i : j, k)$, and $\mathcal{C}(k, s)$ are defined in (3.22), (3.23), and (3.24), respectively[4].

[4]Note that we can obtain $\mathcal{C}(k, s)$ in (4.11) from (3.24) by replacing $L + L_a$ with $L_{(k)}$.

## D. Average BER

In this section, we apply the closed-form results of the previous section to analyze the performance of our proposed combining scheme over Rayleigh fading channels. More specifically, we first examine its average BER by using the well-known MGF-based approach [5, Sec. 9.2.3]. We then look into the complexity tradeoff by quantifying the average number of path estimations, the average number of SNR comparisons, and the SHO overhead it requires.

Fig. 7 represents the average BER of BPSK versus the average SNR per branch, $\overline{\gamma}$, of the proposed schemes for various values of $\gamma_T$ over i.i.d. Rayleigh fading channels when $N = 4, L_1 = L_2 = L_3 = L_4 = 4$, and $L_c = 3$. For comparison purpose, we also plot the average BER of BPSK with $L_c$-MRC, $L_c/L_1$-GSC, and $L_c/L_{(N)}$-GSC. From this figure, it is clear that the higher the threshold, the better the performance, as one expects. As a check, we can see that when the threshold is too large (i.e., $\gamma_T = 15$ dB) or too small (i.e., $\gamma_T = -5$ dB), both schemes have almost the same performance which correspond to the performance of $L_c/L_{(N)}$-GSC for the high threshold and $L_c/L_1$-GSC for the low threshold. For the mid-range of the output threshold (i.e., $\gamma_T = 5$ dB), the full scanning scheme has slightly better performance than the sequential scanning scheme. However, with this slight (negligible) performance loss, the sequential scanning scheme can save the usage of the network resources compared to the full scanning scheme since it can dramatically reduce the unnecessary path estimations, SNR comparisons, and the SHO overhead as we show in what follows.

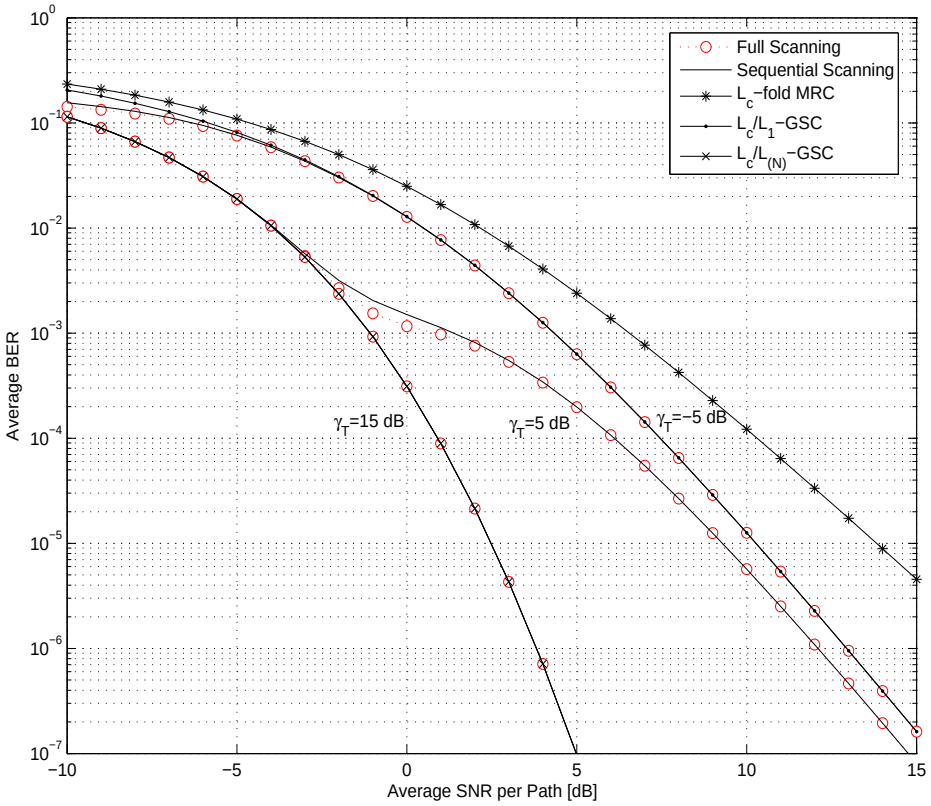


Fig. 7. Average BER of BPSK versus the average SNR per path, $\overline{\gamma}$, of the full scanning and sequential scanning schemes, MRC, and GSC for various values of $\gamma_T$ over i.i.d. Rayleigh fading channels with $N = 4, L_1 = L_2 = L_3 = L_4 = 4$, and $L_c = 3$.

## E. Complexity Comparison

### 1. Average Number of Path Estimations

In this subsection, we quantify the complexity of the proposed schemes by calculating the average number of path estimations needed during the SHO process.

#### a. Case I - Full Scanning

With this case, the RAKE receiver estimates $L_1$ paths in the case of $\Gamma_{L_c:L_1} \geq \gamma_T$ or $L_{(N)}$ in the case of $\Gamma_{L_c:L_1} < \gamma_T$. Hence, we can easily quantify the average number of path estimations, denoted by $E_{Full}$, as

$$E_{Full} = L_1 \Pr\left[\Gamma_{L_c:L_1} \geq \gamma_T\right] + L_{(N)} \Pr\left[\Gamma_{L_c:L_1} < \gamma_T\right], \tag{4.12}$$

which reduces to

$$E_{Full} = L_1 + (L_{(N)} - L_1) F_{\Gamma_{L_c:L_1}}(\gamma_T). \tag{4.13}$$

#### b. Case II - Sequential Scanning

In this scheme, we can write the average number of path estimations, denoted by $E_{Seq}$, in the following summation form:

$$E_{Seq} = \sum_{l=1}^{N} L_{(l)} \cdot \pi_l, \tag{4.14}$$

where $\pi_l$ is the probability that $L_{(l)}$ paths are estimated. Based on the mode of operation in Section IV.B.2.b in Page 34, we have

$$\pi_l = \begin{cases} \Pr\left[\Gamma_{L_c:L_1} \geq \gamma_T\right], & l = 1; \\ \Pr\left[\Gamma_{L_c:L_{(l-1)}} < \gamma_T, \Gamma_{L_c:L_{(l)}} \geq \gamma_T\right], & 1 < l < N; \\ \Pr\left[\Gamma_{L_c:L_{(N-1)}} < \gamma_T\right], & l = N. \end{cases} \tag{4.15}$$

By the similar approach used in order to get (4.8), the joint probability in (4.15) can be obtained as

$$\begin{aligned}&\Pr\left[\Gamma_{L_c:L_{(l-1)}} < \gamma_T, \Gamma_{L_c:L_{(l)}} \geq \gamma_T\right] \\ &= \Pr[\gamma_T \leq \Gamma_{L_c:L_{(l)}}] - \frac{1-\Pr[\Gamma_{L_c:L_{(l-1)}} < \gamma_T]}{1-\Pr[\Gamma_{L_c:L_{(l)}-1} < \gamma_T]} \times \left(\Pr[\gamma_T \leq \Gamma_{L_c:L_{(l)}}] - \mathcal{K}(l)\right),\end{aligned} \tag{4.16}$$

where

$$\begin{aligned}\mathcal{K}(l) &= \Pr\left[\Gamma_{L_c:L_{(l)}-1} < \gamma_T, \Gamma_{L_c:L_{(l)}} \geq \gamma_T\right] \\ &= e^{-\frac{\gamma_T}{\overline{\gamma}}} \left(\frac{\gamma_T}{\overline{\gamma}}\right)^{L_c} \sum_{t=0}^{L_{(l)}-L_c-1} \sum_{u=0}^{L_c-1} \frac{(-1)^{t+u}\binom{L_{(l)}-1}{L_c, L_{(l)}-L_c-t-1, t}}{(L_c-u-1)!\left((t+1)\gamma_T/(\overline{\gamma}L_c)\right)^{u+1}} \\ &\quad \times \left[1 - e^{-\frac{(t+1)\gamma_T}{\overline{\gamma}L_c}} \sum_{v=0}^{u} \left(\frac{(t+1)\gamma_T}{\overline{\gamma}L_c}\right)^{v} / v!\right].\end{aligned} \tag{4.17}$$

After successive substitutions from (4.17) to (4.14), we can express the average number of path estimations, $E_{Seq}$, as

$$\begin{aligned}E_{Seq} &= L_{(1)}\left(1 - F_{\Gamma_{L_c:L_1}}(\gamma_T)\right) + L_{(N)} F_{\Gamma_{L_c:L_{(N-1)}}}(\gamma_T) \\ &\quad + \sum_{l=2}^{N-1} L_{(l)} \Bigg(1 - F_{\Gamma_{L_c:L_{(l)}}}(\gamma_T) - \frac{1 - F_{\Gamma_{L_c:L_{(l-1)}}}(\gamma_T)}{1 - F_{\Gamma_{L_c:L_{(l)}-1}}(\gamma_T)} \\ &\quad \times \left(1 - F_{\Gamma_{L_c:L_{(l)}}}(\gamma_T) - \mathcal{K}(l)\right)\Bigg).\end{aligned} \tag{4.18}$$

Fig. 8 shows the average number of path estimations versus the output threshold, $\gamma_T$, of the proposed schemes, MRC, and GSC for various values of $L_c$ over i.i.d. Rayleigh fading channels when $N = 4, L_1 = L_2 = L_3 = L_4 = 4$, and $\overline{\gamma} = 0$ dB. Note that $L_c$-MRC and $L_c/L_{(N)}$-GSC always require $L_c$ and $L_{(N)}$ estimations, respectively. From this figure, we can clearly see that the sequential scanning scheme leads to a considerably less path estimation load. For a better illustration of the tradeoff between complexity and performance, Fig. 9 shows the average BER of BPSK versus

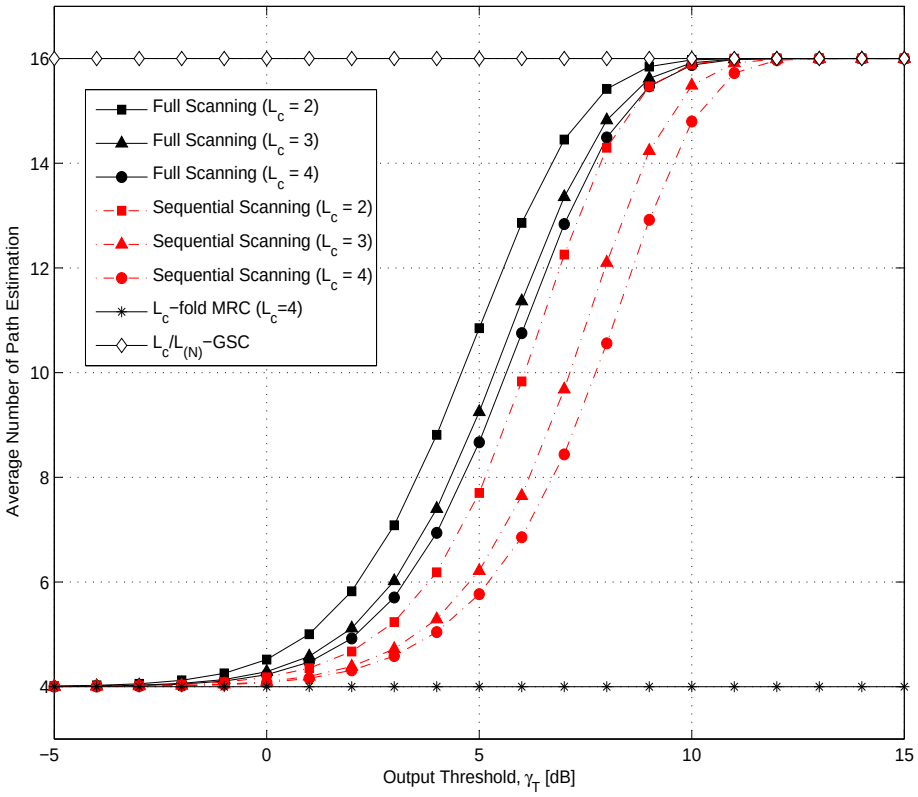


Fig. 8. Average number of path estimation versus the output threshold, $\gamma_T$, of the full scanning and sequential scanning schemes, MRC, and GSC for various values of $L_c$ over i.i.d. Rayleigh fading channels with $N = 4, L_1 = L_2 = L_3 = L_4 = 4$, and $\overline{\gamma} = 0$ dB.

the output threshold, $\gamma_T$, of the proposed schemes, MRC, and GSC for the same parameters. As mentioned earlier, the full scanning scheme shows a very slight performance improvement and the error rate of both proposed schemes decreases to that of $L_c/L_{(N)}$-GSC when the output threshold increases. Considering Figs. 8 and 9 together, we observe that the proposed schemes can save a certain amount of estimation load with a slight performance loss compared to GSC if the transmitted power is properly selected such as, for example, the average received SNR is 6∼8 dB below

the required target threshold for our chosen set of parameters.

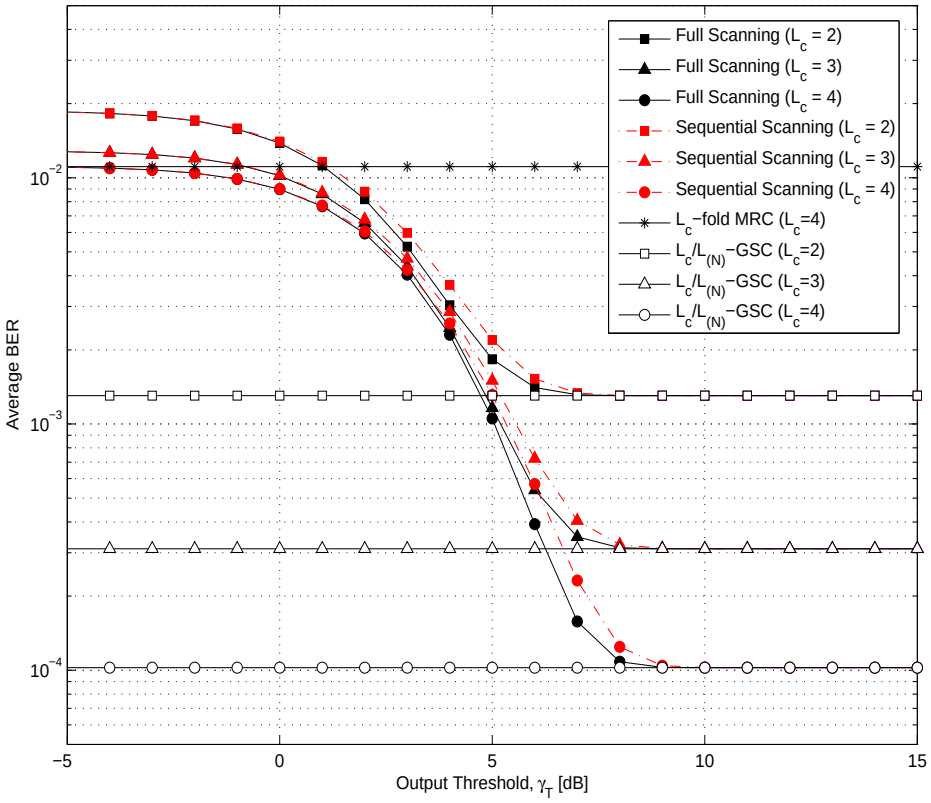


Fig. 9. Average BER of BPSK versus the output threshold, $\gamma_T$, of the full scanning and sequential scanning schemes, MRC, and GSC for various values of $L_c$ over i.i.d. Rayleigh fading channels with $N = 4, L_1 = L_2 = L_3 = L_4 = 4$, and $\overline{\gamma} = 0$ dB.

### 2. Average Number of SNR Comparisons

As another complexity measure, in this subsection we evaluate the average number of required SNR comparisons. Noting that the average number of SNR comparisons for $i/j$-GSC, denoted by $C_{GSC(i,j)}$, can be obtained as

$$C_{GSC(i,j)} = \sum_{k=1}^{\min[i,j-i]} (j-k), \tag{4.19}$$

we can express the average number of SNR comparisons for the full scanning scheme and the sequential scanning scheme as

$$C_{Full} = C_{GSC(L_c,L_1)} \Pr\left[\Gamma_{L_c:L_1} \geq \gamma_T\right] + C_{GSC(L_c,L_{(N)})} \Pr\left[\Gamma_{L_c:L_1} < \gamma_T\right] \tag{4.20}$$

and

$$C_{Seq} = \sum_{l=1}^{N} C_{GSC(L_c,L_{(l)})} \cdot \pi_l, \tag{4.21}$$

respectively, where $\pi_l$ is defined in (4.15).

Fig. 10 represents the average number of SNR comparisons versus the output threshold, $\gamma_T$, of the proposed schemes and GSC for various values of $L_c$ over i.i.d. Rayleigh fading channels when $N = 4, L_1 = L_2 = L_3 = L_4 = 4$, and $\overline{\gamma} = 0$ dB. Note that our proposed schemes are both acting as $L_c/L_{(N)}$-GSC when the output threshold becomes large. Hence, we can observe that the average number of SNR comparisons of the proposed schemes converges to that of GSC as $\gamma_T$ increases. Also we can see that our proposed schemes show a reduction of SNR comparison load and the reduction offered by the sequential scanning scheme is bigger than the one given by the full scanning scheme, for example, when $\gamma_T$ is between 0 to 10 dB.

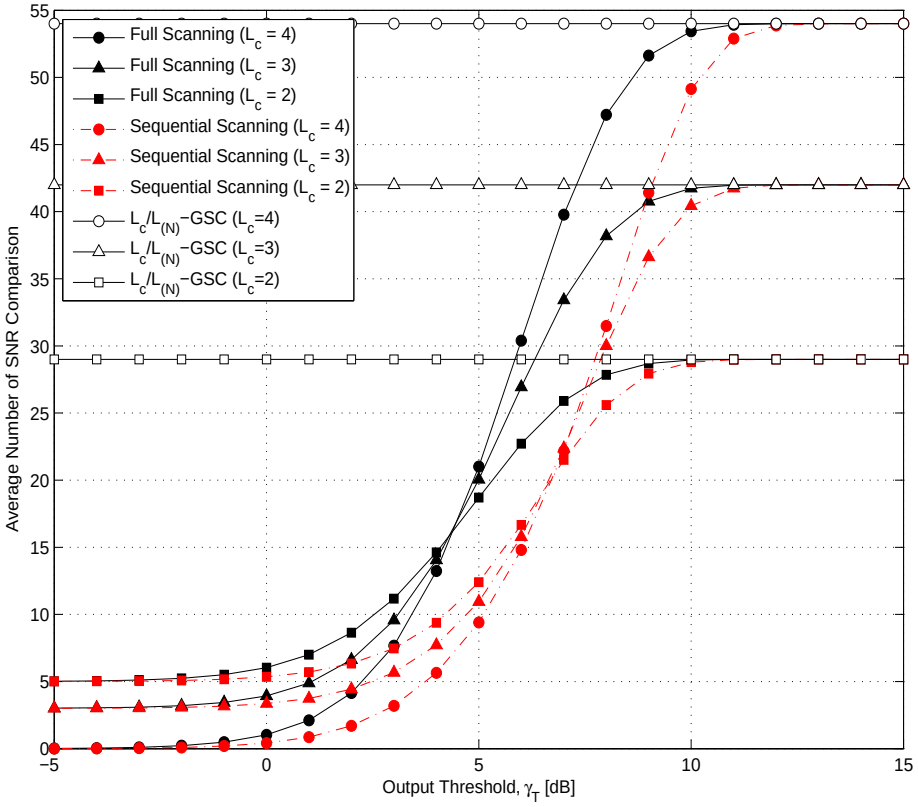


Fig. 10. Average number of SNR comparison versus the output threshold, $\gamma_T$, of the full scanning and sequential scanning schemes, and GSC for various values of $L_c$ over i.i.d. Rayleigh fading channels with $N = 4, L_1 = L_2 = L_3 = L_4 = 4$, and $\overline{\gamma} = 0$ dB.

### 3. SHO Overhead

The SHO overhead, $\beta$, is defined as [30, Eq. (9.2)]

$$\beta = \sum_{n=1}^{L_c} nP_n - 1, \tag{4.22}$$

where $L_c\,(\leq N)$ is the number of fingers (i.e., the number of active BSs) and $P_n$ is the average probability that the mobile unit uses $n$-way SHO. Note that basically a maximum $L_c$-way SHO is possible and we need to determine which BSs the combined $L_c$ paths are from. Unfortunately, it seems difficult to analyze the SHO overhead in a simple fashion. The major difficulty lies in how to determine how many BSs end up eventually being involved in the SHO (i.e., the number $n$ in $n$-way SHO) after HO is requested. For this reason, we just present some numerical results obtained through Monte-Carlo simulations.

In Fig. 11, we plot the simulation results of SHO overhead versus the output threshold, $\gamma_T$, of the full scanning and sequential scanning schemes for various values of $L_c$ over i.i.d. Rayleigh fading channels for the same parameters used in Figs. 8, 9 and 10. Note that as the output threshold increases we have a higher chance to use $L_c$-way SHO. Compared to the full scanning scheme, for the mid-range of the output threshold the sequential scanning scheme shows a large amount of reduction of the SHO overhead. From this figure together with Fig. 9, we can quantify the SHO overhead reduction of our proposed schemes. For example, if the required threshold is 8 dB above $\overline{\gamma}$ in the case of $L_c = 3$, the full scanning and the sequential scheme shows around 1.3 and 0.4 SHO overhead, respectively, while maintaining the same error rate as GSC (which requires around 1.43 SHO overhead).

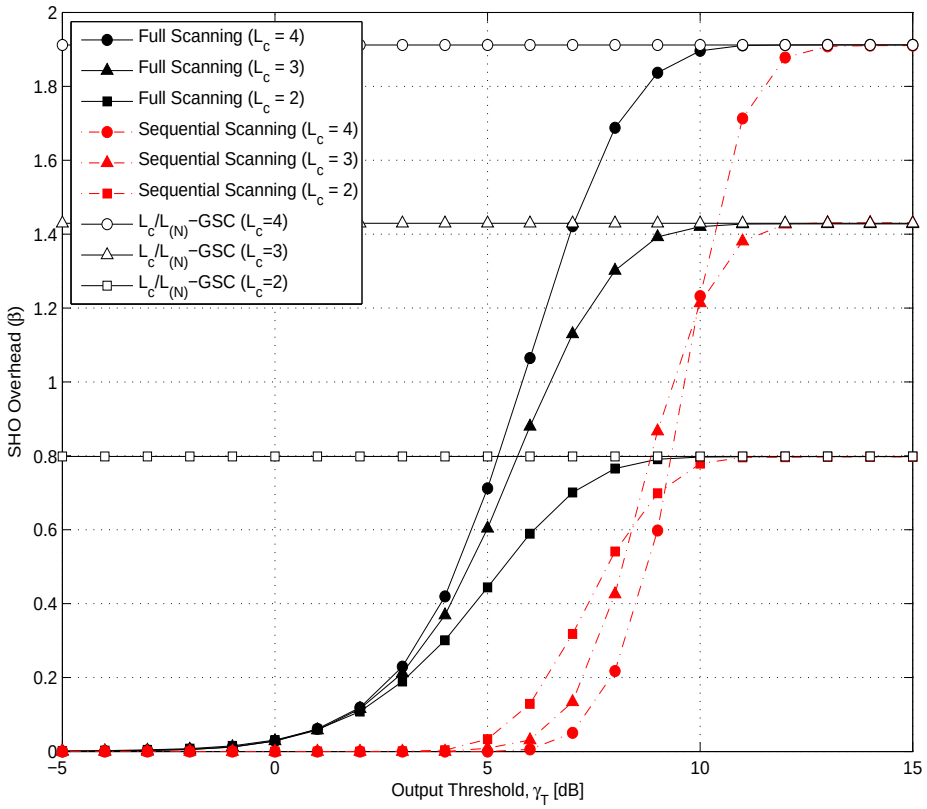


Fig. 11. Simulation results of SHO overhead versus the output threshold, $\gamma_T$, of the full scanning and sequential scanning schemes for various values of $L_c$ over i.i.d. Rayleigh fading channels with $N = 4, L_1 = L_2 = L_3 = L_4 = 4$, and $\overline{\gamma} = 0$ dB.

## F. Conclusion

In this chapter, we generalized the finger assignment scheme proposed in Chapter III. In these schemes, the receiver checks the GSC output SNR from the serving BS against a certain pre-determined output threshold. If the output SNR is below this threshold, the receiver performs a finger reassignment after using GSC on the paths coming from the serving BS and the target BSs. More specifically, we considered two schemes : a full scanning scheme and a sequential scanning scheme. For both schemes, we derived the statistics of the output SNR, based on which we carried out the performance analysis of the resulting systems. We showed through numerical examples that the new schemes offer commensurate performance in comparison with more complicated GSC-based diversity systems while requiring a smaller estimation load and SHO overhead.

# CHAPTER V

# FINGER REPLACEMENT SCHEME WITH TWO BASE STATIONS

## A. Introduction

In this chapter, we propose an alternative finger combining scheme that is also applicable to the SHO region and further reduces the SHO overhead at the expense of a certain degradation in performance in comparison with the scheme proposed in Chapter III (which we will accurately quantify in the body of this chapter). For convenience sake, we call this alternative scheme in this chapter as *a block change scheme* and the scheme in Chapter III as *a full GSC scheme*. With the block change scheme, like the full GSC scheme when the output SNR falls below the target SNR, the receiver scans the additional $L_a$ resolvable paths from the target BS while unlike the full GSC scheme, the receiver compares the sum of the SNRs of the $L_s(\leq L_c)$ strongest paths among the $L_a$ paths from the target BS with the sum of the $L_s$ weakest SNRs among the currently used $L_c$ paths from the serving BS, and selects the better group to form $L_c$ paths again. Note that the block change scheme just compares two blocks with equal size of $L_s$ and as such, avoids reordering all the paths which is essential for the full GSC scheme. Therefore, a further reduction in SNR comparisons and SHO overhead can be obtained.

In this chapter, we show a general comprehensive framework for the assessment of the block change scheme by providing analytical results for i.i.d. fading environments[1]. More specifically, in our derivations we tackle the joint PDF of two adjacent partial sums of order statistics in order to obtain the statistics of the receiver output

[1]In Chapter VII, more practical channel environments, such as non-identical/correlated fading channels and outdated channel estimation, are considered.

SNR.

This chapter is organized as follows. In Section V.B, we present the channel and system model under consideration as well as the mode of operation of the proposed scheme. Based on this mode of operation, we derive in Section V.C the statistics of the combined SNR in the form of finite integrations of elementary functions. These results are next applied in Section V.D to the performance analysis of the average BER of the proposed scheme. Section V.E illustrates the tradeoff of complexity versus performance by quantifying the average number of path estimations, the average number of SNR comparisons, and the SHO overhead of the proposed scheme. Finally, Section V.F provides some concluding remarks.

## B. System Model

### 1. System and Channel Model

Basically, we follow the same system and channel model described in Section III.B.1 in Page 11. Hence, the faded instantaneous received SNR, $\gamma_i$, of the $i$th resolvable path follows the same exponential distribution with the common average faded SNR, $\overline{\gamma}$, where $i = 1, 2, \cdots, L + L_a$, $L$ and $L_a$ are the number of resolvable paths from the serving and target BSs, respectively.

We also consider the mobile unit with an $L_c$ finger RAKE receiver. More specifically, we assume that in the SHO region, the mobile unit is able to resolve the $L$ multi-paths from the serving BS and the $L_a$ paths from the target BS, and depending on the channel conditions only the $L_c$ paths among the $L$ or $L+L_a$ paths are used for RAKE reception according to the mode of operation described in the next section.

## 2. Mode of Operation

As the mobile unit enters the SHO region, the RAKE receiver relies at first on the $L$ resolvable paths gathered from the serving BS and as such, starts with $L_c/L$-GSC. Then, the total received SNR after GSC is given by $\Gamma_{L_c:L}$ where $\Gamma_{i:j}$ is the sum of the $i$ largest SNRs among $j$ ones, i.e., $\Gamma_{i:j} = \sum_{k=1}^{i} \gamma_{k:j}$ where $\gamma_{k:j}$ is the $k$th order statistics (see [18] for terminology). At the beginning of every time slot, the receiver compares the received SNR, $\Gamma_{L_c:L}$, with a certain target SNR, denoted by $\gamma_T$. If $\Gamma_{L_c:L}$ is greater than or equal to $\gamma_T$, a one-way SHO is used and no finger replacement is needed. On the other hand, whenever $\Gamma_{L_c:L}$ falls below $\gamma_T$, a two-way SHO is attempted. In this case, the RAKE receiver compares the sums of two groups, the sum of the $L_s$ smallest paths among the $L_c$ currently used paths from the serving BS (i.e., $\sum_{i=L_c-L_s+1}^{L_s} \gamma_{i:L}$) and the sum of the $L_s$ strongest paths from the target BS (i.e., $\sum_{i=1}^{L_s} \gamma_{i:L_a}$). Then, the receiver replaces the $L_s$ smallest paths which are currently used with the best group. Note that no replacement occurs if the sum of the $L_s$ strongest additional paths from the target BS is less than the sum of the $L_s$ weakest paths among the $L_c$ strongest paths from the serving BS.

For simplicity, if we let

$$Y = \sum_{i=1}^{L_c-L_s} \gamma_{i:L}, \tag{5.1}$$

$$Z = \sum_{i=L_c-L_s+1}^{L_c} \gamma_{i:L}, \tag{5.2}$$

and

$$W = \sum_{i=1}^{L_s} \gamma_{i:L_a}, \tag{5.3}$$

then, based on the above mode of operation, the final combined SNR, $\gamma_t$, is then given

by

$$\gamma_t = \begin{cases} Y + \max\{Z, W\}, & 0 \le Y + Z < \gamma_T; \\ Y + Z, & Y + Z \ge \gamma_T. \end{cases} \tag{5.4}$$

C. Statistics of the Combined SNR

In this section, we derive the statistics of the combined SNR of the proposed scheme. In order to do that, we need to consider the joint PDF of two adjacent partial sums of order statistics. Hence, first we provide an analytical framework for the joint PDF of two partial sums of order statistics which is later on used for the statistics of the combined SNR.

1. CDF

From (5.4), the CDF of $\gamma_t$, $F_{\gamma_t}(x)$, can be written as

$$\begin{aligned} F_{\gamma_t}(x) &= \begin{cases} \Pr\left[Y + \max\{Z, W\} < x\right], & 0 \le x < \gamma_T; \\ \Pr\left[\gamma_T \le Y + Z < x\right] & \\ + \Pr[Y + \max\{Z, W\} < x, Y + Z < \gamma_T], & x \ge \gamma_T \end{cases} \\ &= \begin{cases} \Pr\left[Z \ge W, Y + Z < x\right] + \Pr\left[Z < W, Y + W < x\right], & 0 \le x < \gamma_T; \\ \Pr\left[\gamma_T \le Y + Z < x\right] + \Pr[Z \ge W, Y + Z < \gamma_T] & \\ + \Pr[Z < W, Y + W < x, Y + Z < \gamma_T], & x \ge \gamma_T. \end{cases} \end{aligned} \tag{5.5}$$

Noting that $\Pr\left[\gamma_T \le Y + Z < x\right]$ can be easily calculated from the CDF of $L_c/L$-GSC (see (3.20)) and that $W$ is independent of $Y$ and $Z$, we can obtain the other

joint probabilities in (5.5) as

$$\Pr[Z \geq W, Y + Z < x] = \int_0^x \int_0^{x-y} \int_w^{x-y} f_{Y,Z}(y,z) f_W(w) dz dw dy, \tag{5.6}$$

$$\Pr[Z < W, Y + W < x] = \int_0^x \int_0^{x-y} \int_0^{w} f_{Y,Z}(y,z) f_W(w) dz dw dy, \tag{5.7}$$

$$\Pr[Z \geq W, Y + Z < \gamma_T] = \int_0^{\gamma_T} \int_0^{\gamma_T - y} \int_w^{\gamma_T - y} f_{Y,Z}(y,z) f_W(w) dz dw dy, \tag{5.8}$$

and

$$\begin{aligned} &\Pr[Z < W, Y + W < x, Y + Z < \gamma_T] \\ &= \int_0^{\gamma_T} \int_0^{x-y} \int_0^{\min\{w, \gamma_T - y\}} f_{Y,Z}(y,z) f_W(w) dz dw dy. \end{aligned} \tag{5.9}$$

Since $f_W(w)$ is the well-known PDF of $L_s/L_a$-GSC (see (3.19)), we just need to find the joint PDF of $Y$ and $Z$, $f_{Y,Z}(y,z)$. For better illustration, let $l = L_c - L_s$ and $k = L_c$. Then, the order statistics of $L$ resolvable paths can be viewed as

$$\underbrace{\overbrace{\gamma_{1:L}, \cdots, \gamma_{l-1:L}}^{A=\sum_{i=1}^{l-1}\gamma_{i:L}}, \gamma_{l:L}}_{Y=\sum_{i=1}^{l}\gamma_{i:L}}, \underbrace{\overbrace{\gamma_{l+1:L}, \cdots, \gamma_{k-1:L}}^{B=\sum_{i=l+1}^{k-1}\gamma_{i:L}}, \gamma_{k:L}}_{Z=\sum_{i=l+1}^{k}\gamma_{i:L}}, \gamma_{k+1:L}, \cdots, \gamma_{L:L}. \tag{5.10}$$

We start from the joint PDF of $A, \gamma_{l:L}, B$, and $\gamma_{k:L}$. Applying the Bayesian rule, we can write the joint PDF, $f_{A,\gamma_{l:L},B,\gamma_{k:L}}(a,\alpha,b,\beta)$, as

$$\begin{aligned} &f_{A,\gamma_{l:L},B,\gamma_{k:L}}(a,\alpha,b,\beta) \\ &= f_{\gamma_{l:L}}(\alpha) \cdot f_{\gamma_{k:L}|\gamma_{l:L}=\alpha}(\beta) \cdot f_{A|\gamma_{l:L}=\alpha,\gamma_{k:L}=\beta}(a) \cdot f_{B|\gamma_{l:L}=\alpha,\gamma_{k:L}=\beta,A=a}(b). \end{aligned} \tag{5.11}$$

After obtaining all PDFs in (5.11) (see Appendix C for detailed derivations), we can write a closed-form expression for the joint PDF, $f_{A,\gamma_{l:L},B,\gamma_{k:L}}(a,\alpha,b,\beta)$, for i.i.d.

Rayleigh fading channels as

$$
\begin{aligned}
&f_{A,\gamma_{l:L},B,\gamma_{k:L}}(a,\alpha,b,\beta) \qquad (5.12)\\
&= \frac{L!e^{-(a+\alpha+b+\beta)/\overline{\gamma}}(1-e^{-\beta/\overline{\gamma}})^{L-k}[a-(l-1)\alpha]^{l-2}}{(L-k)!(k-l-1)!(k-l-2)!(l-1)!(l-2)!\overline{\gamma}^{k}}\\
&\quad\times\sum_{j=0}^{k-l-1}\binom{k-l-1}{j}(-1)^j[b-\beta(k-l-j-1)-\alpha j]^{k-l-2}\\
&\quad\times\mathcal{U}(\alpha)\mathcal{U}(\alpha-\beta)\mathcal{U}(a-(l-1)\alpha)\mathcal{U}(b-\beta(k-l-j-1)-\alpha j),\\
&\quad 0<(k-l-1)\beta<b<(k-l-1)\alpha.
\end{aligned}
$$

Since $Y = A + \gamma_{l:L}$ and $Z = B + \gamma_{k:L}$, we can obtain the joint pdf of $Y$ and $Z$, $f_{Y,Z}(y,z)$, from (5.12) by integrating out $\gamma_{l:L}$ and $\gamma_{k:L}$ as

$$
f_{Y,Z}(y,z) = \int_0^{\frac{z}{k-l}}\int_{\frac{z}{k-l}}^{\frac{y}{l}} f_{A,\gamma_{l:L},B,\gamma_{k:L}}(y-\alpha,\alpha,z-\beta,\beta)d\alpha d\beta, \quad y > \frac{l}{k-l}z. \qquad (5.13)
$$

Note that (5.13) involves only finite integrations of elementary functions and as such, this joint probability can be easily calculated with mathematical software, such as Mathematica. Also note that (5.13) is valid when $l \geq 2$ and $k \geq l+2$. All other cases can be easily obtained as

$$
f_{Y,Z}(y,z) = \begin{cases}
\int_0^{\frac{z}{k-1}} f_{\gamma_{1:L},B,\gamma_{k:L}}(y,z-\beta,\beta)d\beta, & l=1, k\geq l+2, y>\frac{1}{k-1}z;\\
\int_z^{\frac{y}{l}} f_{A,\gamma_{l:L},\gamma_{l+1:L}}(y-\alpha,\alpha,z)d\alpha, & l\geq 2, k=l+1, y>lz;\\
f_{\gamma_{1:L},\gamma_{2:L}}(y,z), & l=1,k=2,y>z,
\end{cases} \qquad (5.14)
$$

where

$$\begin{aligned} f_{\gamma_{1:L},B,\gamma_{k:L}}(\alpha,b,\beta) &= f_{\gamma_{1:L}}(\alpha)\cdot f_{\gamma_{k:L}|\gamma_{1:L}=\alpha}(\beta)\cdot f_{B|\gamma_{1:L}=\alpha,\gamma_{k:L}=\beta}(b) \\ &= \frac{L!e^{-(\alpha+b+\beta)/\overline{\gamma}}(1-e^{-\beta/\overline{\gamma}})^{L-k}}{(L-k)!(k-2)!(k-3)!\overline{\gamma}^{k}} \\ &\quad\times\sum_{j=0}^{k-2}\binom{k-2}{j}(-1)^{j}[b-\beta(k-j-2)-\alpha j]^{k-3} \\ &\quad\times\mathcal{U}(\alpha)\mathcal{U}(\alpha-\beta)\mathcal{U}(b-\beta(k-j-2)-\alpha j), \end{aligned} \tag{5.15}$$

$$\begin{aligned} f_{A,\gamma_{l:L},\gamma_{l+1:L}}(a,\alpha,\beta) &= f_{\gamma_{l:L}}(\alpha)\cdot f_{\gamma_{l+1:L}|\gamma_{l:L}=\alpha}(\beta)\cdot f_{A|\gamma_{l:L}=\alpha,\gamma_{l+1:L}=\beta}(a) \\ &= \frac{L!e^{-(a+\alpha+\beta)/\overline{\gamma}}(1-e^{-\beta/\overline{\gamma}})^{L-l-1}}{(L-l-1)!(l-1)!(l-2)!\overline{\gamma}^{l+1}}[a-(l-1)\alpha]^{l-2} \\ &\quad\times\mathcal{U}(\alpha)\mathcal{U}(\alpha-\beta)\mathcal{U}(a-(l-1)\alpha), \end{aligned} \tag{5.16}$$

and

$$\begin{aligned} f_{\gamma_{1:L},\gamma_{2:L}}(\alpha,\beta) &= f_{\gamma_{1:L}}(\alpha)\cdot f_{\gamma_{2:L}|\gamma_{1:L}=\alpha}(\beta) \\ &= \frac{L(L-1)}{\overline{\gamma}^{2}}e^{-(\alpha+\beta)/\overline{\gamma}}(1-e^{-\beta/\overline{\gamma}})^{L-2}\mathcal{U}(\alpha)\mathcal{U}(\alpha-\beta). \end{aligned} \tag{5.17}$$

Considering (5.13) and (5.14) together with (5.6)-(5.9), the CDF of $\gamma_t$, $F_{\gamma_t}(x)$, in (5.5) can be obtained.

## 2. PDF

By using the Leibnitz's rule [32, Eq. (6.40)] and differentiating (5.5) with respect to $x$, we can obtain after some manipulations the following generic expression for the

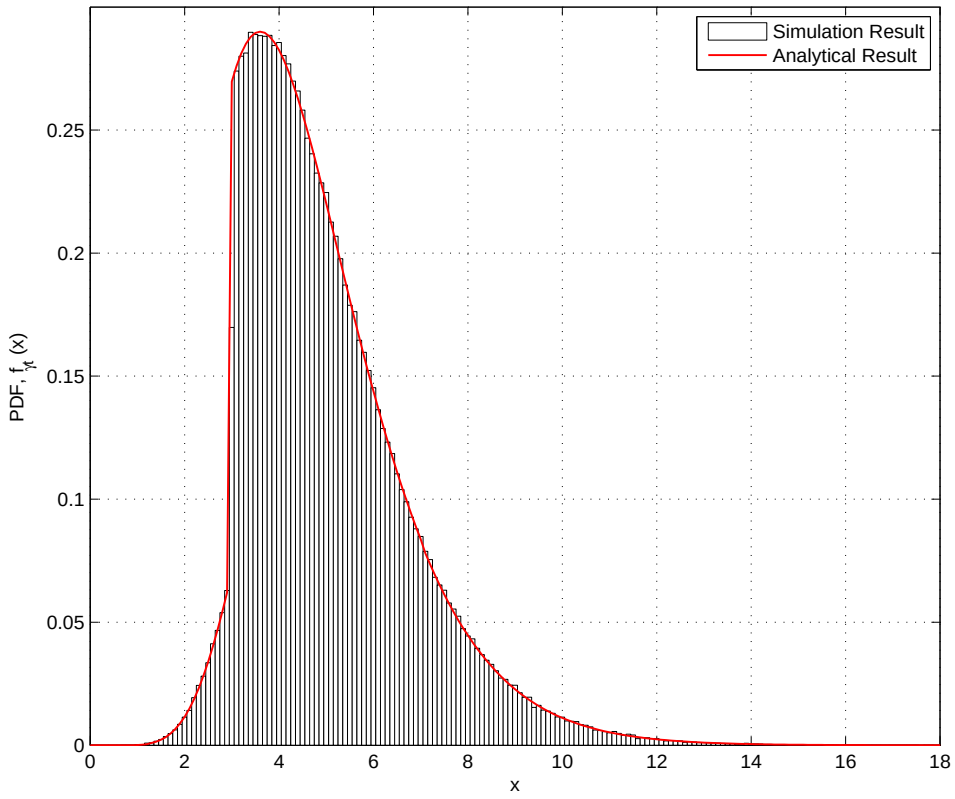


Fig. 12. PDF comparison between the simulation and the analytical results when $L = 5, L_a = 5, L_c = 3, L_s = 2, \gamma_T = 3$, and $\overline{\gamma} = 1$.

PDF of the combined SNR, $\gamma_t$, as

$$f_{\gamma_t}(x) = \begin{cases} \int_0^x \Big( f_{Y,Z}(y, x-y) F_W(x-y) & \\ + f_W(x-y) \int_0^{x-y} f_{Y,Z}(y,z) dz \Big) dy, & 0 \le x < \gamma_T; \\ f_{Y+Z}(x) + \int_0^{\gamma_T} \Big( f_W(x-y) \int_0^{\gamma_T - y} f_{Y,Z}(y,z) dz \Big) dy, & x \ge \gamma_T, \end{cases} \quad (5.18)$$

where $f_{Y,Z}(\cdot,\cdot)$ is defined in (5.13) and (5.14), $f_W(\cdot)$ and $f_{Y+Z}(\cdot)$ are the PDFs of $L_s/L_a$-GSC and $L_c/L$-GSC, respectively, and $F_W(\cdot)$ is the CDF of $L_s/L_a$-GSC. The general forms of the PDF and CDF of $i/j$-GSC output SNR for i.i.d. Rayleigh case

are given in (3.19) and (3.20), respectively. To verify the correctness of our analysis, we compare in Fig. 12 the PDF in (5.18) with Monte Carlo simulation results. It is clear from this figure that there is an excellent match between the analytical and simulation results.

## D. Average BER

In this section, we apply the results from the previous section to the performance analysis of our proposed combining scheme over i.i.d. Rayleigh fading channels. More specifically, by presenting some selected numerical examples, we examine its average BER. The average BER can be calculated by finding the expected value of the conditional probability of error. For example, the average BER for BPSK can be expressed as

$$P_b(E) = \int_0^\infty Q(\sqrt{2x}) f_{\gamma_t}(x) dx, \tag{5.19}$$

where $Q(\cdot)$ is the Gaussian $Q$-function, defined as $Q(x) = \frac{1}{\sqrt{2\pi}} \int_x^\infty e^{-t^2/2} dt$.

In Fig. 13, we consider the effect of the switching threshold on the performance by representing the average BER of BPSK versus the average SNR per path, $\overline{\gamma}$, of the Block Change scheme proposed in this chapter and the full GSC scheme in Chapter III for various values of $\gamma_T$ over i.i.d. Rayleigh fading channels when $L = 5, L_a = 5, L_c = 3$, and $L_s = 2$. From this figure, it is clear that the higher the threshold, the better the performance, as we expect intuitively. Note that when $\overline{\gamma}$ becomes larger, the combined SNR is typically large enough in a way that the receiver does not need to rely on the additional paths from the target BS. Hence, we can observe that in good channel conditions (i.e., $\overline{\gamma}$ is relatively large compared to $\gamma_T$), both schemes become insensitive to variations in $\gamma_T$. Also note that when the switching threshold is small, both schemes have almost the same performance since the additional paths

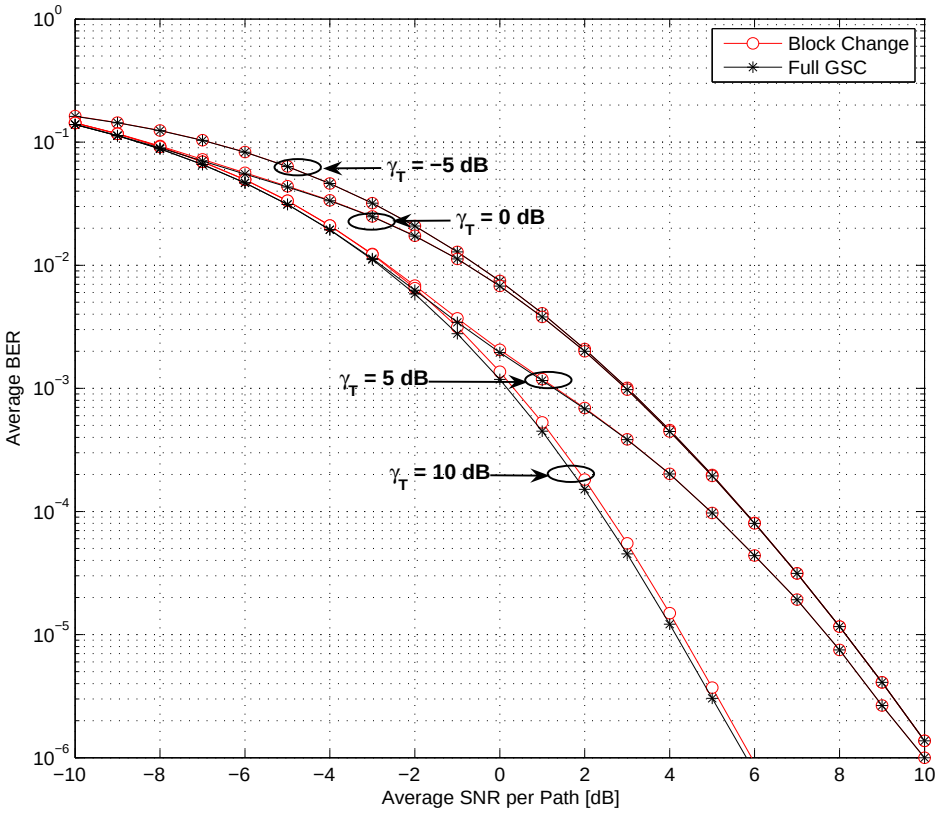


Fig. 13. Average BER of BPSK versus the average SNR per path, $\overline{\gamma}$, of the block change and the full GSC schemes for various values of $\gamma_T$ over i.i.d. Rayleigh fading channels when $L = 5, L_a = 5, L_c = 3$, and $L_s = 2$.

are not necessary. On the other hand, in the case of large threshold values, the full GSC scheme shows better performance since with the full GSC scheme, instead of comparing and replacing blocks, the $L_c$ largest paths are selected among the $L + L_a$ ones.

In Fig. 14, we vary the block size, $L_s$, with two values of $\gamma_T$. We can see that for the low threshold, the variations of the block size do not affect the performance since in this case no replacement is needed. However, when the threshold is set high, we can observe the performance difference according to the value of $L_s$. For our chosen

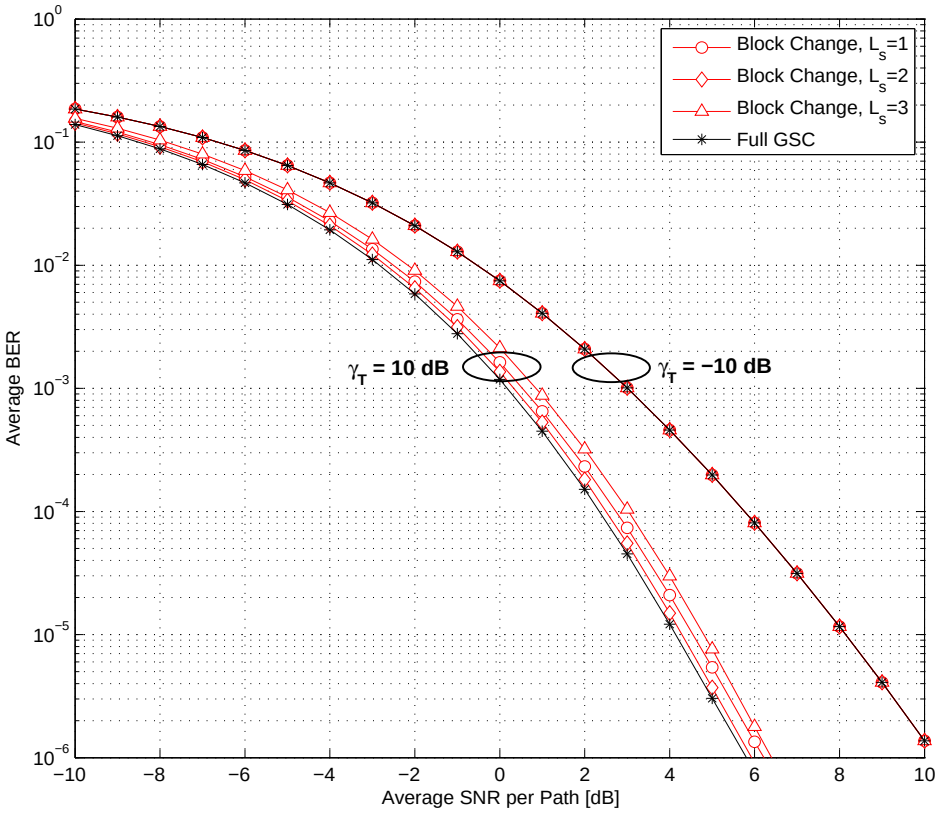


Fig. 14. Average BER of BPSK versus the average SNR per path, $\overline{\gamma}$, of the block change and the full GSC schemes for various values of $L_s$ and $\gamma_T$ over i.i.d. Rayleigh fading channels when $L = 5, L_a = 5$ and $L_c = 3$.

set of parameters, the best performance which is very close to that of the full GSC scheme can be acquired when $L_s = 2$. This is because if $L_s = 1$, we have little benefit from the additional paths while if $L_s = 3$, we have more chances to lose the better paths during the replacement process.

## E. Complexity Comparison

As shown in the previous section, because the paths with strongest SNR values are selected whenever needed, the full GSC scheme always provides the better performance than the block change scheme. However, with the block change scheme considered in this chapter, we can reduce the load induced by a full reordering process of all the paths at a slight sacrifice of performance. In this section, we investigate this complexity tradeoff issue by quantifying the average number of path estimations, the average number of SNR comparisons, and the SHO overhead.

### 1. Average Number of Path Estimations

With the proposed scheme, the RAKE receiver estimates the $L$ paths in the case of $\Gamma_{L_c:L} \geq \gamma_T$ or $L + L_a$ in the case of $\Gamma_{L_c:L} < \gamma_T$. Hence, the average number of path estimations of the block change scheme is same as that of the Full GSC scheme which is given in (3.28).

### 2. Average Number of SNR Comparisons

As another complexity measure, in this subsection we evaluate the average number of required SNR comparisons. Noting that the average number of SNR comparisons for $i/j$-GSC, denoted by $C_{GSC(i,j)}$, can be obtained as

$$C_{GSC(i,j)} = \sum_{k=1}^{\min[i,j-i]} (j-k), \tag{5.20}$$

we can express the average number of SNR comparisons for the full GSC scheme and the block change scheme as

$$C_{Full} = \Pr\left[\Gamma_{L_c:L} \geq \gamma_T\right] C_{GSC(L_c,L)} + \Pr\left[\Gamma_{L_c:L} < \gamma_T\right] C_{GSC(L_c,L+L_a)} \tag{5.21}$$

and

$$C_{Block} = C_{GSC(L_c,L)} + \Pr\left[\Gamma_{L_c:L} < \gamma_T\right]\left(C_{GSC(L_s,L_c)} + C_{GSC(L_s,L_a)} + 1\right), \tag{5.22}$$

respectively.

### 3. SHO Overhead

In this section, we investigate the probability of the SHO attempt and the SHO overhead of the proposed scheme. Since the SHO is attempted whenever $\Gamma_{L_c:L}$ is below $\gamma_T$, the probability of the SHO attempt is same as the outage probability of $L_c/L$-GSC evaluated at $\gamma_T$, i.e., $F_{\Gamma_{L_c:L}}(\gamma_T)$. The SHO overhead, denoted by $\beta$, is commonly used to quantify the SHO activity in a network and is defined as [30, Eq. (9.2)]

$$\beta = \sum_{n=1}^{N} nP_n - 1, \tag{5.23}$$

where $N$ is the number of active BSs and $P_n$ is the average probability that the mobile unit uses $n$-way SHO. Based on the mode of operation in Section V.B.2 in Page 52, $P_1$ and $P_2$ can be defined as

$$P_1 = \begin{cases} \Pr\left[Y + Z \geq \gamma_T\right] + \Pr\left[Y + Z < \gamma_T, Z \geq W\right], & L_s < L_c; \\ 1, & L_s = L_c, \end{cases} \tag{5.24}$$

and

$$P_2 = 1 - P_1. \tag{5.25}$$

Substituting (5.24) and (5.25) into (5.23), we can express the SHO overhead, $\beta$, as

$$\begin{aligned}\beta &= P_1 + 2P_2 - 1 \qquad (5.26)\\ &= \begin{cases} F_{Y+Z}(\gamma_T)\Pr\left[Z < W | Y+Z < \gamma_T\right], & L_s < L_c; \\ 0, & L_s = L_c. \end{cases}\end{aligned}$$

Note that $F_{Y+Z}(\gamma_T)$ is the CDF of $L_c/L$-GSC output SNR evaluated at $\gamma_T$. Since $W$ is independent to $Z$ and $Y$, we can calculate the conditional probability, $\Pr[Z < W|Y+Z<\gamma_T]$, as

$$\Pr\left[Z < W | Y+Z < \gamma_T\right] = \int_0^\infty F_{Z|Y+Z<\gamma_T}(x) f_W(x) dx. \qquad (5.27)$$

The conditional CDF in (5.27) can be written as

$$\begin{aligned}F_{Z|Y+Z<\gamma_T}(x) &= \frac{\Pr\left[Z < x, Y+Z < \gamma_T\right]}{\Pr\left[Y+Z<\gamma_T\right]} \qquad (5.28)\\ &= \frac{1}{F_{Y+Z}(\gamma_T)} \begin{cases} \int_0^x \int_{lz/(k-l)}^{\gamma_T - z} f_{Y,Z}(y,z) dy dz, & 0 \le x < \frac{k-l}{k}\gamma_T; \\ \int_0^{(k-l)\gamma_T/k} \int_{lz/(k-l)}^{\gamma_T - z} f_{Y,Z}(y,z) dy dz, & x \ge \frac{k-l}{k}\gamma_T, \end{cases}\end{aligned}$$

where $f_{Y,Z}(y,z)$ can be obtained from (5.13) or (5.14). After successive substitutions from (5.28) to (5.26), we can finally obtain the SHO overhead.

In Fig. 15, we plot (a) the average number of SNR comparisons, (b) the average BER, and (c) the SHO overhead versus the output threshold, $\gamma_T$, of the block change and the Full GSC schemes for various values of $L_s$ over i.i.d. Rayleigh fading channels when $L = 5, L_a = 5, L_c = 3$, and $\overline{\gamma} = 0$ dB. For comparison purpose, we also plot those for conventional $L_c/(L+L_a)$-GSC. Note that the full GSC scheme is acting as $L_c/(L+L_a)$-GSC when the output threshold becomes large. Hence, we can observe from all the sub-figures that the full GSC scheme converges to GSC as $\gamma_T$ increases.

Recall that the block change scheme has the same path estimation load as the full

GSC scheme. However, from Fig. 15 (a), we can see that the block change scheme leads to a great reduction of the SNR comparison load compared to the full GSC scheme. For example, let us consider the case that $\gamma_T > 8$ dB and $L_s = 2$. In this case, the reduction of the SNR comparison load is maximized compared to the full GSC scheme. However, from Fig. 15 (b), we can observe in the same SNR region a very slight performance loss of the Block Change scheme compared to the full GSC as well as the conventional GSC schemes.

For the SHO overhead, simulation results are also presented in Fig. 15 (c) to verify our analysis. It is clear from this figure that the receiver has a higher chance to use 2-way SHO as $L_s$ decreases. This is because as $L_s$ decreases, the probability that the sum of the $L_s$ smallest paths among the $L_c$ currently used paths from the serving BS is less than the sum of the $L_s$ strongest paths from the target BS is increasing and as such, we have a higher chance to replace groups. From this figure together with Fig. 15 (b), we can quantify the tradeoff between the SHO overhead and performance. Again, let us consider the case that $\gamma_T > 8$ dB and $L_s = 2$. In this case, note the reduction of SHO overhead at the expense of a slight performance loss in comparison to the full GSC scheme.

In Fig. 16, we plot the complexity tradeoff when $L_c = 4$. We can clearly see from this figure that using more fingers can further reduce the complexity with a slight performance loss.

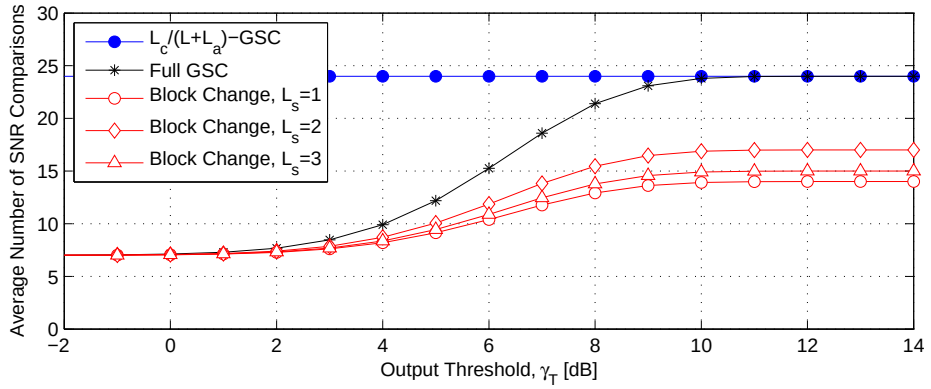


(a) Average Number of SNR Comparisons

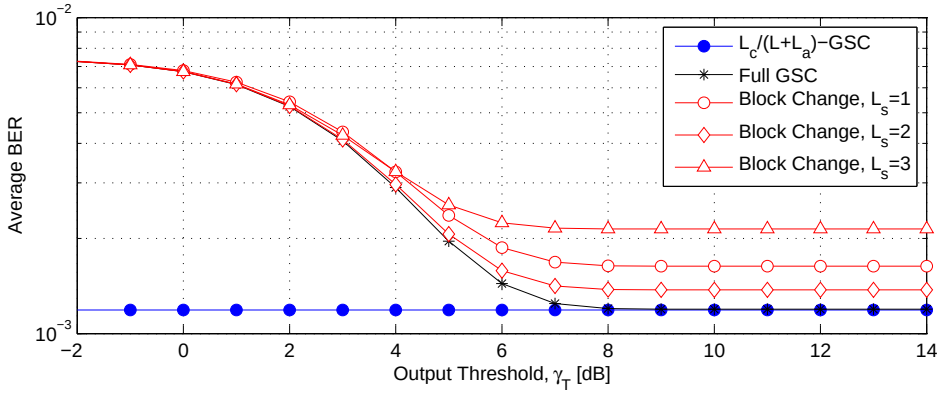


(b) Average BER

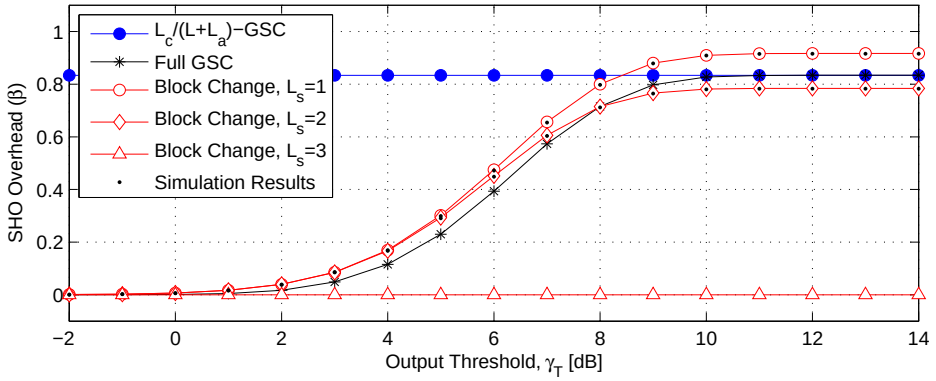


(c) SHO Overhead

Fig. 15. Complexity tradeoff versus the output threshold, $\gamma_T$, of the block change and the full GSC schemes, and conventional GSC for various values of $L_s$ over i.i.d. Rayleigh fading channels with $L = 5, L_a = 5, L_c = 3$, and $\overline{\gamma} = 0$ dB.

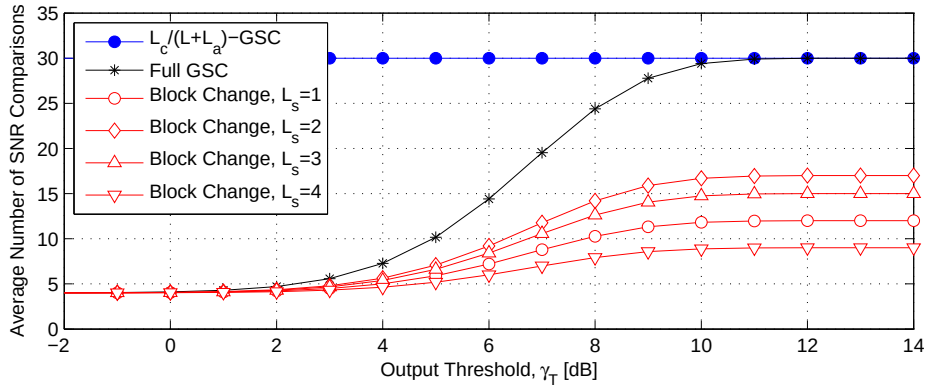


(a) Average Number of SNR Comparisons

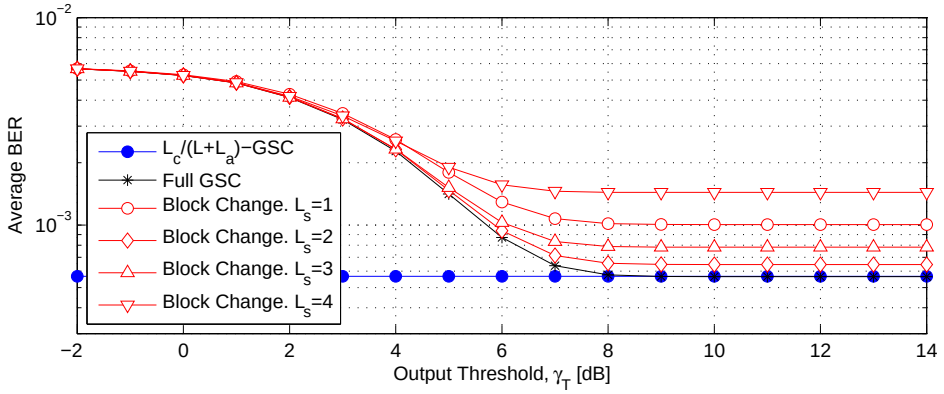


(b) Average BER

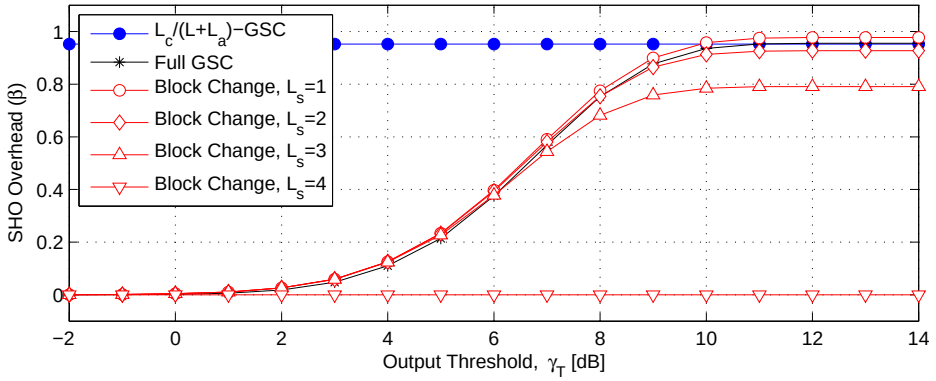


(c) SHO Overhead

Fig. 16. Complexity tradeoff versus the output threshold, $\gamma_T$, of the block change and the full GSC schemes, and conventional GSC for various values of $L_s$ over i.i.d. Rayleigh fading channels with $L = 5, L_a = 5, L_c = 4$, and $\overline{\gamma} = 0$ dB.

## F. Conclusion

In this chapter, we proposed a new finger replacement scheme for RAKE reception in the SHO region. We provided a general comprehensive framework for the assessment of the proposed scheme by offering analytical results for i.i.d. fading environments. We showed through numerical examples that the proposed scheme can save a certain amount of complexity and SHO overhead with a very slight performance loss compared to the previously proposed scheme.

# CHAPTER VI

# FINGER REPLACEMENT SCHEME WITH MULTIPLE BASE STATIONS

## A. Introduction

In Chapter V, an alternative finger selection scheme (namely the block change scheme) for the SHO region was proposed to further reduce the SHO overhead at the expense of a certain degradation in performance. With this scheme, when the output SNR falls below the target SNR, the receiver scans the additional resolvable paths from the target BS. But, unlike the full GSC scheme in Chapter III, the receiver compares the sum of the SNRs of the strongest paths among the paths from the target BS with the sum of the weakest SNRs among the currently used paths from the serving BS, and selects the better group. This block change scheme compares two blocks with equal size and as such, avoids reordering all the paths which is required for the full GSC scheme in Chapter III. Therefore, a reduction in path estimations, SNR comparisons, and SHO overhead can be obtained.

In this chapter, we generalize the results of Chapter V to the multi-BS situation. Similar to Chapter IV, we propose two scanning schemes denoted as *the full scanning scheme* and *the sequential scanning scheme*. Both scanning schemes employ block comparison instead of full GSC used in Chapter IV. For the sake of clarity, we call the proposed scheme in this chapter as *the replacement scheme* and the scheme in Chapter IV as *the reassignment scheme*.

We present a general comprehensive framework for the performance and the complexity assessment of the replacement scheme by providing analytical results for i.i.d.

fading environments[1]. More specifically, in our derivations we accurately quantify the complexity measures of interest and statistics of the receiver output SNR which are used to analyze the performance of the proposed scheme over i.i.d. fading channels.

The remainder of this chapter is organized as follows. In Section VI.B, we present the channel and system model under consideration as well as the mode of operation of the proposed scheme. Based on this mode of operation, we illustrate in Section VI.C the complexity of the proposed schemes by quantifying the average number of path estimations, the average number of SNR comparisons, and the SHO overhead. We then derive the expressions for the statistics of the combined SNR in Section VI.D. These results are next applied to the performance analysis of the proposed systems in Section VI.E. Finally, Section VI.F provides some concluding remarks.

## B. System Model

### 1. System and Channel Model

Similar to the system and channel model described in Section IV.B.1 in Page 33, we assume that in the SHO region, $N$ BSs are active and there are a total of $L_{(N)}$ resolvable paths where $L_{(N)} = \sum_{n=1}^{N} L_n$ and $L_n$ is the number of resolvable paths from the $n$th BS. Each resolvable path whose instantaneous SNR is $\gamma$ follows the same exponential distribution with the common average faded SNR, $\overline{\gamma}$.

In the SHO region, according to the mode of operation described in the next section, only $L_c$ out of $L_{(n)}, 1 \leq n \leq N$, paths are used for RAKE reception.

[1]In Chapter VII, more practical channel environments, such as non-identical/correlated fading channels and outdated channel estimation, are considered.

## 2. Mode of Operation

Without loss of generality, let $L_1$ be the number of resolvable paths from the serving BS and $L_2$, $L_3$, $\cdots$, $L_N$ be those from the target BSs. In the SHO region, the receiver is assumed at first to rely only on $L_1$ resolvable paths and as such, starts with $L_c/L_1$-GSC.

For simplicity, if we let

$$Y = \sum_{i=1}^{L_c - L_s} \gamma_{i:L_1} \tag{6.1}$$

and

$$W_n = \begin{cases} \sum_{i=L_c-L_s+1}^{L_c} \gamma_{i:L_n}, & n = 1; \\ \sum_{i=1}^{L_s} \gamma_{i:L_n}, & n = 2, \cdots, N, \end{cases} \tag{6.2}$$

where $\gamma_{i:L_n}$ is the $i$th order statistics out of $L_n$ (see [18] for terminology), then the received output SNR after GSC is given by $Y + W_1$. At the beginning of every time slot, the receiver compares the GSC output SNR, $Y + W_1$, with a certain target SNR, denoted by $\gamma_T$. If $Y + W_1$ is greater than or equal to $\gamma_T$, a one-way SHO is used and no finger replacement is needed. On the other hand, whenever $Y + W_1$ falls below $\gamma_T$, the receiver attempts a two-way SHO by starting to scan additional paths from the target BSs. More specifically, we consider two different scanning schemes described below.

### a. Case I - Full Scanning

In this case, when $Y + W_1 < \gamma_T$, the RAKE at once scans all target BSs and compares all $W_n$, that is, the sum of the $L_s$ smallest paths among the $L_c$ currently used paths from the serving BS (i.e., $W_1$) and the sums of the $L_s$ strongest paths from each target BS (i.e., $W_i, 2 \leq i \leq N$). Then, the receiver replaces $W_1$ with the largest one.

Hence, the final combined SNR, denoted by $\gamma_{Full}$, is mathematically given by

$$\gamma_{Full} = \begin{cases} Y + W_1, & Y + W_1 \geq \gamma_T; \\ Y + \max\{W_1, \cdots, W_N\}, & Y + W_1 < \gamma_T. \end{cases} \tag{6.3}$$

Note that even in the case of $Y + W_1 < \gamma_T$, no replacement will occur if $W_1 = \max\{W_1, \cdots, W_N\}$.

b. Case II - Sequential Scanning

In this case, when $Y + W_1 < \gamma_T$, the RAKE receiver estimates $L_2$ paths from the first target BS and replaces $W_1$ with $W_2$. The receiver then checks whether the combined SNR, $Y + W_2$, is above $\gamma_T$ or not. By sequentially scanning the remaining target BSs, this process is repeated until either the combined SNR, $Y + W_i, 2 \leq i \leq N$, is above $\gamma_T$ or all the $N$ BSs are examined. In the later case, since the SNRs of all the paths are known, the receiver selects the largest $W_n$. Based on this mode of operation, we can see that the final combined SNR, denoted by $\gamma_{Seq}$, is mathematically given by

$$\gamma_{Seq} = \begin{cases} Y + W_1, & Y + W_1 \geq \gamma_T; \\ Y + W_i, & Y + W_j < \gamma_T, Y + W_i \geq \gamma_T \\ & \text{for } j = 1, \cdots, i-1 \text{ and } i = 2, \cdots, N; \\ Y + \max\{W_1, \cdots, W_N\}, & Y + W_n < \gamma_T \text{ for } n = 1, \cdots, N. \end{cases} \tag{6.4}$$

C. Complexity Comparison

In this section, we look into the complexity of the proposed schemes by accurately quantifying the average number of path estimations, the average number of SNR comparisons, and the SHO overhead which are required during the SHO process of these schemes.

### 1. Average Number of Path Estimations

#### a. Case I - Full Scanning

With this scheme, the RAKE receiver estimates $L_1$ paths in the case of $Y + W_1 \geq \gamma_T$ or $L_{(N)}$ in the case of $Y + W_1 < \gamma_T$. Hence, we can easily quantify the average number of path estimations, denoted by $E_{Full}$, as

$$E_{Full} = L_1 \Pr\left[Y + W_1 \geq \gamma_T\right] + L_{(N)} \Pr\left[Y + W_1 < \gamma_T\right], \tag{6.5}$$

which reduces to

$$E_{Full} = L_1 + (L_{(N)} - L_1) F_{Y+W_1}(\gamma_T), \tag{6.6}$$

where $F_{Y+W_1}(\cdot)$ is the CDF of $L_c/L_1$-GSC output SNR.

#### b. Case II - Sequential Scanning

In this scheme, we can write the average number of path estimations, denoted by $E_{Seq}$, in the following summation form:

$$E_{Seq} = \sum_{n=1}^{N} L_{(n)} \cdot \pi_n, \tag{6.7}$$

where $\pi_n$ is the probability that $L_{(n)}$ paths are estimated. Based on the mode of operation in Section VI.B.2.b in Page 71, we have

$$\pi_n = \begin{cases} \Pr\left[Y + W_1 \geq \gamma_T\right], & n = 1; \\ \Pr[Y + W_1 < \gamma_T, \cdots, Y + W_{n-1} < \gamma_T, Y + W_n \geq \gamma_T], & 1 < n < N; \\ \Pr[Y + W_1 < \gamma_T, \cdots, Y + W_{N-1} < \gamma_T], & n = N. \end{cases} \tag{6.8}$$

Note that $W_n$ are independent while $Y + W_n$ are correlated. Hence, by conditioning on $Y$, the joint probabilities in (6.8) can be calculated as

$$\begin{aligned} &\Pr[Y + W_1 < \gamma_T, \cdots, Y + W_{n-1} < \gamma_T, Y + W_n \geq \gamma_T] \\ &= \int_0^{\gamma_T} f_Y(y) F_{W_1|Y=y}(\gamma_T - y) \left( \prod_{m=2}^{n-1} F_{W_m}(\gamma_T - y) \right) (1 - F_{W_n}(\gamma_T - y))\, dy \end{aligned} \tag{6.9}$$

and

$$\begin{aligned} &\Pr[Y + W_1 < \gamma_T, \cdots, Y + W_{N-1} < \gamma_T] \\ &= \int_0^{\gamma_T} f_Y(y) F_{W_1|Y=y}(\gamma_T - y) \prod_{m=2}^{N-1} F_{W_m}(\gamma_T - y) dy, \end{aligned} \tag{6.10}$$

respectively, where $f_Y(\cdot)$ is the PDF of $(L_c - L_s)/L_1$-GSC output SNR, $F_{W_m}(\cdot)$ and $F_{W_n}(\cdot)$ are the CDFs of $L_s/L_m$-GSC and $L_s/L_n$-GSC output SNR, respectively, and

$$F_{W_1|Y=y}(x) = \begin{cases} \frac{\int_0^x f_{Y,W_1}(y,w_1) dw_1}{f_Y(y)}, & 0 \leq x < \frac{L_s}{L_c - L_s} y; \\ 1, & x \geq \frac{L_s}{L_c - L_s} y. \end{cases} \tag{6.11}$$

Note that the general forms of the PDF and CDF of $i/j$-GSC output SNR for i.i.d. Rayleigh case are given in (3.19) and (3.20), respectively. In (6.11), $f_{Y,W_1}(\cdot,\cdot)$ is the joint PDF of two adjacent partial sums, $Y$ and $W_1$, of order statistics and can be found in (5.13). After successive substitutions from (6.11) to (6.7), we can analytically obtain the average number of path estimations.

### 2. Average Number of SNR Comparisons

As an another complexity measure, in this subsection we evaluate the average number of required SNR comparisons. Noting that the average number of SNR comparisons

for $i/j$-GSC, denoted by $C_{GSC(i,j)}$, can be obtained as

$$C_{GSC(i,j)} = \sum_{k=1}^{\min[i,j-i]} (j-k), \tag{6.12}$$

we can express the average number of SNR comparisons for the full scanning scheme and the sequential scanning scheme as

$$\begin{aligned} C_{Full} = C_{GSC(L_c,L_1)} \Pr\left[Y + W_1 \geq \gamma_T\right] + \Bigg( & C_{GSC(L_c,L_1)} + C_{GSC(L_s,L_c)} \\ & + \sum_{n=2}^{N} C_{GSC(L_s,L_n)} + C_{GSC(1,N)} \Bigg) \Pr\left[Y + W_1 < \gamma_T\right] \end{aligned} \tag{6.13}$$

and

$$\begin{aligned} C_{Seq} = {} & C_{GSC(L_c,L_1)} \Pr\left[Y + W_1 \geq \gamma_T\right] \\ & + \sum_{n=2}^{N} \left( C_{GSC(L_c,L_1)} + C_{GSC(L_s,L_c)} + \sum_{i=2}^{n} C_{GSC(L_s,L_i)} \right) \cdot \pi_n \\ & + \left( C_{GSC(L_c,L_1)} + C_{GSC(L_s,L_c)} + \sum_{i=2}^{N} C_{GSC(L_s,L_i)} \right) \cdot \phi_N + C_{GSC(1,N)} \cdot \pi_N, \end{aligned} \tag{6.14}$$

respectively, where $\pi_n$ is defined in (6.8) and

$$\phi_N = \Pr[Y + W_1 < \gamma_T, \cdots, Y + W_{N-1} < \gamma_T, Y + W_N \geq \gamma_T]. \tag{6.15}$$

### 3. SHO Overhead

The SHO overhead, denoted by $\beta$, is commonly used to quantify the SHO activity in a network and is defined as [30, Eq. (9.2)]

$$\beta = \sum_{n=1}^{2} nP_n - 1, \tag{6.16}$$

where $P_n$ is the average probability that the mobile unit uses $n$-way SHO. Note that in the proposed schemes at most two-way SHO is used and both schemes have the same

SHO overhead since in both schemes, one way SHO will be used if $Y + W_1 \geq \gamma_T$ or $Y + W_1 < \gamma_T, W_1 \geq W_i$ for $i = 2, 3, ...N$; otherwise two-way SHO is used. Therefore,

$$\beta = P_2 = 1 - P_1$$

and

$$P_1 = \Pr[Y + W_1 \geq \gamma_T] + \Pr[Y + W_1 < \gamma_T, W_1 = \max\{W_1, \cdots, W_N\}]. \quad (6.17)$$

Using the similar conditioning method, we can express the joint probability in (6.17) as

$$\begin{aligned} &\Pr[Y + W_1 < \gamma_T, W_1 = \max\{W_1, \cdots, W_N\}] \quad (6.18)\\ &= \Pr[Y + W_1 < \gamma_T, W_1 > W_2, \cdots, W_1 > W_N] \\ &= \int_0^{\gamma_T} f_{W_1}(w_1) F_{Y|W_1=w_1}(\gamma_T - w_1) \prod_{i=2}^{N} F_{W_i}(w_i) dw_i. \end{aligned}$$

Successive substitutions from (6.18) to (6.17) lead to the analytical expression for the SHO overhead as

$$\beta = F_{Y+W_1}(\gamma_T) - \int_0^{\gamma_T} f_{W_1}(w_1) F_{Y|W_1=w_1}(\gamma_T - w_1) \prod_{i=2}^{N} F_{W_i}(w_i) dw_i, \quad (6.19)$$

where $f_{W_1}(\cdot)$ is the marginal density of $W_1$ which can be obtained from the joint PDF, $f_{Y,W_1}(\cdot,\cdot)$, as

$$f_{W_1}(w_1) = \int_{\frac{L_c - L_s}{L_s} w_1}^{\infty} f_{Y,W_1}(y, w_1) dy, \quad (6.20)$$

and

$$F_{Y|W_1=w_1}(x) = \begin{cases} 0, & 0 \leq x < \frac{L_c - L_s}{L_s} w_1; \\ \frac{\int_{\frac{L_c - L_s}{L_s} w_1}^{x} f_{Y,W_1}(y, w_1) dy}{f_{W_1}(w_1)}, & x \geq \frac{L_c - L_s}{L_s} w_1. \end{cases} \quad (6.21)$$

In Fig. 17, we plot (a) the average number of path estimations, (b) the average number of SNR comparisons, and (c) the SHO overhead versus the output threshold, $\gamma_T$, of the proposed replacement scheme for various values of $L_s$ over i.i.d. Rayleigh fading channels when $N = 4, L_1 = L_2 = L_3 = L_4 = 5, L_c = 3$, and $\overline{\gamma} = 0$ dB. For comparison purpose, we also plot those for the reassignment scheme[2] proposed in Chapter IV and conventional $L_c/L_{(N)}$-GSC. Recall from Chapter IV that the reassignment scheme is acting as $L_c/L_{(N)}$-GSC when the output threshold becomes large. Hence, we can observe from all the sub-figures that the reassignment scheme converges to GSC as $\gamma_T$ increases.

Although both the replacement and reassignment schemes have almost the same path estimation load (see Fig. 17 (a)), it can be seen from Fig. 17 (b) that the replacement scheme leads to a great reduction of the SNR comparison load compared to the reassignment scheme and the amount of the reduction increases as $\gamma_T$ increases or the block size, $L_s$, decreases.

For the SHO overhead, it is clear from Fig. 17 (c) that both schemes have a higher chance to rely on the target BSs as $\gamma_T$ increases. Note that unlike the reassignment scheme, the proposed replacement scheme selects the acceptable paths from at most two BSs in any case. Hence, the maximum value of the SHO overhead for the replacement scheme is 1, which essentially leads to a reduction of the SHO overhead compared to the reassignment scheme. Also we can see that in our proposed scheme the smaller block size provides a slightly higher SHO overhead for large $\gamma_T$. This is because as $L_s$ decreases, the probability that the sum of the $L_s$ smallest paths among the $L_c$ currently used paths from the serving BS is less than the sums of the

[2]Note that the analytical results in Chapter IV are based on the approximation methods used in Chapter III. Although this approximation methods have proved to be precise, for more accurate comparison in this chapter, we use the simulation results for the reassignment scheme.

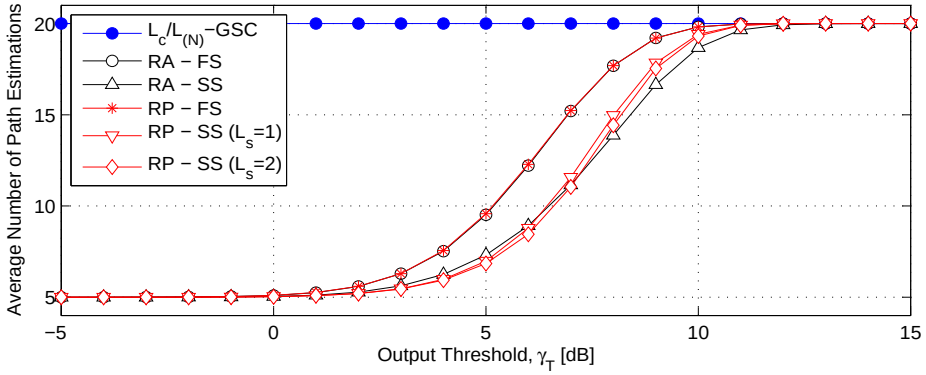


(a) Average Number of Path Estimations

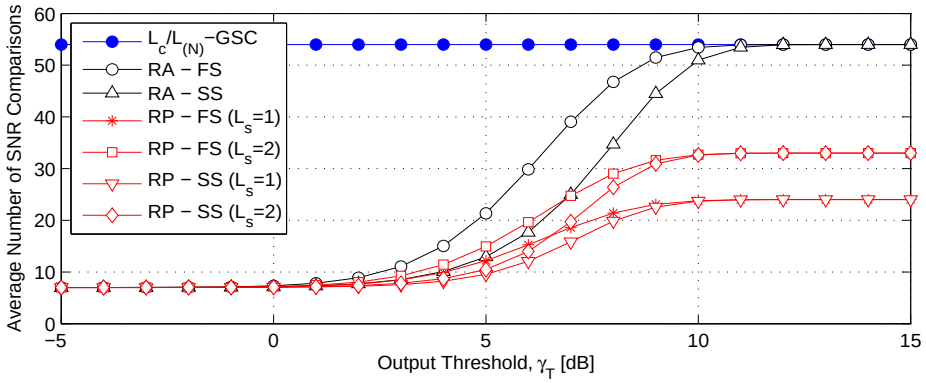


(b) Average Number of SNR Comparisons

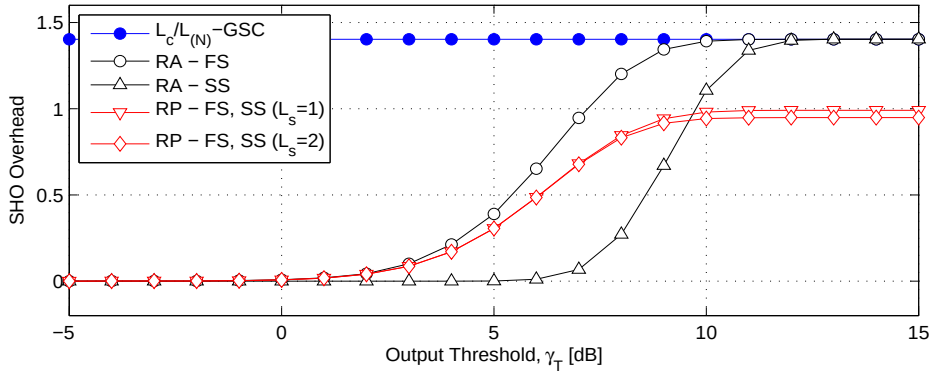


(c) SHO Overhead

Fig. 17. Complexity tradeoff versus the output threshold, $\gamma_T$, of the Reassignment (RA) and Replacement (RP) schemes with the Full Scanning (FS) and Sequential Scanning (SS), and conventional GSC over i.i.d. Rayleigh fading channels when $N = 4, L_1 = \cdots = L_4 = 5, L_c = 3$, and $\overline{\gamma} = 0$ dB.

$L_s$ strongest paths from the target BSs is increasing and as such, we have a higher chance to replace groups.

In summary, from the complexity point of view, our proposed scheme offers a big advantage over the reassignment scheme as well as conventional $L_c/L_{(N)}$-GSC especially when the output threshold, $\gamma_T$, is relatively higher than the average SNR per path, $\overline{\gamma}$. In what follows, we obtain the analytical expressions for the statistics of the output SNR, based on which we quantify the average BER of the proposed scheme and as such, a comprehensive investigation of the tradeoff between complexity and performance is feasible.

## D. Statistics of the Combined SNR

Based on the mode of operation in Section VI.B.2 in Page 70, we derive in this section the statistics of the combined SNR of the proposed scheme.

### 1. Case I - Full Scanning

From (6.3), the CDF of the combined SNR, $\gamma_{Full}$, can be written as

$$\begin{aligned} F_{\gamma_{Full}}(x) &= \Pr[\gamma_{Full} < x] \\ &= \Pr[\gamma_T \leq Y + W_1 < x] \\ &\quad + \Pr[Y + W_1 < \gamma_T, Y + \max\{W_1, \cdots, W_N\} < x]. \end{aligned} \tag{6.22}$$

Following the similar conditioning approach, we have

$$\begin{aligned} &\Pr[Y + W_1 < \gamma_T, Y + \max\{W_1, \cdots, W_N\} < x] \\ &= \int_0^{\min\{x,\gamma_T\}} f_Y(y) F_{W_1|Y=y}\left(\min\{x, \gamma_T\} - y\right) \prod_{i=2}^{N} F_{W_i}(x - y) dy. \end{aligned} \tag{6.23}$$

Substituting (6.23) into (6.22), we can obtain the analytical expression for the CDF of $\gamma_{Full}$ as

$$F_{\gamma_{Full}}(x) = \begin{cases} \int_0^x f_Y(y) F_{W_1|Y=y}(x-y) \prod_{i=2}^{N} F_{W_i}(x-y) dy, & 0 \le x < \gamma_T; \\ F_{Y+W_1}(x) - F_{Y+W_1}(\gamma_T) & \\ + \int_0^{\gamma_T} f_Y(y) F_{W_1|Y=y}(\gamma_T - y) \prod_{i=2}^{N} F_{W_i}(x-y) dy, & x \ge \gamma_T. \end{cases} \tag{6.24}$$

If we assume that the number of resolvable paths from each BS are the same (i.e., $L_1 = \cdots = L_N$), then by using the Leibnitz's rule [32, Eq. (6.40)] and differentiating (6.24) with respect to $x$, we can obtain after some manipulations the following generic expression for the PDF of the combined SNR, $\gamma_{Full}$, as

$$f_{\gamma_{Full}}(x) = \begin{cases} \int_0^x f_Y(y) \Big( f_{W_1|Y=y}(x-y) \left(F_{W_2}(x-y)\right)^{N-1} & \\ + F_{W_1|Y=y}(x-y) (N-1) (F_{W_2}(x-y))^{N-2} f_{W_2}(x-y) \Big) dy, & 0 \le x < \gamma_T; \\ f_{Y+W_1}(x) + \int_0^{\gamma_T} f_Y(y) F_{W_1|Y=y}(\gamma_T - y) & \\ \times (N-1) (F_{W_2}(x-y))^{N-2} f_{W_2}(x-y) dy, & x \ge \gamma_T, \end{cases} \tag{6.25}$$

where

$$f_{W_1|Y=y}(x) = \begin{cases} \frac{f_{Y,W_1}(y,x)}{f_Y(y)}, & 0 \le x < \frac{L_s}{L_c - L_s} y; \\ 0, & x \ge \frac{L_s}{L_c - L_s} y. \end{cases} \tag{6.26}$$

## 2. Case II - Sequential Scanning

From (6.4), the CDF of the combined SNR, $\gamma_{Seq}$, can be calculated as

$$\begin{aligned} F_{\gamma_{Seq}}(x) &= \Pr[\gamma_{Seq} < x] \\ &= \Pr[\gamma_T \le Y + W_1 < x] \\ &\quad + \sum_{i=2}^{N} \Pr[Y + W_1 < \gamma_T, \cdots, Y + W_{i-1} < \gamma_T, \gamma_T \le Y + W_i < x] \\ &\quad + \Pr[Y + W_1 < \gamma_T, \cdots, Y + W_N < \gamma_T, Y + \max\{W_1, \cdots, W_N\} < x]. \end{aligned} \tag{6.27}$$

All the joint probabilities in (6.27) can be expressed using the same conditioning approach, leading to

$$F_{\gamma_{Seq}}(x) = \begin{cases} \int_0^x f_Y(y) F_{W_1|Y=y}(x-y) \prod_{i=2}^{N} F_{W_i}(x-y) dy, & 0 \le x < \gamma_T; \\ F_{Y+W_1}(x) - F_{Y+W_1}(\gamma_T) & \\ + \sum_{i=2}^{N} \Big( \int_0^{\gamma_T} f_Y(y) F_{W_1|Y=y}(\gamma_T - y) \times & \\ \Big( \prod_{j=2}^{i-1} F_{W_j}(\gamma_T - y) \Big) \left( F_{W_i}(x-y) - F_{W_i}(\gamma_T - y) \right) \Big) dy & \\ + \int_0^{\gamma_T} f_Y(y) F_{W_1|Y=y}(\gamma_T - y) \prod_{i=2}^{N} F_{W_i}(\gamma_T - y) dy, & x \ge \gamma_T. \end{cases} \tag{6.28}$$

For $L_1 = \cdots = L_N$, we can obtain the PDF of $\gamma_{Seq}$ as

$$f_{\gamma_{Seq}}(x) = \begin{cases} \int_0^x f_Y(y) \Big( f_{W_1|Y=y}(x-y) \left( F_{W_2}(x-y) \right)^{N-1} & \\ + F_{W_1|Y=y}(x-y) (N-1) (F_{W_2}(x-y))^{N-2} f_{W_2}(x-y) \Big) dy, & 0 \le x < \gamma_T; \\ f_{Y+W_1}(x) + \int_0^{\gamma_T} f_Y(y) F_{W_1|Y=y}(\gamma_T - y) f_{W_2}(x-y) & \\ \times \frac{1 - (F_{W_2}(\gamma_T - y))^{N-1}}{1 - F_{W_2}(\gamma_T - y)} dy, & x \ge \gamma_T. \end{cases} \tag{6.29}$$

E. Average BER

In this section, we apply the results from the previous section to the performance analysis of our proposed combining schemes over i.i.d. Rayleigh fading channels. More specifically, by presenting some selected numerical examples, we examine its average BER. The average BER can be calculated by finding the expected value of the conditional probability of error. For example, the average BER for BPSK can be expressed as

$$P_b(E) = \int_0^\infty Q(\sqrt{2x}) f(x) dx, \tag{6.30}$$

where $Q(\cdot)$ is the Gaussian $Q$-function, defined as $Q(x) = \frac{1}{\sqrt{2\pi}} \int_x^\infty e^{-t^2/2} dt$ and $f(x)$ is the PDF of the combined SNR which is obtained in (6.25) for the full scanning scheme and in (6.29) for the sequential scanning scheme.

Fig. 18 presents the average BER of BPSK versus the average SNR per path, $\overline{\gamma}$, of the proposed replacement scheme with the full scanning and the sequential scanning for various values of $\gamma_T$ over i.i.d. Rayleigh fading channels when $N = 4, L_1 = L_2 = L_3 = L_4 = 5$, and $L_c = 3$. From this figure, it is clear that the higher the threshold, the better the performance, as one expects. Both scanning schemes show almost the same performance when the threshold is too small (i.e., $\gamma_T = -5$ dB) or too large (i.e., $\gamma_T = 15$ dB). We also observe that when the threshold is large, both schemes will benefit from larger $L_s$. This is because when the replacement is needed we have little benefit from the additional paths if $L_s = 1$ compared to the case of $L_s = 2$ while for the low threshold, the variation of the block size do not affect the performance since in this case that no replacement is needed. For the mid-range of the output threshold (i.e., $\gamma_T = 5$ dB), the full scanning scheme has slightly better performance than the sequential scanning scheme over the medium SNR range. However, as shown in Fig. 17, with this slight (negligible) performance loss, the sequential scanning scheme

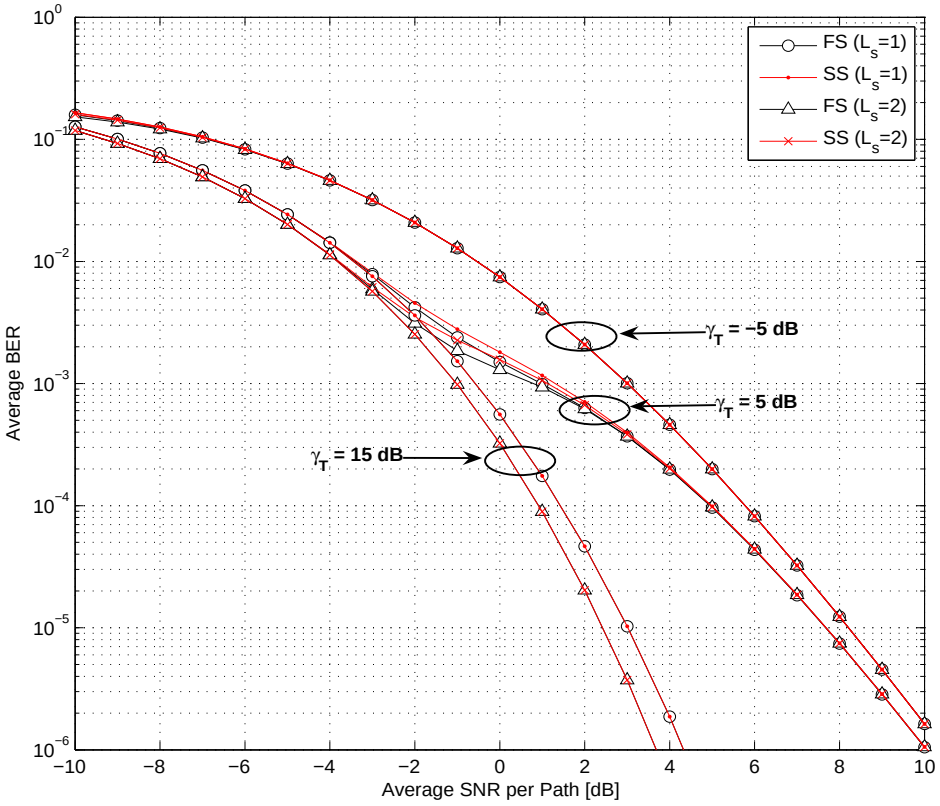


Fig. 18. Average BER of BPSK versus the average SNR per path, $\overline{\gamma}$, of the proposed scheme with the Full Scanning (FS) and Sequential Scanning (SS) for various values of $\gamma_T$ and $L_s$ over i.i.d. Rayleigh fading channels when $N = 4, L_1 = \cdots = L_4 = 5$, and $L_c = 3$.

can reduce the unnecessary path estimations and SNR comparisons compared to the full scanning scheme.

In Fig. 19, we compare the error performance of the replacement scheme to that of the reassignment scheme when $L_s = 2$ and other parameters are the same as in Fig. 18. For the full scanning scheme (Fig. 19 (a)), since the paths with largest SNR values are selected whenever needed, the reassignment scheme always provides the better performance than the replacement scheme. However, with the sequential

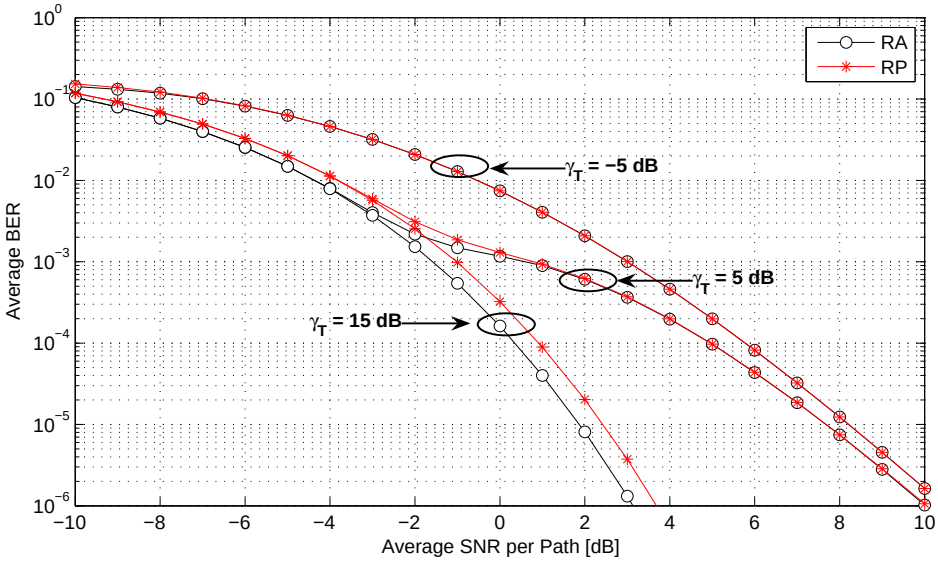


(a) Full Scanning Scheme

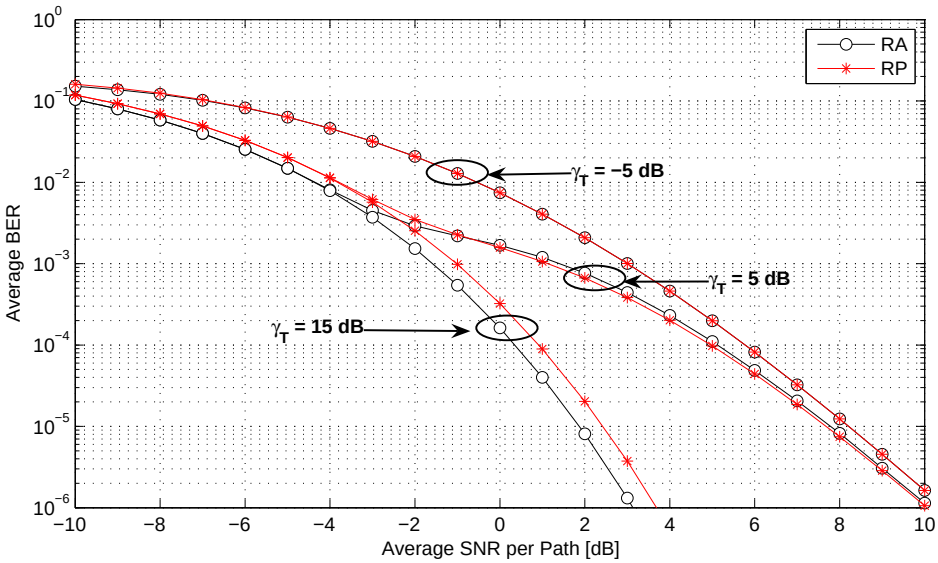


(b) Sequential Scanning Scheme

Fig. 19. Average BER of BPSK versus the average SNR per path, $\overline{\gamma}$, of the Reassignment (RA) and Replacement (RP) schemes for various values of $\gamma_T$ over i.i.d. Rayleigh fading channels when $N = 4, L_1 = \cdots = L_4 = 5, L_c = 3$, and $L_s = 2$.

scanning scheme (Fig. 19 (b)), we can observe that while the performance of the reassignment scheme is better than that of the replacement scheme for most cases, the replacement scheme performs better for the high average SNR region ($\overline{\gamma} > 0$ dB) and medium values of the threshold ($\gamma_T = 5$ dB). This can be interpreted as that in this case, in order to exceed the output threshold the replacement scheme has to scan more and more BSs and as such, there is a higher chance to acquire a block with better quality while the reassignment scheme needs less BSs to meet that threshold requirement.

## F. Conclusion

In this chapter, we generalized the finger replacement scheme proposed in Chapter V by considering two path scanning schemes : a full scanning scheme and a sequential scanning scheme. For both schemes, we provided a general comprehensive framework for the assessment of these proposed schemes by offering analytical results for i.i.d. fading environments. We showed through numerical examples that the proposed schemes can save a certain amount of complexity with a negligible performance loss compared to the previously proposed schemes.

# CHAPTER VII

# PRACTICAL STUDY OF FINGER ASSIGNMENT SCHEMES

## A. Introduction

Recall that in Chapters III and V, by considering macroscopic diversity schemes with two BSs (one serving and one target BSs), we proposed and analyzed new finger assignment schemes (namely *the full GSC scheme* in Chapter III and *the block change scheme* in Chapter V) that maintain a low complexity and reduce the usage of the network resources in the SHO region. The main idea behind these scheme is that, in the SHO region, the receiver uses the additional network resources from the target BS only if needed.

More specifically, with the full GSC scheme considered in Chapter III, whenever the received signal is unsatisfactory, the receiver scans the additional resolvable paths from the target BS and selects the strongest paths among the total available paths from both the serving and the target BSs. It has been shown that this scheme can reduce the unnecessary path estimations and the SHO overhead compared to the conventional GSC scheme in the SHO region. In Chapter V, an alternative finger selection scheme, denoted as the block change scheme, for the SHO region was proposed to further reduce the SHO overhead at the expense of a certain degradation in performance. With this scheme, when the output SNR falls below the target SNR, the receiver scans the additional resolvable paths from the target BS. But, unlike the full GSC scheme in Chapter III, the receiver compares the sum of the SNRs of the strongest paths among the paths from the target BS with the sum of the weakest SNRs among the currently used paths from the serving BS, and selects the better group. This scheme compares two blocks with equal size and as such, avoids reordering all

the paths which is required for the full GSC scheme. Therefore, a reduction in path estimations, SNR comparisons, and SHO overhead can be obtained.

The schemes proposed in Chapters III and V were generalized to the multi-BS situation in Chapters IV and VI, respectively, by developing two different path scanning schemes denoted as *the full scanning scheme* and *the sequential scanning scheme*. With the full scanning scheme, whenever the received signal becomes unsatisfactory, the RAKE receiver scans all the available paths from all potential target BSs while with the sequential scanning scheme, the RAKE receiver sequentially scans the target BSs until the combined SNR is satisfactory or all potential target BSs are scanned. For the sake of clarity, we called the proposed scheme in Chapter IV as *the reassignment scheme* and the scheme in Chapter VI as *the replacement scheme*.

For analytical tractability, Chapters III-VI assumed i.i.d. Rayleigh fading channels and perfect channel estimation, and as such, these chapters were able to offer (i) some closed-form expressions for the statistics of the output SNR and (ii) analytical-based study of the tradeoff among error performance, SNR comparison and path estimation load, and SHO overhead. However, there are a number of real-life scenarios in which this i.i.d. assumption in is not valid especially in multi-path diversity over frequency-selective channels, and as such, the study on the impact of various realistic fading channels is very important.

In this chapter, we look into the schemes proposed in Chapters III-VI in more practical fading environments. More specifically, we consider through various computer simulations the effects of path unbalance as well as path correlation on the performance. The impact of outdated or imperfect channel estimation is also investigated. The main contribution of this chapter is to present a general comprehensive framework for the performance evaluation of the proposed schemes for non-i.i.d. fading channels and under outdated/imperfect channel estimates. We show that pro-

posed schemes are also applicable to practical fading conditions. More importantly, the simulation results show that the block change/replacement scheme shows in comparison to the full GSC/reassignment scheme a considerable robustness to channel estimation errors.

This chapter organized as follows. In Section VII.B, we present the channel model under consideration. More specifically we consider the effect of path unbalance/correlation and outdated/imperfect channel estimates. In Section VII.C, we compare the average BER performance of the schemes proposed in Chapters III-VI over practical channel environments. Finally, Section VII.D provides some concluding remarks.

## B. Channel Model

### 1. Effect of Path Unbalance/Correlation

In practice, the i.i.d. fading scenario on the diversity paths is not always realistic due to, for example, the different adjacent multi-path routes with path-loss and the resulting unbalance and correlation among paths. We assess through the computer simulations the effect of non-identically distributed paths with correlation on the performance of the proposed schemes. More specifically, instead of the uniform power delay profile (PDP) considered so far, we now consider an exponentially decaying PDP, for which $\overline{\gamma}_j = \overline{\gamma}_1 e^{-\delta(j-1)}$ where $\overline{\gamma}_j$ is the average SNR of the $j$-th path out of total available resolvable paths from each BS and $\delta$ is the average fading power decaying factor. For the correlated paths, we consider the constant and exponential correlation models. For the constant correlation model, the same power correlation coefficient, $\rho \in [0, 1]$, is assumed between all the path pairs while the exponential correlation model assumes an exponential power correlation coefficient, $\rho^{|j-j'|}$, between

any pair of paths, $\gamma_j$ and $\gamma_{j'}$. Note that $\delta = 0$ means identically distributed paths and $\rho = 0$ means independent fading paths. When we set $\delta = 0$ and $\rho = 0$, we revert to the i.i.d. fading channels.

### 2. Effect of Outdated or Imperfect Channel Estimations

In general, diversity combining techniques rely, to a large extent, on accurate channel estimation. As a typical first step in performance analysis, perfect estimation was assumed so far. However, in practice these estimates must be obtained in the presence of noise and time delay. Hence, the effects of channel estimation error or channel decorrelation on the performance of diversity systems is of interest. We study the effect of outdated or imperfect channel estimates on the performance. For simplicity, all the diversity paths are assumed to be i.i.d. Let $\gamma_i^\tau$ be the estimated received signal power. Due to imperfect or outdated channel estimates, $\gamma_i^\tau$ may or may not be the same as $\gamma_i$. Hence, we can assume that $\gamma_i^\tau$ is the correlated sample from $\gamma_i$ with a power correlation factor, $\rho^\tau \in [0, 1]$, between $\gamma_i$ and $\gamma_i^\tau$. Here, $\rho^\tau$ can be viewed as a measure of channel fluctuation rate and a measure of the channel estimation quality as well. As an example, from the well-known Clark's model, we know $\rho^\tau = J_0^2(2\pi f_D \tau)$ [3, Section 2.1.1] where $J_0()$ is the zero-order Bessel function of the first kind, $\tau$ is the time delay, and $f_D$ is the maximum Doppler frequency shift. Note that $\rho^\tau = 0$ means completely outdated channel estimates while $\rho^\tau = 1$ an up-to-date and perfect channel estimates.

## C. BER Comparison

### 1. Full GSC vs. Block Change

In Fig. 20, we plot the average BER of BPSK versus $\overline{\gamma}_1$ of the full GSC and the block change schemes over an exponentially decaying PDP with (a) an exponential correlation and (b) a constant correlation across the multi-paths. In all cases, the full GSC scheme shows a slightly better performance as observed in the i.i.d. case analyzed in Chapter V (see Fig. 13). These results also show that PDP induces a non-negligible degradation in the performance and therefore must be taken into account for the accurate prediction of the performance of proposed schemes. Moreover, we can observe that constant correlation suffers a minor performance degradation in comparison to exponential correlation.

Fig. 21 compares the effect of the correlation factor, $\rho^\tau$, on the average BER of BPSK of the full GSC and the block change schemes for several values of the output threshold, $\gamma_T$, over i.i.d. Rayleigh fading channels. We can see from these curves that in all cases the diversity gain offered by the proposed schemes decreases as $\rho^\tau$ decreases, as expected. It is very notable that contrary to the analysis over perfect channel estimations, the block change scheme shows a lower error probability than the full GSC scheme when $\rho^\tau = 0$ and 0.5 for $\gamma_T = 5$ and 15 dB. Recall that the block change scheme compares two sums of paths from the serving and target BSs while the full GSC scheme relies on the SNR of each path. Therefore, the block change scheme is more robust to the channel estimation errors especially when the comparisons of the two sums are needed. In other words, the more often the combined SNR is below the threshold, the less sensitive to the channel estimation error the block change scheme is while the more sensitive the full GSC scheme is.

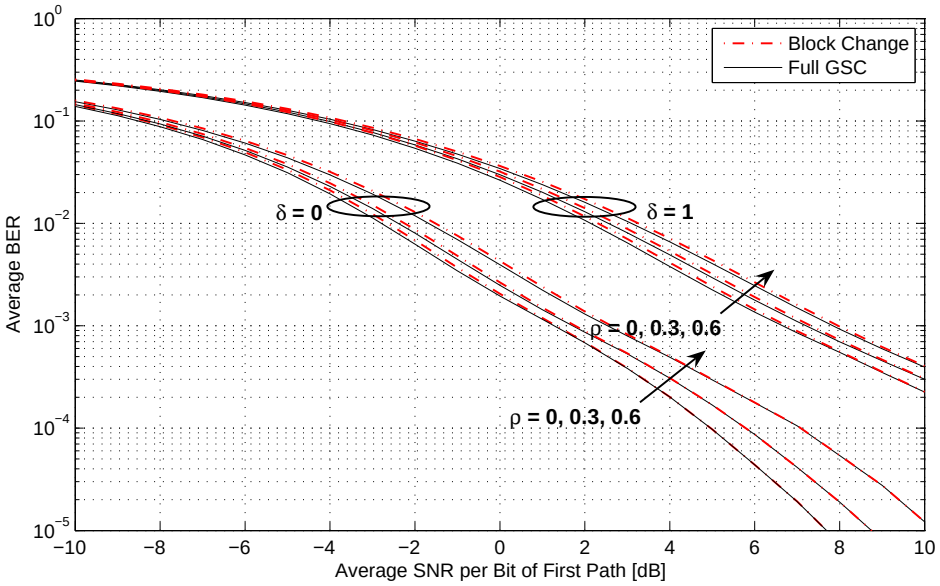


(a) Exponential Correlation

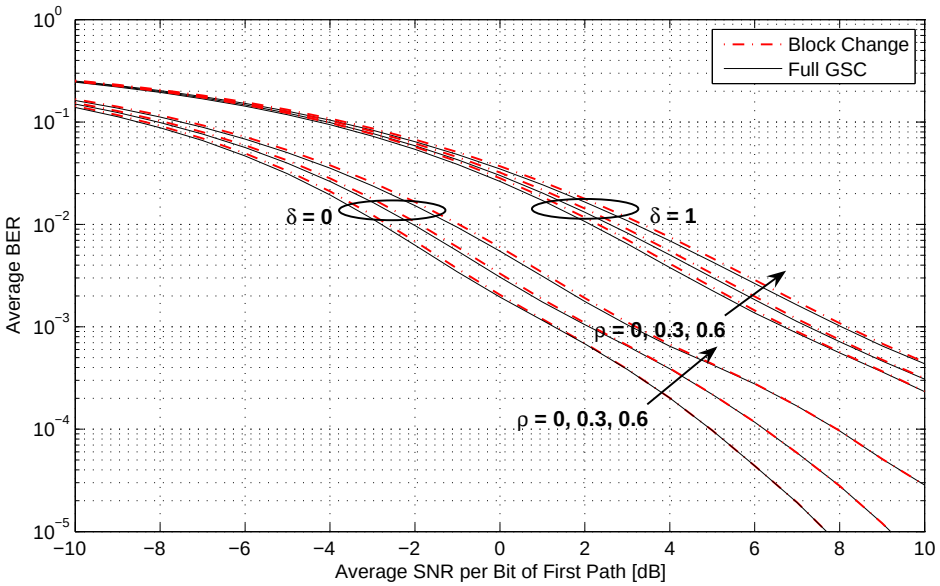


(b) Constant Correlation

Fig. 20. Average BER of BPSK versus the average SNR of first path, $\overline{\gamma}_1$, of the block change and the full GSC schemes over non-identical/correlated Rayleigh fading channels when $L = 5, L_a = 5, L_c = 3, L_s = 2$, and $\gamma_T = 5$ dB.

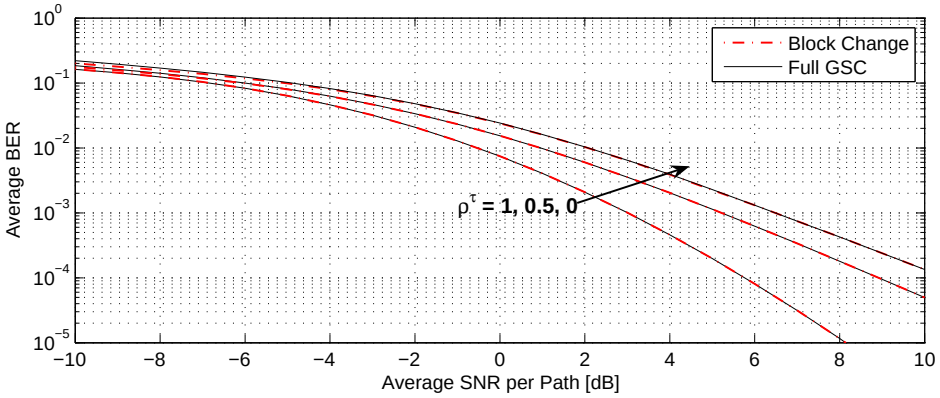


(a) $\gamma_T = -5$ dB

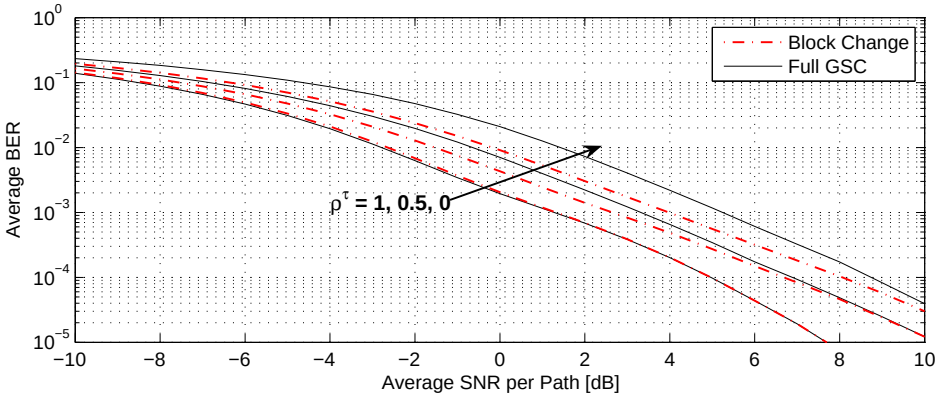


(b) $\gamma_T = 5$ dB

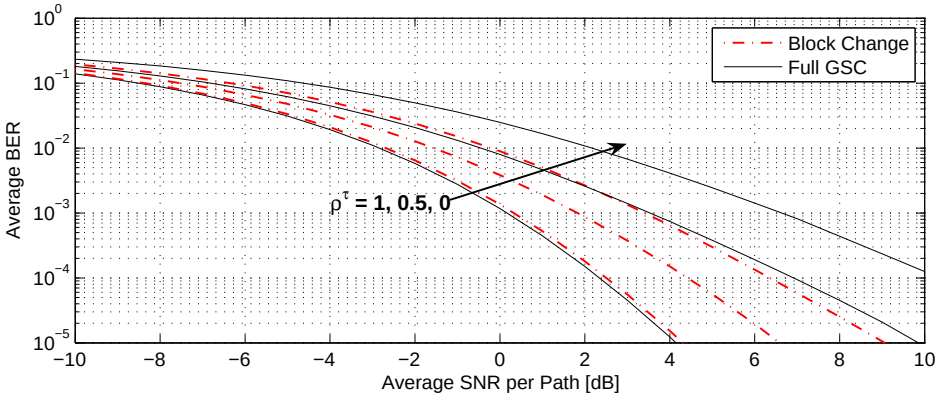


(c) $\gamma_T = 15$ dB

Fig. 21. Average BER of BPSK versus the average SNR per path, $\overline{\gamma}$, of the block change and the full GSC schemes with outdated channel estimation over i.i.d. Rayleigh fading channels when $L = 5, L_a = 5, L_c = 3$, and $L_s = 2$.

### 2. Reassignment vs. Replacement

In Fig. 22, we plot the average BER of BPSK versus $\overline{\gamma}_1$ of the replacement and the reassignment schemes over an exponentially decaying PDP with an exponential correlation across the multi-paths. These results show that the PDP and the correlation among paths induce a non-negligible degradation in the performance and therefore must be taken into account for the accurate prediction of the performance of proposed schemes. In all cases, we can see the same relationship between the replacement and the reassignment schemes as observed in Chapter VI (see Fig. 19).

Fig. 23 compares the effect of the correlation factor, $\rho^{\tau}$, on the average BER of BPSK of the replacement and the reassignment schemes with the full scanning for several values of the output threshold, $\gamma_T$, over i.i.d. Rayleigh fading channels. We can see from these curves that in all cases the diversity gain offered by the proposed schemes decreases as $\rho^{\tau}$ decreases, as expected. It is very notable that contrary to the analysis over perfect channel estimations, the replacement scheme shows a lower error probability than the reassignment scheme when $\rho^{\tau} = 0$ and 0.5 for $\gamma_T = 5$ and 15 dB. Recall that the replacement scheme compares two sums of paths from the serving and target BSs while the reassignment scheme relies on the SNR of each path. Therefore, the replacement scheme is more robust to the channel estimation errors especially when the comparisons of the two sums are needed. In other words, the more often the combined SNR is below the threshold, the less sensitive to the channel estimation error the replacement scheme is while the more sensitive the reassignment scheme is.

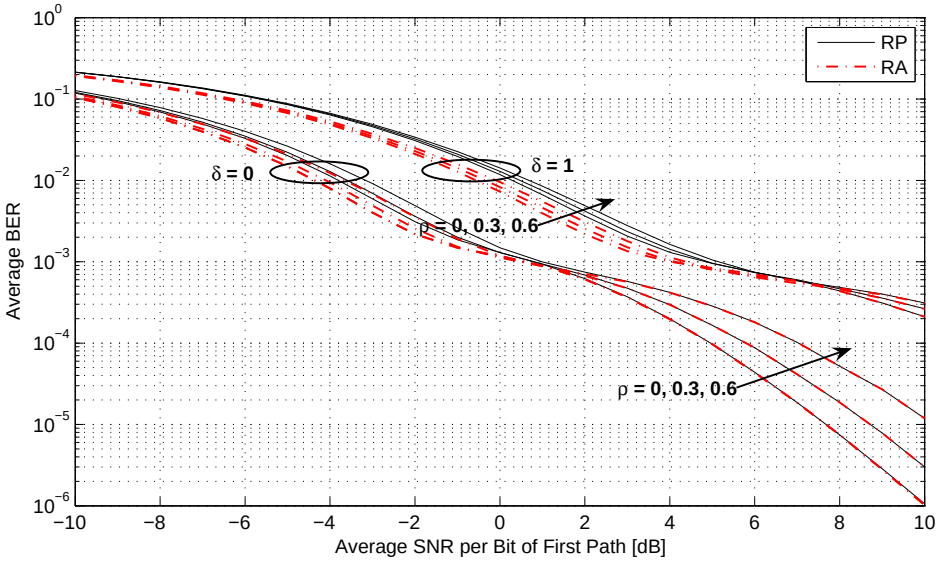


(a) Full Scanning Scheme

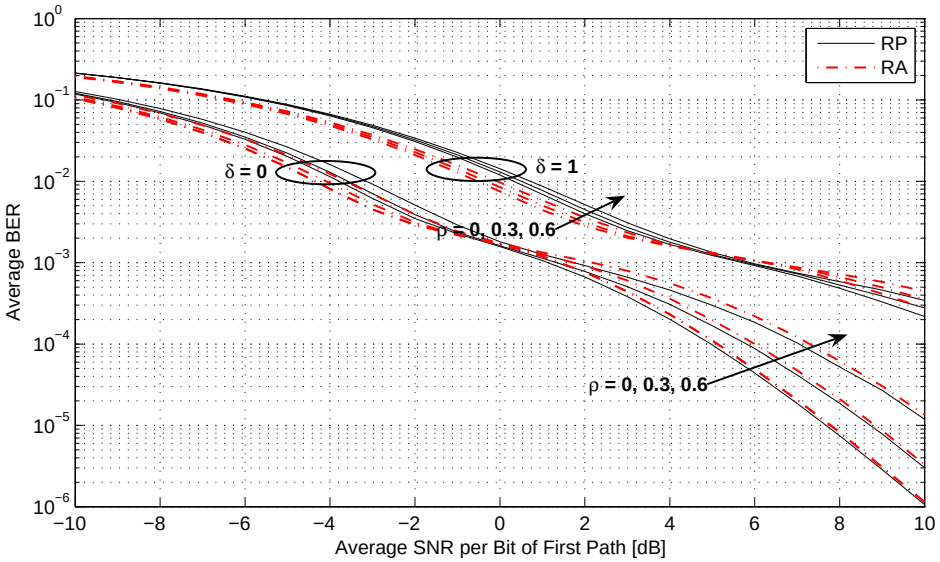


(b) Sequential Scanning Scheme

Fig. 22. Average BER of BPSK versus the average SNR of first path, $\overline{\gamma}_1$, of the Reassignment (RA) and Replacement (RP) schemes over non-identical/exponentially correlated Rayleigh fading channels when $N = 4, L_1 = \cdots = L_4 = 5, L_c = 3, L_s = 2$, and $\gamma_T = 5$ dB.

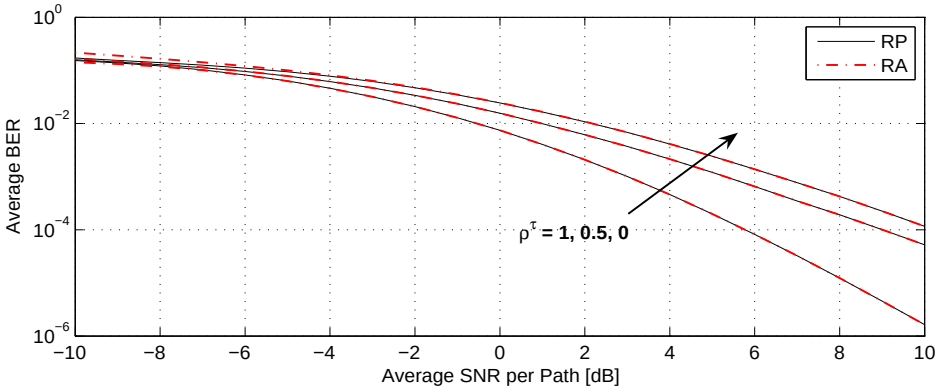


(a) $\gamma_T = -5$ dB

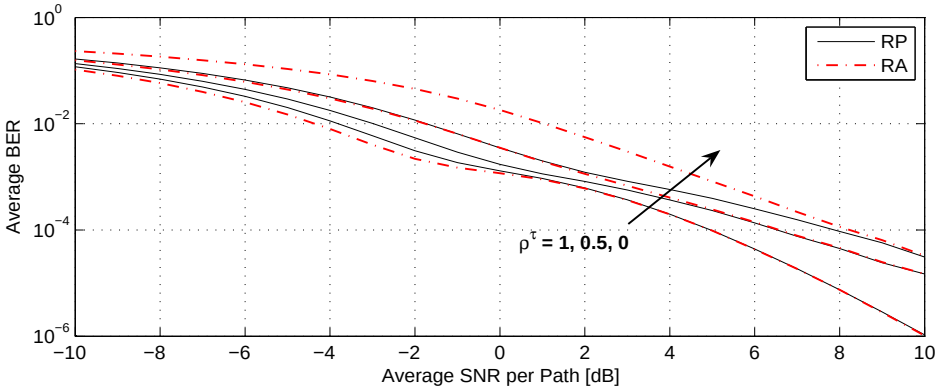


(b) $\gamma_T = 5$ dB

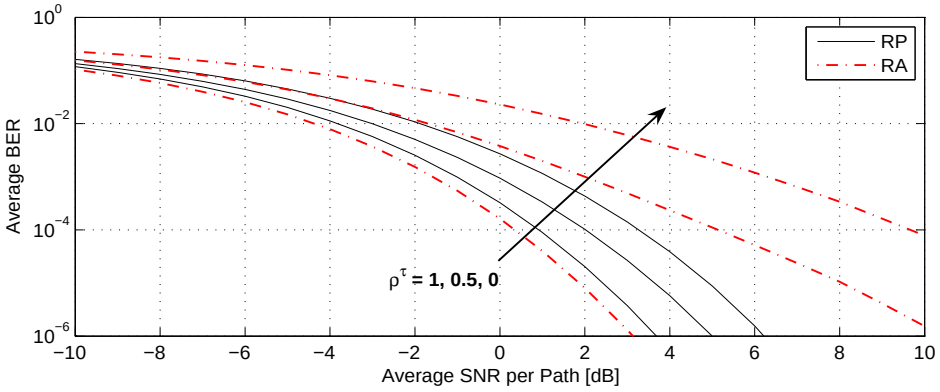


(c) $\gamma_T = 15$ dB

Fig. 23. Average BER of BPSK versus the average SNR per path, $\overline{\gamma}$, of the Reassignment (RA) and Replacement (RP) schemes for the full Scanning with outdated channel estimation over i.i.d. Rayleigh fading channels when $N = 4, L_1 = \cdots = L_4 = 5, L_c = 3$, and $L_s = 2$.

## D. Conclusion

In this chapter, we examined the effects of various practical considerations on the performance of some newly proposed finger assignment schemes for RAKE reception in the SHO region which were previously analyzed over ideal i.i.d. fading environments in Chapters III-VI. Through computer simulations, we considered the impact of an exponentially decaying PDP as well as a fading correlation among paths. The effect of outdated or imperfect channel estimations was also evaluated. In summary, with the analytical methods presented in Chapters III-VI and the simulation results presented in this chapter, we are providing a general comprehensive framework for the assessment of the proposed finger assignment schemes.

# CHAPTER VIII

# FINGER MANAGEMENT SCHEME FOR MINIMUM CALL DROP

## A. Introduction

Bearing in mind that our previous efforts focused on schemes that minimize the use of network resources, we consider in this chapter other finger management schemes that are designed to minimize call drops. More specifically, we propose two finger management schemes denoted by *distributed GSC* and *distributed MS GSC* schemes. The main idea behind these newly proposed schemes is that they try to "balance" SNR/paths among as many BSs as possible so that if the mobile unit ends up loosing connection with one BS (due for example to the corner effect), we can keep a great proportion of the total initially combined SNR and as such, minimize the possibility of call drops. With distributed GSC, we apply the conventional GSC scheme to each BS by distributing the combined paths among the active BSs. On the other hand, with distributed MS GSC, we apply the conventional MS GSC to each BS by distributing the combined paths. The main contribution of this chapter is to provide an analytical framework deriving the average error probability of our proposed schemes. Some selected numerical results show that our proposed schemes considerably outperform the conventional ones when there is a high chance of loosing a BS.

The remainder of this chapter is organized as follows. In Section VIII.B, we present the channel and system model under consideration as well as the mode of operation of the proposed schemes. Based on this mode of operation, we derive the expressions for the average error rate of the proposed schemes in Section VIII.C. Section VIII.D quantifies the average number of combined paths of the proposed distributed MS GSC scheme to investigate the tradeoff between complexity and per-

formance. Finally, Section VIII.E provides some concluding remarks.

## B. System Model

### 1. System and Channel Model

With the same system and channel model in Section III.B.1 in Page 11, we further assume that there are $L_1$ and $L_2$ available paths from BS1 and BS2, respectively. In the SHO region, according to the mode of operation described in the next section, at most $L_c$ out of the $L_1 + L_2$ available paths are used for RAKE reception.

### 2. Mode of Operation

We distinguish the combined SNRs from each BS by letting $\gamma_{B_1}$ and $\gamma_{B_2}$ be the combined SNRs of the paths from BS1 and BS2, respectively. In both schemes, we assume first that the receiver estimates all the resolvable paths.

#### a. Distributed GSC

With this scheme, the receiver selects and combines the $L_{c_1}$ largest paths among $L_1$ ones and the $L_{c_2}$ largest paths among $L_2$ ones, respectively, where $L_{c_1} + L_{c_2} = L_c\,(\leq L_1, L_2)$. Hence, $\gamma_{B_1}$ and $\gamma_{B_2}$ are the combined output SNRs of $L_{c_1}/L_1$-GSC and $L_{c_2}/L_2$-GSC, respectively.

#### b. Distributed MS GSC

With this scheme, the receiver selects the least number of the best paths such that the combined SNRs, $\gamma_{B_1}$ and $\gamma_{B_2}$, are greater than the predetermined thresholds, $\gamma_{T_1}$ and $\gamma_{T_2}$, respectively. More specifically, starting from the best path from BS1, the receiver tries to increase the combined SNR, $\gamma_{B_1}$, above the threshold, $\gamma_{T_1}$, by combining an

increasing number of diversity paths. This process is performed until either $\gamma_{B_1}$ is above $\gamma_{T_1}$ or the best $L_{c_1}$ paths out of $L_1$ ones are combined. In the later case, the receiver acts as a traditional $L_{c_1}/L_1$-GSC combiner. The same algorithm is applied to BS2 along with the chosen design parameters, $L_{c_2}$ and $\gamma_{T_2}$, where $\gamma_{T_1} + \gamma_{T_2} = \gamma_T$ and $\gamma_T$ is the final output threshold. Hence, $\gamma_{B_1}$ and $\gamma_{B_2}$ are the combined output SNRs of $L_{c_1}/L_1$-MS GSC and $L_{c_2}/L_2$-MS GSC, respectively.

It is important to note that, in both conventional and proposed distributed schemes, while it is of course clear that MS GSC is always outperformed by GSC, MS GSC will use on average less number of combined paths to reach a certain threshold and as such, save the processing power on the mobile units receiving data on the down-link. In addition, in comparison to the conventional schemes, the proposed distributed schemes with minimum call drop criterion will show better performance when the signals coming from one BS are completely lost. In the next section, we investigate this issue by exactly quantifying the average error rate of the proposed schemes in terms of the probabilities of loosing BSs.

## C. Average BER

In this section, we analyze the average error rate of the proposed schemes. If we assume that $P_1$ and $P_2$ are the probabilities of loosing BS1 and BS2, respectively, then the final combined SNR, denoted by $\gamma_t$, is mathematically given by

$$\begin{aligned}\gamma_t &= (1-P_1)(1-P_2)(\gamma_{B_1}+\gamma_{B_2}) + (1-P_1)P_2\gamma_{B_1} + (1-P_2)P_1\gamma_{B_2} \qquad (8.1)\\ &= (1-P_1)\gamma_{B_1} + (1-P_2)\gamma_{B_2}.\end{aligned}$$

Note that although we consider two BSs for the illustration purpose, an extension to multi-BS case is straightforward[1]. Since two random variables, $(1-P_1)\gamma_{B_1}$ and $(1-P_2)\gamma_{B_2}$, in (8.1) are independent, we can express the MGF of $\gamma_t$ as a product of the MGFs of these two random variables as

$$\begin{aligned}\mathcal{M}_{\gamma_t}(s) &= \mathcal{M}_{(1-P_1)\gamma_{B_1}}(s)\cdot\mathcal{M}_{(1-P_2)\gamma_{B_2}}(s) \\ &= \mathcal{M}_{\gamma_{B_1}}((1-P_1)s)\cdot\mathcal{M}_{\gamma_{B_2}}((1-P_2)s).\end{aligned} \tag{8.2}$$

The MGF-based method for the evaluation of the average error rate over fading channels can be used [5, Sec. 9.2.3]. For example, the average BER of BPSK signals is given by

$$\begin{aligned}P_B(E) &= \frac{1}{\pi}\int_0^{\pi/2}\mathcal{M}_{\gamma_t}\left(\frac{-1}{\sin^2\phi}\right)d\phi \\ &= \frac{1}{\pi}\int_0^{\pi/2}\mathcal{M}_{\gamma_{B_1}}\left(\frac{P_1-1}{\sin^2\phi}\right)\mathcal{M}_{\gamma_{B_2}}\left(\frac{P_2-1}{\sin^2\phi}\right)d\phi.\end{aligned} \tag{8.3}$$

### 1. Distributed GSC

With the distributed GSC scheme, the MGFs, $\mathcal{M}_{\gamma_{B_1}}(\cdot)$ and $\mathcal{M}_{\gamma_{B_2}}(\cdot)$, in (8.3) are the MGFs of the $L_{c_1}/L_1$-GSC and $L_{c_2}/L_2$-GSC output SNRs, respectively. The general form of the MGF of $l/L$-GSC for independent and identically distributed (i.i.d.) Rayleigh case can be found in [5, Eq. (9.430)] as

$$\mathcal{M}_{GSC}(s) = (1-\overline{\gamma}s)^{-l+1}\sum_{j=0}^{L-l}\frac{(-1)^j\binom{L}{l}\binom{L-l}{j}}{1+\frac{j}{l}-\overline{\gamma}s}. \tag{8.4}$$

After substitution of (8.4) into (8.3) and some manipulations, (8.3) specializes

[1]For example, in the case of $N$ BSs, $\gamma_t = \sum_{n=1}^{N}(1-P_n)\gamma_{B_n}$ where $P_n$ is the probability of loosing $n$th BS and $\gamma_{B_n}$ is the combined SNR of the paths from the $n$th BS.

to

$$P_B(E) = \binom{L_1}{L_{c_1}} \binom{L_2}{L_{c_2}} \sum_{i=0}^{L_1-L_{c_1}} \sum_{j=0}^{L_2-L_{c_2}} (-1)^{i+j} \binom{L_1-L_{c_1}}{i} \binom{L_2-L_{c_2}}{j} \times \frac{1}{(1+i/L_{c_1})(1+j/L_{c_2})} \frac{1}{\pi} \int_0^{\frac{\pi}{2}} \prod_{n=1}^{4} \left( \frac{\sin^2\phi}{\sin^2\phi + c_n} \right)^{r_n} d\phi, \tag{8.5}$$

where

$$c_1 = \frac{(1-P_1)\overline{\gamma}}{1+i/L_{c_1}}, \quad c_2 = \frac{(1-P_2)\overline{\gamma}}{1+j/L_{c_2}}, \quad c_3 = (1-P_1)\overline{\gamma}, \quad c_4 = (1-P_2)\overline{\gamma},$$

$$r_1 = 1, \quad r_2 = 1, \quad r_3 = L_{c_1} - 1, \quad r_4 = L_{c_2} - 1.$$

Since the integral in (8.5) can be found in closed form (see [5, Eq. (5A.74)]), (8.5) presents the final desired closed-form result for the average BER of the distributed GSC scheme.

Fig. 24 shows the average BER of BPSK of the proposed distributed GSC scheme as a function of the average SNR per path, $\overline{\gamma}$, over i.i.d. Rayleigh fading channels. For comparison purpose, we also plot through computer simulations the average BER of the conventional GSC scheme. Note that the conventional GSC scheme acts as $L_c/(L_1+L_2)$-GSC where $L_c = L_{c_1} + L_{c_2}$ while the distributed GSC scheme uses the combinational form of $L_{c_1}/L_1$-GSC and $L_{c_2}/L_2$-GSC, and as such, a certain number of paths from one BS are always secured. Therefore, we can clearly see from this figure that by evenly distributing paths to BSs, the distributed GSC scheme shows a comparable or better performance in comparison to the conventional GSC scheme especially when the probability of loosing one BS is increasing. To better illustrate the benefit of our proposed scheme, we present in Fig. 25 the average BER in terms of the probability of loosing BS2, $P_2$, for fixed values of $\overline{\gamma}$. We can observe from this figure that, for example, for our chosen set of parameters, the proposed distributed scheme outperforms the conventional scheme when $P_2 > 0.5$.

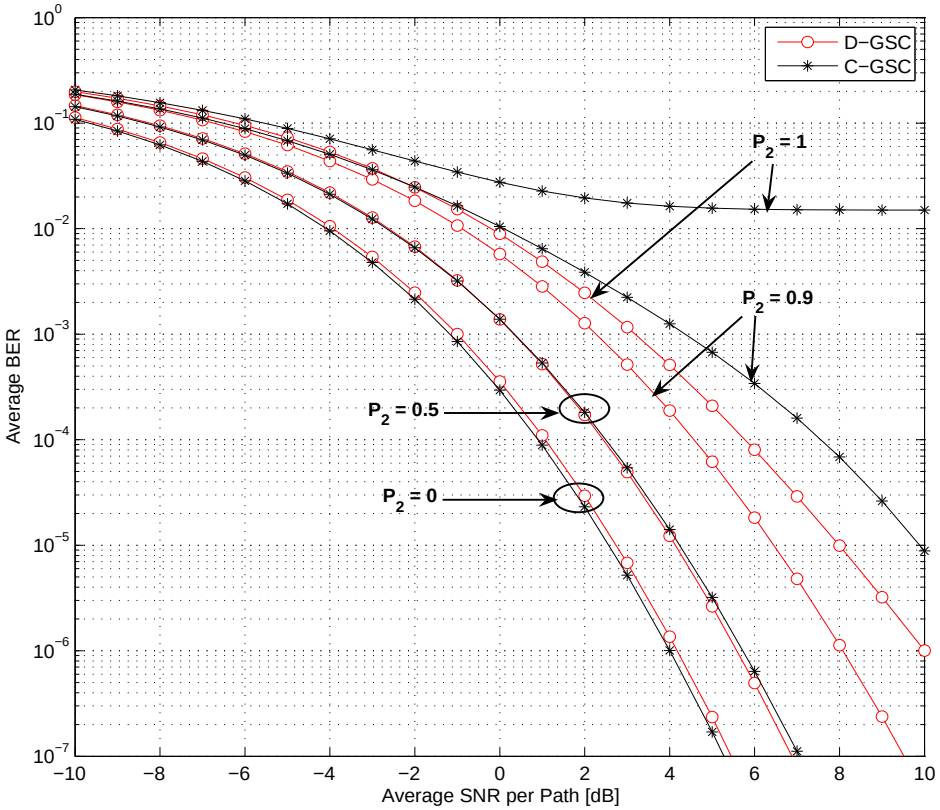


Fig. 24. Average BER of BPSK versus the average SNR per path, $\overline{\gamma}$, of distributed GSC (D-GSC) and conventional GSC (C-GSC) for various values of $P_2$ over i.i.d. Rayleigh fading channels when $L_1 = L_2 = 6, L_{c_1} = L_{c_2} = 2$, and $P_1 = 0$.

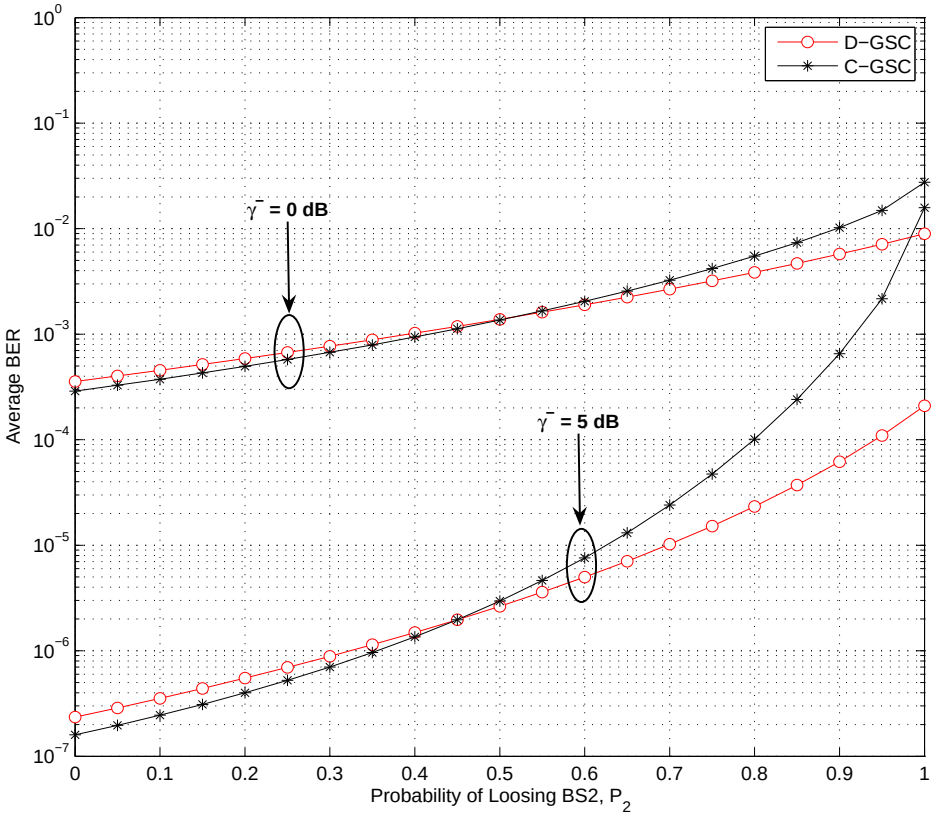


Fig. 25. Average BER of BPSK versus the probability of loosing BS2, $P_2$, of distributed GSC (D-GSC) and conventional GSC (C-GSC) for various values of $\overline{\gamma}$ over i.i.d. Rayleigh fading channels when $L_1 = L_2 = 6, L_{c_1} = L_{c_2} = 2$, and $P_1 = 0$.

## 2. Distributed MS GSC

Similar to the distributed GSC scheme, we just need to replace the MGFs, $\mathcal{M}_{\gamma_{B_1}}(\cdot)$ and $\mathcal{M}_{\gamma_{B_2}}(\cdot)$, in (8.3) with the MGFs of the $L_{c_1}/L_1$-MS GSC and $L_{c_2}/L_2$-MS GSC output SNRs, respectively. The general form of the MGF of $l/L$-MS GSC for i.i.d. Rayleigh case is given by [23, Eq. (35)][2]

$$\begin{aligned}
&\mathcal{M}_{MSGSC}(s) \qquad (8.6)\\
&= L\sum_{j=0}^{L-1}\binom{L-1}{j}(-1)^j\frac{e^{-\left(\frac{1+j}{\overline{\gamma}}-s\right)\gamma_T}}{1+j-\overline{\gamma}s}+\sum_{i=2}^{l}\binom{L}{i}\left[\sum_{m=0}^{i-1}\frac{(1-i)^m}{(i-1-m)!}\left(\frac{i\gamma_T}{\overline{\gamma}}\right)^{i-1-m}\right.\\
&\times\mathcal{G}_0(s)+\sum_{j=1}^{L-i}\binom{L-i}{j}(-1)^{j-i+1}\left(\frac{i}{j}\right)^{i-1}\left(\frac{e^{-\left(\frac{1+j/i}{\overline{\gamma}}-s\right)\gamma_T}-e^{-\left(\frac{1+j/i}{\overline{\gamma}}-s\right)\frac{i}{i-1}\gamma_T}}{1+j/i-\overline{\gamma}s}\right.\\
&\left.\left.-\sum_{k=0}^{i-2}\sum_{m=0}^{k}\frac{\left(\frac{i-1}{i}j\right)^m\left(-j\frac{\gamma_T}{\overline{\gamma}}\right)^{k-m}\mathcal{G}_j(s)}{(k-m)!}\right)\right]+\binom{L}{l}\left[\mathcal{F}_l(s)+\sum_{i=1}^{L-l}\binom{L-l}{i}\right.\\
&\left.\times(-1)^{l+i-1}\left(\frac{l}{i}\right)^{l-1}\left(\frac{1-e^{-\left(\frac{1+i/l}{\overline{\gamma}}-s\right)\gamma_T}}{1+i/l-\overline{\gamma}s}-\sum_{m=0}^{l-2}\left(-\frac{i}{l}\right)^m\mathcal{F}_{m+1}(s)\right)\right],
\end{aligned}$$

where

$$\mathcal{G}_x(s)=e^{x\frac{\gamma_T}{\overline{\gamma}}}\frac{\Gamma\left[m+1,\left(\frac{1+x}{\overline{\gamma}}-s\right)\gamma_T\right]-\Gamma\left[m+1,\left(\frac{1+x}{\overline{\gamma}}-s\right)\frac{i}{i-1}\gamma_T\right]}{m!(1+x-\overline{\gamma}s)^{m+1}}, \qquad (8.7)$$

$$\mathcal{F}_x(s)=\frac{\Gamma[x]-\Gamma\left[x,\left(\frac{1}{\overline{\gamma}}-s\right)\gamma_T\right]}{(x-1)!(1-\overline{\gamma}s)^x}, \qquad (8.8)$$

and $\Gamma[\cdot]$ and $\Gamma[\cdot,\cdot]$ are the complete and the incomplete gamma functions, respectively, defined as [31, Sec. 8.3]

$$\Gamma[\alpha]=\int_0^\infty e^{-t}t^{\alpha-1}dt, \quad \Gamma[\alpha,\beta]=\int_\beta^\infty e^{-t}t^{\alpha-1}dt. \qquad (8.9)$$

[2]Note that Eq. (8.6) corrects some minor typos in [23, Eq. (35)].

Thus, substituting (8.6) into (8.3), we can obtain the average BER of the distributed MS GSC scheme.

In Fig. 26, we compare the average BER of the distributed MS GSC scheme with the conventional MS GSC scheme as a function of $\overline{\gamma}$ for different values of $P_2$. Note that, unlike conventional GSC, the conventional MS GSC scheme does not necessarily combine all the $L_c$ best paths if the channel is of satisfactory quality compared to the output threshold. In some cases, for example, using only a few best paths out of all the available paths can be enough to meet our threshold. However, in this case, the conventional MS GSC scheme has the drawback of having a high chance of loosing the few combined paths which can come from only one BS. Curves for the conventional MS GSC in Fig. 26 manifest indeed this phenomenon. For the distributed MS GSC scheme, we distribute the combined paths as well as the threshold between two BSs as evenly as possible and as such, acquiring at least one best path from each BS is guaranteed. Hence, we can clearly see from this figure a great amount of performance improvement of the proposed scheme in comparison to the conventional scheme as $P_2$ increases. This performance gain comes at the cost of an increase in the processing power, which will be investigated in the next section. Fig. 27 presents the average BER in terms of the probability of loosing BS2, $P_2$, for fixed values of $\overline{\gamma}$. As expected, the proposed distributed MS GSC scheme outperforms the conventional scheme for higher values of $\overline{\gamma}$ and $P_2$.

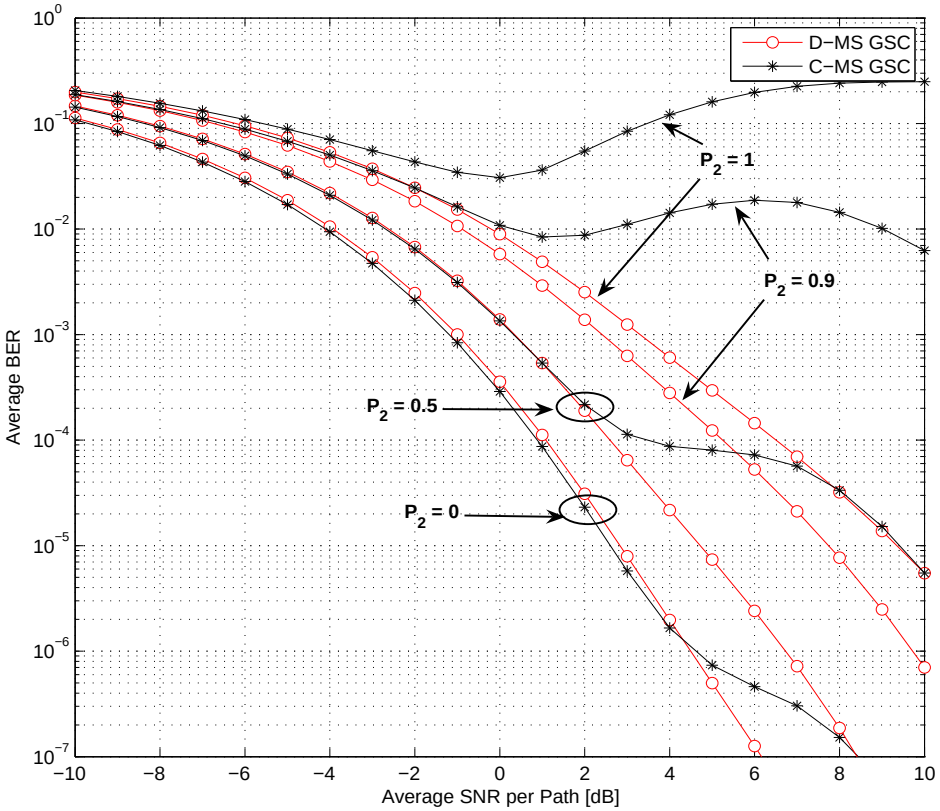


Fig. 26. Average BER of BPSK versus the average SNR per path, $\overline{\gamma}$, of distributed MS GSC (D-MS GSC) and conventional MS GSC (C-MS GSC) for various values of $P_2$ over i.i.d. Rayleigh fading channels when $L_1 = L_2 = 6, L_{c_1} = L_{c_2} = 2, P_1 = 0, \gamma_T = 10$ dB, and $\gamma_{T_1} = \gamma_{T_2} = \frac{\gamma_T}{2}$.

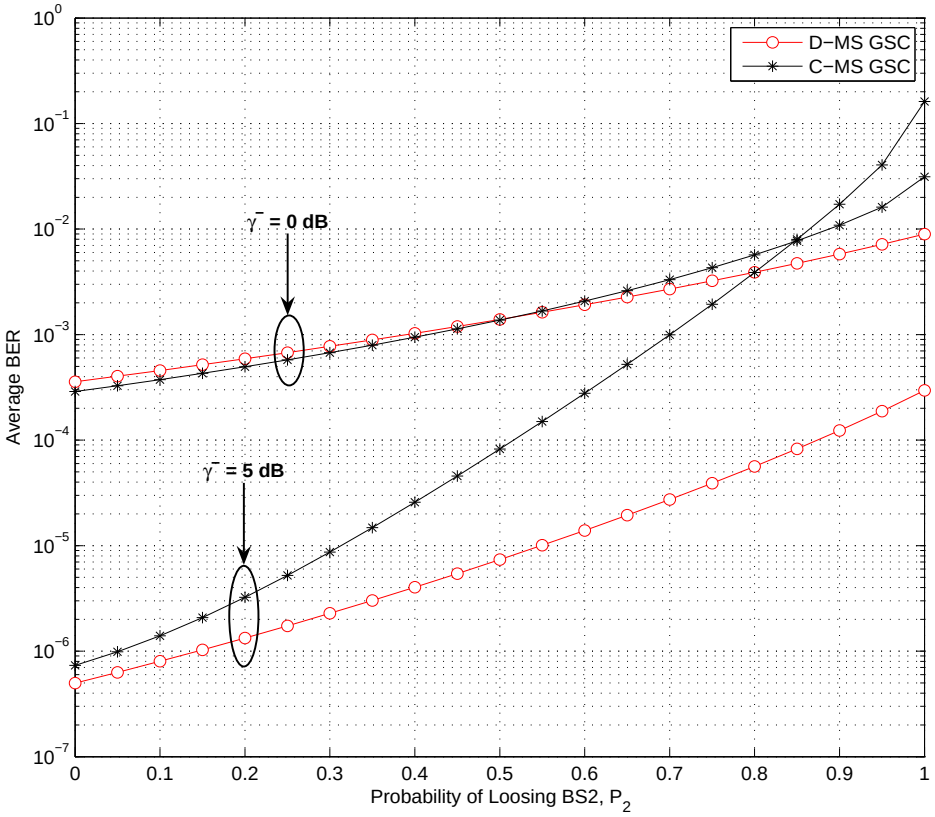


Fig. 27. Average BER of BPSK versus the probability of loosing BS2, $P_2$, of distributed MS GSC (D-MS GSC) and conventional MS GSC (C-MS GSC) for various values of $\overline{\gamma}$ over i.i.d. Rayleigh fading channels when $L_1 = L_2 = 6, L_{c_1} = L_{c_2} = 2, P_1 = 0, \gamma_T = 10$ dB, and $\gamma_{T_1} = \gamma_{T_2} = \frac{\gamma_T}{2}$.

D. Complexity Comparison

As mentioned earlier, in comparison to the conventional GSC scheme, the conventional MS GSC scheme can save receiver processing power by using the least number of combined paths while keeping the combined SNR above a predetermined output threshold. As a quantification of this power savings with MS GSC, the average number of combined paths was analyzed and given by [23, Eq. (16)]

$$\overline{N}_{MSGSC} = 1 + \sum_{i=1}^{L_c-1} F_{\Gamma_{i:L_1+L_2}}(\gamma_T), \tag{8.10}$$

where $\Gamma_{i:j}$ is the sum of the $i$ largest SNRs among $j$ ones and $F_{\Gamma_{i:j}}$ is the well-known CDF of $i/j$-GSC output SNR which is given in (3.20).

Since we are distributing MS GSC selection algorithm to each BS, we can easily obtain the average number of combined paths with distributed MS GSC as

$$\begin{aligned}\overline{N}_{D-MSGSC} = (1-P_1)\left(1 + \sum_{i=1}^{L_{c_1}-1} F_{\Gamma_{i:L_1}}(\gamma_{T_1})\right) \\ +(1-P_2)\left(1 + \sum_{i=1}^{L_{c_2}-1} F_{\Gamma_{i:L_2}}(\gamma_{T_2})\right),\end{aligned} \tag{8.11}$$

where $\gamma_{T_1} + \gamma_{T_2} = \gamma_T$.

Fig. 28 shows the average number of combined paths with the conventional and the distributed MS GSC schemes as a function of the output threshold, $\gamma_T$. As we can see, in both cases the average number of combined paths decreases as $P_2$ increases, but increases as the output threshold increases since the receiver has to combine more paths to raise the combined SNR above the output threshold. Considering Fig. 26 together with Fig. 28, we can observe the complexity tradeoff issue between the proposed and the conventional schemes . For example, if the output threshold is set to 10 dB, for $\overline{\gamma} = 5$ dB and $P_2 = 0.9$, the proposed scheme and the conventional scheme

show $1.2 \times 10^{-4}$ BER and $1.7 \times 10^{-2}$ BER, respectively, while the proposed scheme requires on average only around 0.5 more combined paths than the conventional scheme.

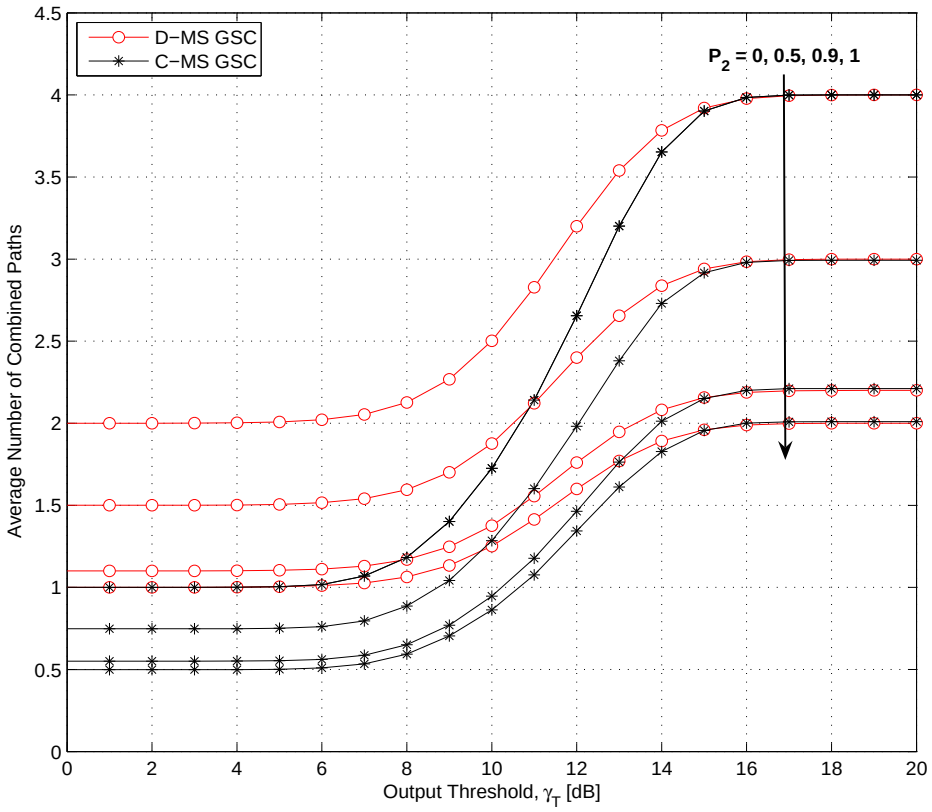


Fig. 28. Average number of combined paths versus the output threshold, $\gamma_T$, of distributed MS GSC (D-MS GSC) and conventional MS GSC (C-MS GSC) for various values of $P_2$ over i.i.d. Rayleigh fading channels when $L_1 = L_2 = 6, L_{c_1} = L_{c_2} = 2, P_1 = 0, \overline{\gamma} = 5$ dB, and $\gamma_{T_1} = \gamma_{T_2} = \frac{\gamma_T}{2}$.

## E. Conclusion

In this chapter, we proposed new finger management schemes for RAKE reception in the SHO region. In particular, we considered distributed versions of the conventional GSC and MS GSC schemes in order to minimize the possibility of call drops in case that one of the active BSs is lost with a certain probability. We provided an analytical framework for the assessment of the proposed schemes by offering generic expressions for the average BER of the proposed distributed schemes for i.i.d. Rayleigh fading environments. We showed through numerical examples that in comparison to the conventional schemes, the proposed distributed schemes offer better error performance when there is a considerable chance of loosing the signals from one of the active BSs.

# CHAPTER IX

# CONCLUSION AND FUTURE WORK

## A. Summary of Conclusions

In this dissertation, various new finger assignment/management schemes for RAKE receivers in the SHO region were proposed and analyzed. Collectively, the main contributions of this dissertation are to provide a comprehensive framework for the assessment of the proposed schemes.

Focusing on the minimum use of network resources, we first presented in Chapters III and IV new finger reassignment schemes in case of two BSs and multiple BSs, respectively. Both schemes implement a new version of GSC-based path selection mechanisms. We derived some important statistics such as PDF, CDF, and MGF of the output SNR, based on which we carried out an extensive performance analysis along with an investigation of the tradeoff between the proposed and the conventional schemes.

In Chapters V and VI, alternative finger combining schemes (namely replacement schemes) were proposed. To further reduce the use of network resources and complexity, these schemes use the block comparison mechanisms instead of the full GSC methods used in the reassignment schemes. It has been shown that the proposed replacement schemes can save a certain amount of complexity with a negligible performance loss compared to the previously proposed schemes in Chapters III and IV.

In Chapter VII, all the schemes analyzed over i.i.d. fading channels in Chapters III-VI were reconsidered in more practical channel environments. More specifically, we examined through computer simulations the effects of path unbalance, path

correlation, and outdated or imperfect channel estimation on the performance. Simulation results showed that our proposed schemes are still applicable in the practical channel environments and that, more interestingly, the replacement schemes are very robust to these practical limitations in comparison to the reassignment schemes.

Noting that the proposed schemes in Chapters III-VII were mainly focusing on how to reduce the network resources, we considered in Chapter VIII the schemes for the minimum call drop achievement in the SHO region as another target criteria. These schemes were designed by evenly distributing the finger paths among BSs such that we can reduce the probability of call drops when a certain BS is totally blocked. We considered distributed GSC and MS GSC schemes and quantified the error performance. The complexity tradeoff issue between the proposed and the conventional schemes was also investigated.

## B. Future Research Directions

It is important to note that in this dissertation we assumed a fixed number of fingers for RAKE receivers and we mainly focused on the macroscopic diversity techniques. However, for example, if only one path from a certain BS is satisfactory to maintain our required quality of service, there is no need to use many other fingers for alternative BSs. Hence, we can save the network resources as well as the receiver complexity and processing power. Only if it is not the case, we need to scan the additional BSs and gradually increase the number of combined paths to meet a certain threshold. In summary, we can design new schemes which are fully utilizing simultaneously temporal diversity from the same BS as well as space diversity from the different BSs. From this point, we can further extend our schemes to joint adaptive microscopic and macroscopic diversity schemes by considering inter and intra SHO among BSs.

# REFERENCES

[1] W. C. Jakes, *Microwave Mobile Communications*, 2nd ed. Piscataway, NJ: IEEE Press, 1994.

[2] J. G. Proakis, *Digital Communications*, 3rd ed. New York, NY: McGraw-Hill, 1995.

[3] G. L. Stüber, *Principles of Mobile Communication*, 2nd ed. Norwell, MA: Kluwer Academic Publishers, 2001.

[4] T. S. Rappaport, *Wireless Communications : Principles and Practice*, 2nd ed. Upper Saddle River, NJ: Prentice Hall, 2002.

[5] M. K. Simon and M.-S. Alouini, *Digital Communication over Fading Channels*, 2nd ed. New York, NY: John Wiley & Sons, 2005.

[6] B. Sklar, *Digital Communications : Fundamentals of Applications*, 2nd ed. Upper Saddle River, NJ: Prentice Hall, 2001.

[7] N. C. Beaulieu, "Introduction to "linear diversity combining techniques"," *Proc. IEEE*, vol. 91, no. 2, pp. 328–356, Feb. 2003.

[8] M. A. Blanco and K. J. Zdunek, "Performance and optimization of switched diversity systems for the detection of signals with Rayleigh fading," *IEEE Trans. Commun.*, vol. COM-27, no. 12, pp. 1887–1895, Dec. 1979.

[9] M. A. Blanco, "Diversity receiver performance in Nakagami fading," in *Proc. IEEE Southeastern Conf.*, Orlando, FL, Apr. 1983.

[10] A. A. Abu-Dayya and N. C. Beaulieu, "Analysis of switched diversity systems on generalized-fading channels," *IEEE Trans. Commun.*, vol. 42, no. 11, pp. 2959–2966, Nov. 1994.

[11] ——, "Switched diversity on Microcellular Ricean channels," *IEEE Trans. Veh. Technol.*, vol. 43, no. 4, pp. 970–976, Nov. 1994.

[12] Y.-C. Ko, M.-S. Alouini, and M. K. Simon, "Analysis and optimization of switched diversity systems," *IEEE Trans. Veh. Technol.*, vol. 49, no. 5, pp. 1813–1831, Sept. 2000.

[13] H.-C. Yang and M.-S. Alouini, "Performance analysis of multibranch switched diversity systems," *IEEE Trans. Commun.*, vol. 51, no. 5, pp. 782–794, May 2003.

[14] C. Tellambura, A. Annamalai, and V. K. Bhargava, "Unified analysis of switched diversity systems in independent and correlated fading channels," *IEEE Trans. Commun.*, vol. 49, no. 11, pp. 1955–1965, Nov. 2001.

[15] H.-C. Yang and M.-S. Alouini, "Generalized switched-and-examine combining (GSEC): A low-complexity combining scheme for diversity-rich environments," *IEEE Trans. Commun.*, vol. 52, no. 10, pp. 1711–1721, Oct. 2004.

[16] T. Eng, N. Kong, and L. B. Milstein, "Comparison of diversity combining techniques for Rayleigh-fading channels," *IEEE Trans. Commun.*, vol. 44, no. 9, pp. 1117–1129, Sept. 1996.

[17] M. Z. Win and J. H. Winters, "Analysis of hybrid selection/maximal-ratio combining in Rayleigh fading," *IEEE Trans. Commun.*, vol. 47, no. 12, pp. 1773–1776, Dec. 1999.

[18] M.-S. Alouini and M. K. Simon, "An MGF-based performance analysis of generalized selection combining over Rayleigh fading channels," *IEEE Trans. Commun.*, vol. 48, no. 3, pp. 401–415, Mar. 2000.

[19] Y. Ma and C. C. Chai, "Unified error probability analysis for generalized selection combining in Nakagami fading channels," *IEEE J. Select. Areas Commun.*, vol. 18, no. 11, pp. 2198–2210, Nov. 2000.

[20] A. Annamalai and C. Tellambura, "Analysis of hybrid selection/maximal-ratio diversity combiner with Gaussian errors," *IEEE Trans. Wireless Commun.*, vol. TWC-1, no. 3, pp. 498–512, July 2002.

[21] S. W. Kim, D. S. Ha, and J. H. Reed, "Minimum selection GSC and adaptive low-power RAKE combining scheme," in *Proc. IEEE Int. Symp. on Circuit and Systems (ISCAS'03)*, Bangkok, Thailand, May 2003.

[22] H.-C. Yang, "Exact performance analysis of minimum-selection generalized selection combining (GSC)," in *Proc. IEEE Int. Conf. on Commun. (ICC'05)*, Seoul, Korea, May 2005.

[23] ——, "New results on ordered statistics and analysis of minimum-selection generalized selection combining (GSC)," *IEEE Trans. Wireless Commun.*, vol. 5, no. 7, pp. 1876–1885, July 2006.

[24] R. K. Mallik, P. Gupta, and Q. T. Zhang, "Minimum selection GSC in independent Rayleigh fading," *IEEE Trans. Veh. Technol.*, vol. 54, no. 3, pp. 1013–1021, May 2005.

[25] M.-S. Alouini and H.-C. Yang, "Minimum estimation and combining generalized selection combining (MEC-GSC)," in *Proc. IEEE Int. Symp. on Information*

*Theory (ISIT'05)*, Adelaide, Australia, Sept. 2005.

[26] H.-C. Yang and M.-S. Alouini, "MRC and GSC diversity combining with an output theshold," *IEEE Trans. Veh. Technol.*, vol. 54, no. 3, pp. 1081–1090, May 2005.

[27] L. Yang and H.-C. Yang, "Performance analysis of output-threshold generalized selection combining (OT-GSC) over Rayleigh fading channels," in *Proc. IEEE Wireless Commun. & Networking Conf. (WCNC'06)*, Las Vegas, NV, Apr. 2006.

[28] R. Price and P. E. Green, "A communication technique for multipath channels," *Proc. IEEE*, vol. 46, pp. 555–570, Mar. 1958.

[29] [Online]. Available: http://www.cdmaonline.com/interactive/workshops/terms1/1035.htm

[30] H. Holma and A. Toskala, *WCDMA for UMTS*, revised ed. New York, NY: John Wiley & Sons, 2001.

[31] I. S. Gradshteyn and I. M. Ryzhik, *Table of Integrals, Series, and Products*, Corrected and Enlarged ed. San Diego, CA: Academic, 1994.

[32] A. Papoulis and S. U. Pillai, *Probability, Random Variables, and Stochastic Processes*, 4th ed. New York, NY: McGraw-Hill, 2002.

[33] H. A. David, *Order Statistics*, 3rd ed. New York, NY: John Wiley & Sons, 2003.

# APPENDIX A

## DERIVATION OF (3.10)

The joint probability $\Pr\left[\gamma_T \leq \Gamma_{L_c:L+L_a} < x, \Gamma_{L_c:L} < \gamma_T\right]$ in (3.7) can be written as

$$\begin{aligned} &\Pr\left[\gamma_T \leq \Gamma_{L_c:L+L_a} < x, \Gamma_{L_c:L} < \gamma_T\right] \\ &\quad = \Pr[\Gamma_{L_c:L} < \gamma_T] \Pr\left[\gamma_T \leq \Gamma_{L_c:L+L_a} < x | \Gamma_{L_c:L} < \gamma_T\right]. \end{aligned} \tag{A.1}$$

For simplicity, if we define the events $A$, $B$, and $C$ as

$$A = \gamma_T \leq \Gamma_{L_c:L+L_a} < x, \tag{A.2}$$

$$B = \Gamma_{L_c:L} < \gamma_T, \tag{A.3}$$

$$C = \Gamma_{L_c:L+L_a-1} < \gamma_T, \tag{A.4}$$

then (A.1) can be rewritten as

$$\begin{aligned} \Pr\left[A, B\right] &= \Pr\left[B\right] \Pr\left[A|B\right] \\ &= \Pr\left[B\right] \left(\Pr\left[A|B, C\right] \Pr\left[C|B\right] + \Pr\left[A|B, \overline{C}\right] \Pr\left[\overline{C}|B\right]\right), \end{aligned} \tag{A.5}$$

where $\overline{C}$ is the complementary set of event $C$, i.e., $\overline{C} = \Gamma_{L_c:L+L_a-1} \geq \gamma_T$. Since event $B$ includes event $C$, we have $\Pr[A|B, C] = \Pr[A|C]$. Note also that when event $B$ and event $\overline{C}$ happened, $\Gamma_{L_c:L}$ and $\Gamma_{L_c:L+L_a-1}$ are sums of different set of exponential random variables. Based on the memoryless property of exponential random variables and noting that given that $\overline{C}$ happened after $B$, $B$ may have little effect on $A$ since a path reassignment happened, we have $\Pr[A|B, \overline{C}] \approx \Pr[A|\overline{C}]$. Therefore, we can

express (A.5) as

$$\begin{aligned}\Pr[A,B] &= \Pr[B]\left(\Pr[A|C]\Pr[C|B] + \Pr\left[A|\overline{C}\right]\Pr\left[\overline{C}|B\right]\right) \\ &= \Pr[B]\left(\frac{\Pr[A,C]}{\Pr[C]}\Pr[B|C]\frac{\Pr[C]}{\Pr[B]} + \frac{\Pr\left[A,\overline{C}\right]}{\Pr\left[\overline{C}\right]}\Pr\left[B|\overline{C}\right]\frac{\Pr\left[\overline{C}\right]}{\Pr[B]}\right) \\ &= \Pr[A,C]\Pr[B|C] + \Pr\left[A,\overline{C}\right]\Pr\left[B|\overline{C}\right].\end{aligned} \tag{A.6}$$

Hence, the joint probability in (A.1) can now be written as

$$\begin{aligned}&\Pr[\gamma_T \le \Gamma_{L_c:L+L_a} < x, \Gamma_{L_c:L} < \gamma_T] \\ &= \Pr[\gamma_T \le \Gamma_{L_c:L+L_a} < x, \Gamma_{L_c:L+L_a-1} < \gamma_T]\Pr[\Gamma_{L_c:L} < \gamma_T | \Gamma_{L_c:L+L_a-1} < \gamma_T] \\ &\quad + \Pr[\gamma_T \le \Gamma_{L_c:L+L_a} < x, \Gamma_{L_c:L+L_a-1} \ge \gamma_T]\Pr[\Gamma_{L_c:L} < \gamma_T | \Gamma_{L_c:L+L_a-1} \ge \gamma_T].\end{aligned} \tag{A.7}$$

Using the following relationships

$$\Pr[\Gamma_{L_c:L} < \gamma_T | \Gamma_{L_c:L+L_a-1} < \gamma_T] = 1, \tag{A.8}$$

$$\begin{aligned}&\Pr[\gamma_T \le \Gamma_{L_c:L+L_a} < x, \Gamma_{L_c:L+L_a-1} \ge \gamma_T] \\ &= \Pr[\gamma_T \le \Gamma_{L_c:L+L_a} < x] - \Pr[\gamma_T \le \Gamma_{L_c:L+L_a} < x, \Gamma_{L_c:L+L_a-1} < \gamma_T],\end{aligned} \tag{A.9}$$

and

$$\Pr[\Gamma_{L_c:L} < \gamma_T | \Gamma_{L_c:L+L_a-1} \ge \gamma_T] = 1 - \frac{1 - \Pr[\Gamma_{L_c:L} < \gamma_T]}{1 - \Pr[\Gamma_{L_c:L+L_a-1} < \gamma_T]}, \tag{A.10}$$

we finally arrive at the desired result given in (3.10).

# APPENDIX B

## CLOSED-FORM EXPRESSION OF SOFT HANDOVER OVERHEAD, $\beta$

$$\beta = \sum_{t=1}^{L-L_c}\sum_{u=0}^{L_c-2}\sum_{k=0}^{L_c-u-2}\binom{L_c-2}{u}\frac{(-1)^{t+u}(L_c-1)^u(L_c-u-2)!L!\overline{\gamma}^{L_c-u-k-1}}{(L-L_c-t)!(L_c-1)!(L_c-2)!t!k!\overline{\gamma}^{L_c}} \quad \text{(B.1)}$$
$$\times\Bigg\{\left[1-\left(1-e^{-\frac{\gamma_T}{L_c\overline{\gamma}}}\right)^{L_a}\right]\left[\frac{\gamma[k+u+1,(L_c+t)\gamma_T/(\overline{\gamma}L_c)]}{(L_c-1)^{-k}\left((L_c+t)/\overline{\gamma}\right)^{k+u+1}}-e^{-\frac{\gamma_T}{\overline{\gamma}}}\right.$$
$$\left.\times\sum_{w=0}^{k}\binom{k}{w}\gamma_T^{k-w}(-1)^w\frac{\gamma[w+u+1,t\gamma_T/(\overline{\gamma}L_c)]}{(t/\overline{\gamma})^{w+u+1}}\right]+\frac{L_a}{\overline{\gamma}}\sum_{l=0}^{L_a-1}\binom{L_a-1}{l}$$
$$\times(-1)^l\Bigg[(L_c-1)^k\Bigg(\frac{(k+u)!\left(1-e^{-(l+1)\gamma_T/(\overline{\gamma}L_c)}\right)}{\left((L_c+t)/\overline{\gamma}\right)^{k+u+1}(l+1)/\overline{\gamma}}$$
$$-\sum_{v=0}^{k+u}\frac{(k+u)!\gamma\left[v+1,(L_c+t+l+1)\gamma_T/(\overline{\gamma}L_c)\right]}{k!\left((L_c+t)/\overline{\gamma}\right)^{k+u-v+1}\left((L_c+t+l+1)/\overline{\gamma}\right)^{v+1}}\Bigg)$$
$$-e^{-\frac{\gamma_T}{\overline{\gamma}}}\sum_{w=0}^{k}\binom{k}{w}\gamma_T^{k-w}(-1)^w\Bigg(\frac{(w+u)!\left(1-e^{-(l+1)\gamma_T/(\overline{\gamma}L_c)}\right)}{(t/\overline{\gamma})^{w+u+1}(l+1)/\overline{\gamma}}$$
$$\left.\left.-\sum_{v=0}^{w+u}\frac{(w+u)!\gamma\left[v+1,(t+l+1)\gamma_T/(\overline{\gamma}L_c)\right]}{v!\left(t/\overline{\gamma}\right)^{w+u+v+1}\left((t+l+1)/\overline{\gamma}\right)^{v+1}}\Bigg)\Bigg]\right\}+\sum_{u=0}^{L_c-2}\sum_{k=0}^{L_c-u-2}\binom{L_c-2}{u}$$
$$\times\frac{(-1)^u(L_c-1)^u(L_c-u-2)!L!\overline{\gamma}^{L_c-u-k-1}}{(L-L_c)!(L_c-1)!(L_c-2)!k!\overline{\gamma}^{L_c}}\Bigg\{\left[1-\left(1-e^{-\frac{\gamma_T}{L_c\overline{\gamma}}}\right)^{L_a}\right]$$
$$\times\left[\frac{\gamma[k+u+1,L_c\gamma_T/(\overline{\gamma}L_c)]}{(L_c-1)^{-k}\left(L_c/\overline{\gamma}\right)^{k+u+1}}-e^{-\frac{\gamma_T}{\overline{\gamma}}}\sum_{w=0}^{k}\binom{k}{w}\gamma_T^{k-w}(-1)^w\frac{\left(\gamma_T/L_c\right)^{w+u+1}}{w+u+1}\right]$$
$$+\frac{L_a}{\overline{\gamma}}\sum_{l=0}^{L_a-1}\binom{L_a-1}{l}(-1)^l\Bigg[(L_c-1)^k\Bigg(\frac{(k+u)!\left(1-e^{-(l+1)\gamma_T/(\overline{\gamma}L_c)}\right)}{\left(L_c/\overline{\gamma}\right)^{k+u+1}(l+1)/\overline{\gamma}}$$
$$-\sum_{v=0}^{k+u}\frac{(k+u)!\gamma\left[v+1,(L_c+l+1)\gamma_T/(\overline{\gamma}L_c)\right]}{k!\left(L_c/\overline{\gamma}\right)^{k+u-v+1}\left((L_c+l+1)/\overline{\gamma}\right)^{v+1}}\Bigg)$$
$$-e^{-\frac{\gamma_T}{\overline{\gamma}}}\sum_{w=0}^{k}\binom{k}{w}\frac{\gamma_T^{k-w}(-1)^w\gamma\left[w+u+2,(l+1)\gamma_T/(\overline{\gamma}L_c)\right]}{(w+u+1)\left((l+1)/\overline{\gamma}\right)^{w+u+2}}\Bigg]\Bigg\}.$$

# APPENDIX C

## DERIVATION OF (5.12)

The generic expression of $f_{\gamma_{l:L}}(\alpha)$ in (5.11) can be found in [33, Eq. (2.1.6)] as

$$f_{\gamma_{l:L}}(\alpha) = \frac{L!}{(L-l)!(l-1)!}[F_\gamma(\alpha)]^{L-l}[1-F_\gamma(\alpha)]^{l-1}f_\gamma(\alpha), \quad \alpha > 0. \tag{C.1}$$

Now we consider three conditional PDFs in (5.11): (i) $f_{\gamma_{k:L}|\gamma_{l:L}=\alpha}(\beta)$, (ii) $f_{A|\gamma_{l:L}=\alpha,\gamma_{k:L}=\beta}(a)$, and (iii) $f_{B|\gamma_{l:L}=\alpha,\gamma_{k:L}=\beta,A=a}(b)$.

**(i)** $f_{\gamma_{k:L}|\gamma_{l:L}=\alpha}(\beta)$

Using [33, Eqs. (2.1.6)(2.2.1)], we can easily obtain the conditional PDF, $f_{\gamma_{k:L}|\gamma_{l:L}=\alpha}(\beta)$, as

$$\begin{aligned} &f_{\gamma_{k:L}|\gamma_{l:L}=\alpha}(\beta) \\ &= \frac{(L-l)!}{(k-l-1)!(L-k)!}\frac{F_\gamma(\beta)^{L-k}f_\gamma(\beta)(F_\gamma(\alpha)-F_\gamma(\beta))^{k-l-1}}{F_\gamma(\alpha)^{L-l}}, \quad 0<\beta<\alpha. \end{aligned} \tag{C.2}$$

This conditional distribution can be interpreted in another way by noting that the conditional distribution of the $k$th order statistics of $L$ i.i.d. random samples given that the $l$th$(l < k)$ order statistics is $\alpha$ is the same as the distribution of the $k$th order statistics of $L-l$ different i.i.d. random variables whose PDF is the truncated PDF of the original random variables on the right at $\alpha$.

**(ii)** $f_{A|\gamma_{l:L}=\alpha,\gamma_{k:L}=\beta}(a)$

According to Theorem 2.5 in [33], the order statistics of samples from a continuous distribution form a Markov chain. Also note that the ordering operation does not

affect the statistics of the sum of random variables. Therefore, the conditional distribution of the sum of the first $l-1$ order statistics given that the $l$th and $k$th ($l<k$) order statistics are equal to $\alpha$ and $\beta$, respectively, is the same as the distribution of the sum of $l-1$ different i.i.d. random variables whose PDF is the truncated PDF of the original random variable on the left at $\alpha$, i.e.,

$$\begin{aligned} f_{A|\gamma_{l:L}=\alpha,\gamma_{k:L}=\beta}(a) &= f_{A|\gamma_{l:L}=\alpha}(a) \\ &= f_{\sum_{i=1}^{l-1}\gamma_i^+}(a), \quad 0<(l-1)\alpha<a, \end{aligned} \tag{C.3}$$

where $f_{\gamma_i^+}(x)=\frac{f_\gamma(x)}{1-F_\gamma(\alpha)},\ x\geq\alpha$.

**(iii)** $f_{B|\gamma_{l:L}=\alpha,\gamma_{k:L}=\beta,A=a}(b)$

In the same manner used above, the conditional PDF of $\sum_{i=l+1}^{k-1}\gamma_{i:L}$ given $\gamma_{l:L}=\alpha$, $\gamma_{k:L}=\beta$, and $\sum_{i=1}^{l-1}\gamma_{i:L}=a$ is the PDF of the sum of $k-l-1$ random variables with PDF truncated at $\alpha$ from right and $\beta$ from left, i.e.,

$$\begin{aligned} f_{B|\gamma_{l:L}=\alpha,\gamma_{k:L}=\beta,A=a}(b) &= f_{B|\gamma_{l:L}=\alpha,\gamma_{k:L}=\beta}(b) \\ &= f_{\sum_{i=1}^{k-l-1}\gamma_i^\pm}(b), \quad 0<(k-l-1)\beta<b<(k-l-1)\alpha, \end{aligned} \tag{C.4}$$

where $f_{\gamma_i^\pm}(x)=\frac{f_\gamma(x)}{F_\gamma(\alpha)-F_\gamma(\beta)},\ \beta\leq x\leq\alpha$.

For the i.i.d. Rayleigh fading scenarios, after substituting (3.1) and (3.2) into (C.1) and (C.2), the PDF, $f_{\gamma_{l:L}}(\alpha)$, and the conditional PDF, $f_{\gamma_{k:L}|\gamma_{l:L}=\alpha}(\beta)$, specialize to

$$f_{\gamma_{l:L}}(\alpha)=\frac{L!}{(L-l)!(l-1)!\overline{\gamma}}\left(1-e^{-\alpha/\overline{\gamma}}\right)^{L-l}e^{-l\alpha/\overline{\gamma}}\mathcal{U}(\alpha) \tag{C.5}$$

and

$$f_{\gamma_{k:L}|\gamma_{l:L}=\alpha}(\beta)=\frac{(L-l)!(1-e^{-\beta/\overline{\gamma}})^{L-k}e^{-\beta/\overline{\gamma}}(e^{-\beta/\overline{\gamma}}-e^{-\alpha/\overline{\gamma}})^{k-l-1}}{(k-l-1)!(L-k)!\overline{\gamma}(1-e^{-\alpha/\overline{\gamma}})^{L-l}}\mathcal{U}(\alpha-\beta), \tag{C.6}$$

respectively, where $\mathcal{U}(\cdot)$ is the unit step function. It can be also shown that $f_{\gamma_i^+}(x)$ and $f_{\gamma_i^\pm}(x)$ specialize to

$$f_{\gamma_i^+}(x) = \frac{e^{-(x-\alpha)/\overline{\gamma}}}{\overline{\gamma}}, \quad x \geq \alpha \tag{C.7}$$

and

$$f_{\gamma_i^\pm}(x) = \frac{e^{-x/\overline{\gamma}}}{\overline{\gamma}\left(e^{-\beta/\overline{\gamma}} - e^{-\alpha/\overline{\gamma}}\right)}, \quad \beta \leq x \leq \alpha, \tag{C.8}$$

respectively. Hence, the moment generating function (MGF) of $\gamma_i^+$ and $\gamma_i^\pm$ can be shown as

$$\mathcal{M}_{\gamma_i^+}(s) = \int_\alpha^\infty f_{\gamma_i^+}(x)e^{sx}dx = \frac{e^{s\alpha}}{1 - s\overline{\gamma}} \tag{C.9}$$

and

$$\mathcal{M}_{\gamma_i^\pm}(s) = \int_\beta^\alpha f_{\gamma_i^\pm}(x)e^{sx}dx = \frac{e^{s\beta-\beta/\overline{\gamma}} - e^{s\alpha-\alpha/\overline{\gamma}}}{(e^{-\beta/\overline{\gamma}} - e^{-\alpha/\overline{\gamma}})(1 - s\overline{\gamma})}, \tag{C.10}$$

respectively. Noting that the MGF of $\sum_{i=1}^{l-1}\gamma_i^+$ and $\sum_{i=1}^{k-l-1}\gamma_i^\pm$ are equal to $[\mathcal{M}_{\gamma_i^+}(s)]^{l-1}$ and $[\mathcal{M}_{\gamma_i^\pm}(s)]^{k-l-1}$, respectively, and using [15, Eq. (34)], we can obtain the closed forms for (C.3) and (C.4) by taking the inverse Laplace transform, $\mathcal{L}^{-1}\{\cdot\}$, as

$$\begin{aligned} f_{A|\gamma_{l:L}=\alpha,\gamma_{k:L}=\beta}(a) &= \mathcal{L}^{-1}\{[\mathcal{M}_{\gamma_i^+}(s)]^{l-1}\} \\ &= \frac{[a-(l-1)\alpha]^{l-2}}{(l-2)!\overline{\gamma}^{l-1}}e^{-[a-(l-1)\alpha]/\overline{\gamma}}\mathcal{U}(a-(l-1)\alpha) \end{aligned} \tag{C.11}$$

and

$$\begin{aligned} f_{B|\gamma_{l:L}=\alpha,\gamma_{k:L}=\beta,A=a}(b) &= \mathcal{L}^{-1}\{[\mathcal{M}_{\gamma_i^\pm}(s)]^{k-l-1}\} \\ &= \sum_{j=0}^{k-l-1}\binom{k-l-1}{j}\frac{(-1)^j e^{-b/\overline{\gamma}}[b-\beta(k-l-j-1)-\alpha j]^{k-l-2}}{[(e^{-\beta/\overline{\gamma}}-e^{-\alpha/\overline{\gamma}})\overline{\gamma}]^{k-l-1}(k-l-2)!} \\ &\quad \times\mathcal{U}(b-\beta(k-l-j-1)-\alpha j), \\ &\quad 0 < (k-l-1)\beta < b < (k-l-1)\alpha, \end{aligned} \tag{C.12}$$

respectively. After substituting (C.5), (C.6), (C.11), and (C.12) into (5.11), we finally arrive at the desired result given in (5.12).

# VITA

Seyeong Choi received his B.S. and M.S. degrees in the Department of Electrical and Communication Engineering at Hanyang University, Seoul, Korea, in 1996 and 1998, respectively. From 1998 through 2001 he worked as a researcher at LGTele-Com's Network R&D Center, Seoul, Korea, operating the CDMA mobile communication networks. He received his Ph.D. degree in the Department of Electrical and Computer Engineering at Texas A&M University, College Station, Texas, in August 2007. His research was co-advised by Dr. Mohamed-Slim Alouini and Dr. Costas N. Georghiades. His research interests include wireless communications, MIMO fading channels, diversity techniques, and system performance evaluation.

He may be reached at the following permanent address and emails.

Seyeong Choi

80-23, Shinchang-Dong, Yongsan-Gu,

Seoul 140-060, Korea

Email : seyeong.choi@qatar.tamu.edu/seyeong.choi@gmail.com